On State-Predictive Servo Controllers for Time-Delay Systems and Their Application to Blood Pressure Control

Eiko Furutani

November, 1996

On State-Predictive Servo Controllers for Time-Delay Systems and Their Application to Blood Pressure Control

Dissertation
Submitted for the Doctor Degree
in Kyoto University

Eiko Furutani

November, 1996

Abstract

In this thesis, a design method of the state-predictive servo system for the plant with a pure delay is proposed and applied to the blood pressure control of living bodies using a hypotensive drug. The state-predictive controller is one of the representative controllers that takes the pure delay of the plant into account, and is effective in control of the plant with comparatively long delay. The thesis consists of three parts.

In the first part, a design method of the state-predictive two-degree-of-freedom LQI servo system is studied. First, a design method of the two-degree-of-freedom LQI servo system in the delay-free case is extended to the case where the plant includes a pure delay. This method enables the designer to determine the tracking characteristics for step references and the feedback characteristics for step disturbances optimally with respect to independent quadratic performance indices, respectively. Then, the properties of the designed state-predictive two-degree-of-freedom servo system is clarified, and the optimal observer that minimizes the deterioration of the maximally attainable disturbance rejection ability is derived. This result about the optimal observer, in combination with the two-degree-of-freedom design method derived at the beginning, constitutes the complete solution to the optimal design problem of the state-predictive two-degree-of-freedom LQI servo system for step references and step disturbances.

In the second part, a robust stability condition of the state-predictive control system is derived under the assumption that the gain and the delay time of the plant model include uncertainties. A method to calculate the stability margin is also established. In the state-predictive controller, the present state of the lumped-parameter part of the plant is predicted using a dynamical model of the plant. So, the performance of the controller much depends upon the accuracy of the model. Hence, in the design of state-predictive controllers, the robust stability analysis is essential. The robust stability condition derived here gives a practically complete solution to this problem for the case of scalar plants in the sense that the controller is ready for the worst case. Namely, the uncertainties of the plant model of scalar plants can be reduced to the uncertainties in the gain and the phase, and the assumption that there exists the

uncertainty in the delay time corresponds to the case of the worst phase shift for a given gain.

In the third part, the state-predictive servo controller is applied to the blood pressure control of living bodies using a hypotensive drug. The final purpose of the research is to apply the obtained result to the blood pressure control of patients under surgical operation and to reduce blood loss, to reduce blood transfusion and to avoid the side-effect of blood transfusion. To attain these effects, the blood pressure must be kept within a narrow range. Since the responses of the blood pressure of living bodies to a hypotensive drug include a considerably large pure delay, the control system must be designed by a method taking the dead time of the responses to the hypotensive drug into account so that highly accurate control is performed. This circumstance motivated the use of a state-predictive servo controller. The control system was applied to a dog experimentally and proved to achieve satisfactorily accurate and robust performance needed in the application to the surgical operations.

Acknowledgements

The author wishes to express his sincere gratitude to Professor Mituhiko Araki of the Department of Electrical Engineering, Kyoto University. His enthusiastic guidance and constant encouragement enabled the author to complete this work. The author is also grateful to Dr. Tomomichi Hagiwara, Associate Professor of Department of Electrical Engineering, Kyoto University, for his stimulating and helpful advice and discussions. The author would like to thank Professor Shunzo Maetani of Research Center on Biomedical Engineering, Kyoto University, and Mr. Tadahiro Sakamoto at First Department of Surgery, Kyoto University for their helpful discussion from the medical viewpoint and assistance in blood pressure control experiments. Gratitude is also due to the members of Professor Araki's research group for their assistance.

Contents

Chapter 1

Introduction

Feedback control is a method in which the input is changed so as to make the error between the reference input and the controlled output smaller, based on the observation of the effect of the past input on the controlled output. When the plant includes a pure delay, the effect of the input does not appear on the output immediately. This means that sufficient information for determining the present input cannot be obtained, and that the effect of the past input on the output cannot be evaluated accurately. For this reason, the performances (i.e. the tracking characteristics, the feedback characteristics, the stability, and so on) of the control system for the plant with a pure delay become worse than those of the plant without a pure delay.

In order to avoid such performance deterioration of the control system for the plant with a pure delay, several methods that the input is determined based on the predicted value of the output obtained by an appropriate prediction mechanism were proposed [42], [32], [22], [16].

The Smith controller [42] is the first and representative method that realized the above idea. It has a transfer function model of the plant in itself and equivalently realizes a closed-loop system with no delay by predicting the output of the *lumped-parameter part* of the plant (i.e. the part of the plant obtained by removing the pure delay) by the transfer function model. However, the Smith controller has the following drawbacks.

1. The Smith controller cannot stabilize the closed-loop system when the plant is unstable.

2. The Smith controller cannot suppress step disturbances when the plant has a pole (or poles) at the origin. Furthermore, the effects of step disturbances remain for a long time when the plant has a pole (or poles) near the origin.

In order to cope with the second drawback, the Smith controller using an approximate plant model [39], the Smith controller with a disturbance compensator [45] and a two-degree-of-freedom Smith controller [4] were proposed. However, the first drawback was not removed in these modified versions; i.e. these controllers could not stabilize the closed-loop system when the plant is unstable. This is because the first drawback originates from the essential structure of the Smith controller.

On the other hand, the state-predictive controller [32], [22], [16] is a comparatively new proposal. It has a state-space model of the plant in itself and equivalently realizes a closed-loop system with delay-free state feedback by predicting the state of the lumped-parameter part of the plant by the state-space model. This controller can be derived by applying the finite spectrum assignment technique [32] to the plant, and has the following advantages in comparison with the Smith controller.

1. The state-predictive controller can stabilize the closed-loop system even when the plant is unstable.

2. The state-predictive controller can suppress step disturbances completely at the steady state even when the plant has a pole (or poles) at the origin. If the plant model is accurate, the effects of step disturbances can be removed at arbitrarily specified speed even when the plant has a pole (or poles) near the origin.

The present thesis is devoted to establishing a systematic design method of the state-predictive controller.

As for the design of a one-degree-of-freedom state-predictive controller, design methods for the plant with no delay can be used. Namely, after the control system is constructed in accordance with the state-predictive control system structure [32], [22], [16], the feedback gain and the observer gain can be determined by applying an appropriate design method for plants with no delay (for example, the pole-assignment method, the optimal design method with respect to a quadratic performance index, and so on [16]) to the lumped-parameter part of the plant. However, as for the design of the two-degree-of-freedom state-predictive control system, no systematic method has been established. In [2], a two-degree-of-freedom state-predictive control system was studied, but the controller was only for a single-input single-output plant and its feedforward gain was determined by a trial-and-error method.

On the other hand, for the plant without a delay, a systematic two-degree-of-freedom optimal design method has been studied [11], [17], [19] assuming that the state feedback is possible. These researches have made the following common contribution. Namely, they have clarified that, by taking an appropriate 'two-stage design

procedure,' tracking characteristics and feedback characteristics can be adjusted separately. To be precise, the tracking characteristics can be determined optimally in the first stage, and the feedback characteristics can be improved in the second stage by introducing an integral and proportional feedback, without affecting the tracking characteristics determined in the first stage. In particular, under the setting of state feedback, Hagiwara et al. [19] proposed a two-degree-of-freedom *optimal* design method, in which the responses for step references can be determined optimally with respect to a quadratic performance index, and at the same time, the responses for step disturbances can be determined optimally with respect to another quadratic performance index. Moreover, they showed that the responses for step disturbances become quicker as the 'state-weighting matrix' Ξ of the performance index posed on the disturbance responses is made larger, and also gave the asymptotic disturbance responses for $\Xi \to \infty$. (Note that the responses for step references remain the same in this process of improving the responses for step disturbances by adjusting Ξ, as mentioned above.)

A two-degree-of-freedom design method in the output feedback case has been also studied [12], [20]. In particular, Hagiwara et al. [20] focused upon the responses for step disturbances and studied the optimal procedure of determining the feedback gains of the robust servo system, assuming that we employ an arbitrary but fixed observer. To be specific, it is proved that we may use the same feedback gains as those of the state feedback case, whatever observer we may employ. Moreover, it is shown that all the fundamental desirable features are inherited from the state feedback case [19]. In addition, the asymptotic disturbance responses for $\Xi \to \infty$ is given for the output feedback case.

Based on the above background, we study a two-degree-of-freedom design method of an LQI servo system for plant with a pure delay. To put it concretely, we extend the results in the output feedback case [20] to the case where the plant has a pure delay, and study the features of the state-predictive two-degree-of-freedom servo system designed by that procedure. In order to give the complete solution to the optimal design problem of the state-predictive two-degree-of-freedom LQI servo system for step references and step disturbances, the optimal observer for the designed system is derived. Moreover, since the robustness analysis is important in the design of control systems for plants with delays, a robust stability test of the state-predictive control systems is proposed. The test is effective for the Smith controller, too.

As the last step of research, we apply the state-predictive servo controller to the blood pressure control of living bodies using a hypotensive drug. This research is aiming

at the control of the blood pressure of patients under operation, but in this thesis the preliminary studies using dogs are mainly reported. The responses of most functions of living bodies to drugs include more or less a pure delay. When the ratio of the dead time to the time-constant of the response is large, the dead time has a large effect on the response of the overall control system, especially on stability. Blood pressure control is a typical example of such a function. The purposes of our blood pressure control are reducing blood loss in surgical operations, reducing blood transfusion and avoiding the side-effect of blood transfusion. For these purposes, the effect of control becomes more eminent as the blood pressure is kept lower. On the other hand, the blood pressure must be kept at a level higher than the critical value that results in irreversible changes to the body. In order to maintain the blood pressure within such a narrow range bounded by the above two requirements, the control system must be designed by the method taking the dead time of the responses to the hypotensive drug into account. Many blood pressure control systems have been developed [40], [47], [3], [24], [44], [33], [14], [48] (see also [21]), but most of those systems did not take the dead time of responses to drugs into account. Woodruff and Northrop [48] developed a blood pressure control system using the Smith controller, but their control system has a good performance only if the parameters of the controller are fine-tuned. Under such background, we developed a blood pressure control system.

The contents of this thesis are as follows.

In Chapter 2, we make a brief survey of usual state-predictive controllers [32], [22], [16]. Furthermore, we review a two-degree-of-freedom state-predictive servo system proposed by Araki and Watanabe [2].

In Chapter 3, we extend the results for the two-degree-of-freedom LQI servo system in the output feedback case [20] to the case where the plant has a pure delay. It will be proved that the resulting compensator is the same as that for the plant with the delay removed, except the existence of a state prediction mechanism to cope with the delay, and that all the fundamental desirable features are inherited from the delay-free case. Moreover, comparing the obtained asymptotic responses with those of the state feedback case, the deterioration of disturbance rejection ability caused by the introduction of an observer is quantitatively clarified. In addition, by evaluating this performance deterioration, we study a design method of an observer. To be precise, we give a design method of an optimal observer that minimizes the deterioration of the maximally attainable disturbance rejection ability. The derived optimal observers have a close connection with the technique of loop transfer recovery [9], [43].

In state-predictive controllers, the present state of the lumped-parameter part of

the plant is predicted using dynamical models of the plant. Then, the performance of the controllers much depends upon the accuracy of those models. This implies that the control systems can become very sensitive to modeling errors, especially when the response speed is raised excessively. Hence, in the design of state-predictive controllers, the robustness analysis is crucially important. In Chapter 4, we study robust stability conditions in the case where the modeling errors (in the following, referred to as *mismatches*) exist only in the estimates of the gain and the delay time, and we derive a method to obtain the stability margin of state-predictive control systems. Although the assumption of the modeling errors seems to be very restrictive, the results can be practically useful because the assumed modeling errors cover general gain and phase deviation which are practically plausible.

In Chapter 5, we apply the state-predictive servo controller to the blood pressure control using a hypotensive drug. It is proved by experiments that the blood pressure control system using the state-predictive controller exhibits satisfactorily accurate and robust performances needed in the application to the surgical operations.

In the final chapter, Chapter 6, we summarize this thesis, and discuss the future topics.

Chapter 2

State-predictive control systems

As controllers for plants with a cascaded pure delay, the Smith controller [42] and state-predictive controllers [32], [22], [15], [16] are well-known. Both of them have some prediction mechanisms. In the Smith controller, the effect of the manipulating input on the controlled output is predicted. This controller has a defect that it cannot suppress the offset if the plant has a pole at the origin. In order to solve this difficulty, the Smith controller using an approximate plant model [39], the Smith controller with a disturbance compensator [45] and a two-degree-of-freedom Smith controller [4] were proposed. However, these controllers, nor the original Smith controller, cannot stabilize the closed-loop system if the plant is unstable. On the other hand, in state-predictive controllers, the present state of the lumped-parameter part of the plant is predicted, and accordingly, they can stabilize the closed-loop system even for an unstable plant.

In this chapter, we make a brief survey of the usual state-predictive servo controller [32], [22], [16].

2.1 State-predictive servo systems

Consider the plant with a cascaded pure delay T_L on the output side, described by

$$\frac{dx(t)}{dt} = Ax(t) + Bu(t), \tag{2.1}$$

$$y_{\mathrm{A}}(t) = Cx(t), \tag{2.2}$$

$$y(t) = y_{\mathrm{A}}(t - T_L), \tag{2.3}$$

where $u(t)$ is an m-dimensional input, $y(t)$ is an m-dimensional output, $y_{\mathrm{A}}(t)$ is an m-dimensional delay-free output, and $x(t)$ is an n-dimensional state, and (A, B) is controllable and (C, A) is observable. We assume that the state x is not accessible and only y is available. (Even if the delay is on the input side, we can model the system in

the form of (2.1), (2.2) and (2.3). Therefore, the assumption that the delay lies on the output side does not cause any loss of generality.) We refer to (2.1) and (2.2) as the *lumped-parameter part* of the plant, and to (2.3) as the *pure delay part*. The structure of the model is depicted in Fig. 2.1 where

$$G(s) := C(sI - A)^{-1}B \tag{2.4}$$

is the transfer function of the lumped-parameter part.

Now, we derive a state-predictive servo system for this plant. The basic idea is as follows. First, assuming that we can use the state and the delay-free output (i.e., the output of the lumped-parameter part of the plant), we construct a fictitious system. Then, we transform the fictitious system into a physically realizable system using an observer and a prediction mechanism.

We first consider a fictitious *augmented system* of Fig. 2.2, which includes integral compensation in order to attain the robust tracking ability. If we can use the values of $x(t)$ and $y_A(t)$, we can apply the state feedback law to the augmented system:

$$u(t) = [F_1 \quad F_2] \begin{bmatrix} x_I(t) \\ x(t) \end{bmatrix} \tag{2.5}$$

with

$$x_I(t) := \int_0^t \{r(\tau) - Cx(\tau)\}d\tau. \tag{2.6}$$

The feedback gain for the augmented system

$$F_a := [F_1 \quad F_2] \tag{2.7}$$

should be determined so that the closed-loop system has appropriate properties. Thus, we obtain the fictitious servo system of Fig. 2.3.

Now, we derive a physically realizable system from Fig. 2.3. For this purpose, we first make an estimate of the state of the lumped-parameter part by using an observer. Since the available data is the delayed output $y(t) = Cx(t - T_L)$, we design an observer to estimate the past value $x(t - T_L)$ of the state:

$$\begin{aligned} \frac{dq(t)}{dt} &= \hat{A}q(t) + \hat{B}u(t - T_L) - Ky(t), \\ \hat{x}(t - T_L) &= Dq(t) - Ly(t). \end{aligned} \tag{2.8}$$

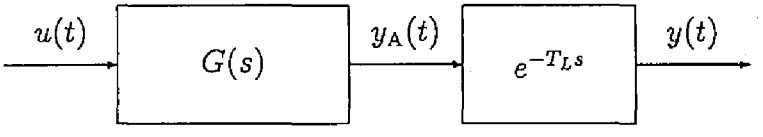

Fig. 2.1: A plant with a pure delay

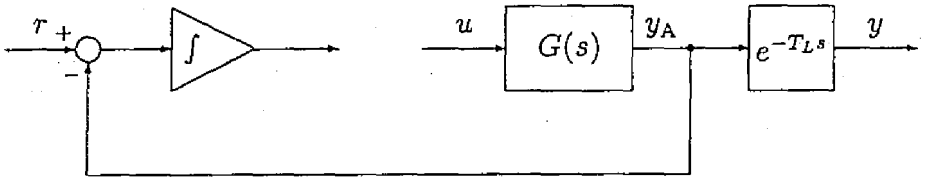

Fig. 2.2: Augmented system for designing the state-predictive servo system

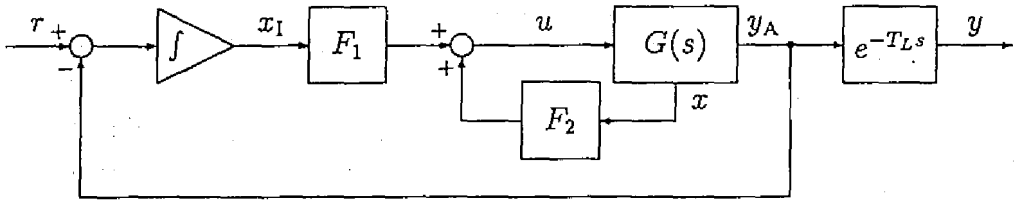

Fig. 2.3: Fictitious servo system

Here, $\hat{x}(t-T_L)$ denotes the estimate of $x(t-T_L)$, $\hat{A}$ is a stable matrix and $\hat{A}$, $\hat{B}$, K, D and L satisfy

$$\begin{aligned} \hat{A}M &= MA + KC, \\ \hat{B} &= MB, \\ I &= DM - LC \end{aligned} \tag{2.9}$$

for a certain M [29]. Next, we predict the values of the state of the lumped-parameter part and the integral error. For this purpose, we use the state transition equation of the augmented system

$$\begin{aligned} \begin{bmatrix} x_I(t) \\ x(t) \end{bmatrix} &= e^{A_a T_L} \begin{bmatrix} x_I(t-T_L) \\ x(t-T_L) \end{bmatrix} + \int_{t-T_L}^{t} e^{A_a(t-\tau)} B_a u(\tau) d\tau \\ &\quad + \int_{t-T_L}^{t} \begin{bmatrix} r(\tau) \\ 0 \end{bmatrix} d\tau \end{aligned} \tag{2.10}$$

with

$$A_a := \begin{bmatrix} 0 & -C \\ 0 & A \end{bmatrix}, \quad B_a := \begin{bmatrix} 0 \\ B \end{bmatrix}. \tag{2.11}$$

Assuming that $y(t) = 0$ $(0 \le t < T_L)$, $\hat{x}_I(t)$, the integral error of the available output from the reference (this corresponds to the output of the integrator which can be implemented in the actual controller), is obtained by

$$\begin{aligned} \hat{x}_I(t) &= \int_0^{t-T_L} \{r(\tau) - Cx(\tau)\} d\tau + \int_{t-T_L}^{t} r(\tau) d\tau \\ &= x_I(t-T_L) + \int_{t-T_L}^{t} r(\tau) d\tau. \end{aligned} \tag{2.12}$$

Replacing $x(t-T_L)$ in (2.10) by the estimate $\hat{x}(t-T_L)$ and substituting the equation obtained by solving (2.12) for $x_1(t-T_L)$ into (2.10), we obtain the predicted value

$$\hat{\bar{x}}_a(t) := \begin{bmatrix} \hat{\bar{x}}_1(t) \\ \hat{\bar{x}}(t-T_L) \end{bmatrix} = e^{A_a T_L} \begin{bmatrix} \hat{x}_1(t) \\ \hat{x}(t-T_L) \end{bmatrix} + \int_{t-T_L}^{t} e^{A_a(t-\tau)} B_a u(\tau) d\tau. \tag{2.13}$$

Here, $\hat{\bar{x}}_1$, $\hat{\bar{x}}$ are the predicted values of the integral error and the state of the lumped-parameter part. If this $\hat{\bar{x}}_a(t)$ is used in place of $[x_I^T(t) \quad x^T(t)]^T$ in (2.5), the feedback law becomes

$$u(t) = [F_1 \quad F_2]\hat{\bar{x}}_a(t). \tag{2.14}$$

As a result, we obtain a one-degree-of-freedom *state-predictive servo system* given in Fig. 2.4. Here, $\mathcal{F}(A_a, B_a, T_L)$ is a finite interval integration operator defined by

$$\mathcal{F}(A_a, B_a, T_L)u := \int_{-T_L}^{0} e^{A_a \tau} B_a u(t+\tau) d\tau, \tag{2.15}$$

and I_{I} and I_{F} are matrices defined by

$$I_{\mathrm{I}} = \begin{bmatrix} I_m \\ 0 \end{bmatrix}, \quad I_{\mathrm{F}} = \begin{bmatrix} 0 \\ I_n \end{bmatrix}, \tag{2.16}$$

where I_i is an i-dimensional unit matrix. If there exist no modeling errors, the responses of this system for reference inputs coincide with those of Fig. 2.3. The parameters of the system can be determined by pole assignment method, optimal design method with respect to a quadratic performance index, and so on.

2.2 Two-degree-of-freedom state-predictive servo system for an SISO plant

In the preceding section, we reviewed one-degree-of-freedom servo system based on state-predictive control. In this section, we make a brief survey of a two-degree-of-freedom state-predictive servo control system proposed by Araki and Watanabe [2]. This system is for an SISO (single-input single-output) plant[1]. The structure of this system is shown in Fig. 2.5. The term χ, one of the inputs of the observer, works as a feedforward from the reference input to the manipulated input, and κ is a parameter for adjusting the tracking characteristics. In addition, κ gives no effect on the feedback characteristics. Therefore, the system of Fig. 2.5 is a two-degree-of-freedom servo system. However, we can adjust κ only by trial-and-error method and no effective adjusting method of the parameter κ is given.

[1]This system can be easily extended to the multivariable case.

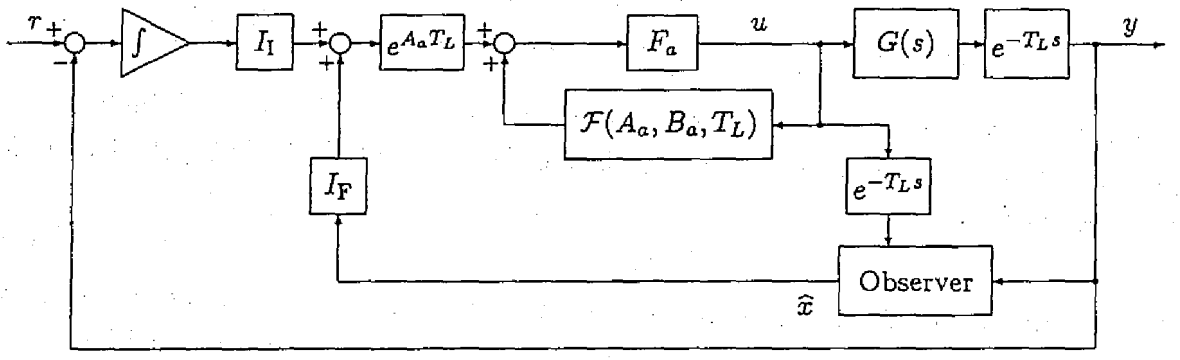

Fig. 2.4: One-degree-of-freedom state-predictive servo system

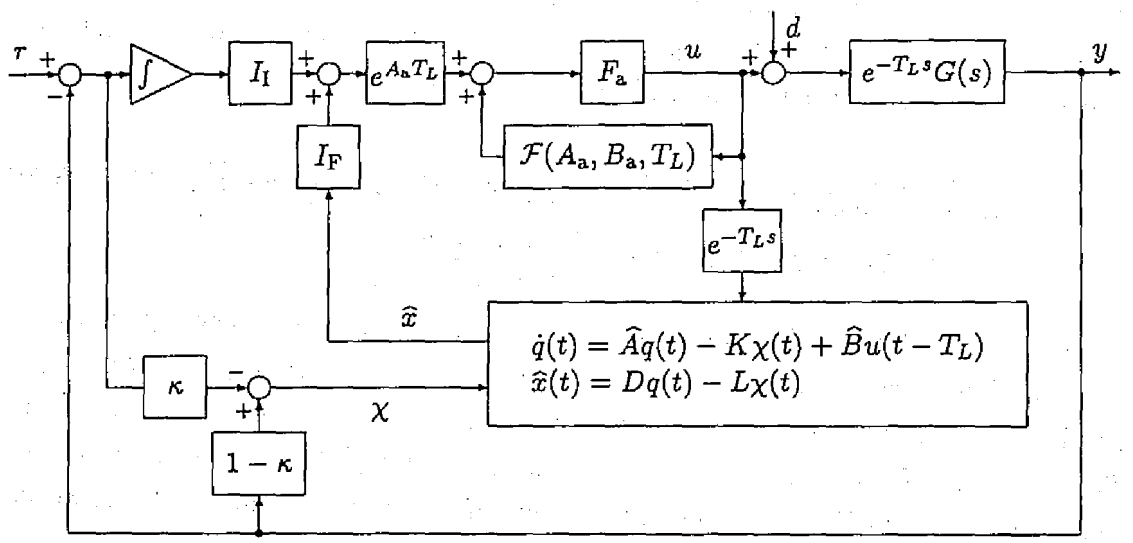

Fig. 2.5: Two-degree-of-freedom state-predictive servo system proposed by Araki and Watanabe [2]

Chapter 3

Two-degree-of-freedom state-predictive LQI servo systems

As mentioned in the preceding chapter, in designing state-predictive controllers, design methods for plants with no delay have been used, that is, control systems are constructed in accordance with state-predictive control system structures [32], [22], and the feedback gain and the observer gain are determined, for example, by pole-assignment method, optimal design method with respect to a quadratic performance index, and so on [16]. On the other hand, no effective design method of two-degree-of-freedom state-predictive control systems has been established. A two-degree-of-freedom state-predictive control system was studied in [2], but its feedforward gain can be determined only by a trial-and-error method.

As for the plants without a delay, an effective two-degree-of-freedom optimal design method was proposed [11], [17], [19], in which the responses for step references can be determined optimally with respect to a quadratic performance index, and at the same time, the responses for step disturbances can be determined optimally with respect to another quadratic performance index. In addition, the extension of this method to the output feedback case was studied [20], [12].

The purpose of this chapter is to extend one of these results [20] to the case in which the plant has a pure delay. It will be proved that the resulting compensator is the same as that for the plant with the delay removed, except the existence of a state prediction mechanism to cope with the delay, and that all the fundamental desirable features are inherited from the delay-free case. Moreover, the asymptotic disturbance responses obtained improving the disturbance rejection ability of the system as much as possible are given, and comparing the obtained asymptotic responses with those of the state feedback case, the deterioration of disturbance rejection ability caused by the introduction of an observer is quantitatively clarified. Furthermore, we study the

problem of designing the optimal observer that minimizes this deterioration under a suitable measure.

3.1 Plant-variable-optimal state-predictive robust servo system

In this section, we describe the basic ideas for the design of two-degree-of-freedom (abbreviated as *2DOF*) robust servo systems for the plant with a pure delay. This is done by an extension of the design method in the delay-free case [20], by introducing a prediction mechanism. The main problems of this chapter (determining the parameters of the two-degree-of-freedom *optimal* robust servo systems for plants with a pure delay, clarifying the performance deterioration caused by the introduction of an observer and determining the parameters of optimal observers for the designed system) will be studied in the subsequent sections, based on these preliminary results.

3.1.1 State-predictive LQ-obs servo system

As in the preceding chapter, consider the plant with a cascaded pure delay T_L on the output side, described by

$$\begin{aligned} \frac{dx(t)}{dt} &= Ax(t) + Bu(t), \\ y_{\mathrm{A}}(t) &= Cx(t), \\ y(t) &= Cx(t - T_L), \end{aligned} \tag{3.1}$$

where $u(t)$ is an m-dimensional input, $y(t)$ is an m-dimensional output, $y_{\mathrm{A}}(t)$ is an m-dimensional delay-free output, and $x(t)$ is an n-dimensional state, and (A, B) is stabilizable and (C, A) is detectable. For this plant, we consider the problem of designing a robust servo system in which the output $y(t)\,(t \geq 0)$ tends to the step reference $r(t) = r$ applied at $t = 0$ in an optimal fashion. In order for this problem to be solvable, we assume [8]

$$\det \begin{bmatrix} A & B \\ C & 0 \end{bmatrix} \neq 0. \tag{3.2}$$

We further assume that the state x is not accessible and only y is available. Under the above condition, x_∞ and u_∞, the steady-state values of $x(t)$ and $u(t)$ respectively that achieve $y(t) \equiv r$, are uniquely determined by

$$\begin{bmatrix} x_\infty \\ u_\infty \end{bmatrix} = \begin{bmatrix} A & B \\ C & 0 \end{bmatrix}^{-1} \begin{bmatrix} 0 \\ r \end{bmatrix}. \tag{3.3}$$

The *errors* of $x(t)$ and $u(t)$ from these steady-state values defined by

$$\begin{aligned} \tilde{x}(t) &:= x(t) - x_\infty, \\ \tilde{u}(t) &:= u(t) - u_\infty, \end{aligned} \tag{3.4}$$

satisfy the equation of the *error system*:

$$\frac{d\tilde{x}(t)}{dt} = A\tilde{x}(t) + B\tilde{u}(t). \tag{3.5}$$

Noting that $y(t)\,(0 \le t < T_L)$ cannot be altered by $u(t)\,(t \ge 0)$, our purpose could be restated as making the output $y(t)\,(t \ge T_L)$ tend to the step reference r, that is, making the errors $\tilde{x}(t)$ and $\tilde{u}(t)$ for $t \ge 0$ tend to zero as quickly as possible. Thus, as in the delay-free case [20] (see also [36]), we pose the performance index

$$J = \int_0^\infty \left(\tilde{x}(t)^T Q \tilde{x}(t) + \tilde{u}(t)^T R \tilde{u}(t)\right)\, dt, \tag{3.6}$$

$$Q \ge 0, \quad R > 0. \tag{3.7}$$

Assuming that $(Q^{1/2}, A)$ is detectable, we obtain the optimal feedback

$$\tilde{u}(t) = F_0 \tilde{x}(t) \tag{3.8}$$

with

$$F_0 := -R^{-1}B^T P, \tag{3.9}$$

where P is the unique positive semidefinite solution of the Riccati equation

$$PA + A^T P - PBR^{-1}B^T P + Q = 0. \tag{3.10}$$

For this F_0, the matrix $A+BF_0$ becomes stable. From (3.3),(3.4) and (3.8), the optimal plant input u is given by

$$\begin{aligned} u(t) &= F_0(x(t) - x_\infty) + u_\infty \\ &= F_0 x(t) + H_0 r(t), \end{aligned} \tag{3.11}$$

where

$$H_0 := -[C(A + BF_0)^{-1}B]^{-1}. \tag{3.12}$$

The closed-loop system obtained by the control law (3.11) is called an *LQ servo system* by state feedback (Fig. 3.1) [17], [19].

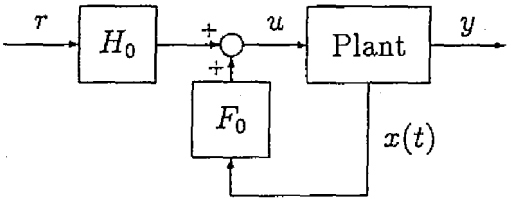

Fig. 3.1: LQ servo system by state feedback

However, since the state x is not accessible by our assumption and since the output $y(t)$ holds the information about $x(t-T_L)$ rather than $x(t)$, we introduce the following observer that estimates the state $x(t-T_L)$ as in Chapter 2 (see also [46]):

$$\begin{aligned} \frac{dq(t)}{dt} &= \widehat{A}q(t) + \widehat{B}u(t-T_L) - Ky(t), \\ \widehat{x}(t-T_L) &= Dq(t) - Ly(t). \end{aligned} \tag{3.13}$$

Here, $\widehat{x}(t-T_L)$ denotes the estimate of $x(t-T_L)$, and we assume that there exists a matrix M satisfying

$$\begin{aligned} \widehat{A}M &= MA + KC, \\ I &= DM - LC, \\ \widehat{B} &= MB, \end{aligned} \tag{3.14}$$

and that $\widehat{A}$ is stable [29]. Furthermore, we introduce $\widehat{\widehat{x}}(\tau|t-T_L)$, an estimate of the state $x(\tau)\,(t-T_L \le \tau \le t)$ calculated from $\widehat{x}(t-T_L)$ using the state transition rule, given by

$$\widehat{\widehat{x}}(\tau|t-T_L) = e^{A(\tau-t+T_L)}\widehat{x}(t-T_L) + \int_{t-T_L}^{\tau} e^{A(\tau-\sigma)}Bu(\sigma)d\sigma. \tag{3.15}$$

Replacing the first term of the right hand side of (3.11) with $F_0\widehat{\widehat{x}}(\tau|t-T_L)|_{\tau=t}$, the control law is given by

$$u(t) = F_0\widehat{\widehat{x}}(t|t-T_L) + H_0 r. \tag{3.16}$$

Here, $\widehat{\widehat{x}}(t|t-T_L)$ is given from (3.15) by

$$\widehat{\widehat{x}}(t|t-T_L) = e^{AT_L}\widehat{x}(t-T_L) + y_f(t), \tag{3.17}$$

where $y_f(t)$ is the *finite interval integration* defined by

$$y_f(t) = \mathcal{F}(A,B,T_L)u := \int_{t-T_L}^{t} e^{A(t-\sigma)}Bu(\sigma)d\sigma, \tag{3.18}$$

which can be formally described by the state equation

$$\begin{aligned} \frac{dx_f(t)}{dt} &= Ax_f(t) + Bu(t), \\ y_f(t) &= x_f(t) - e^{AT_L}x_f(t-T_L), \end{aligned} \tag{3.19}$$

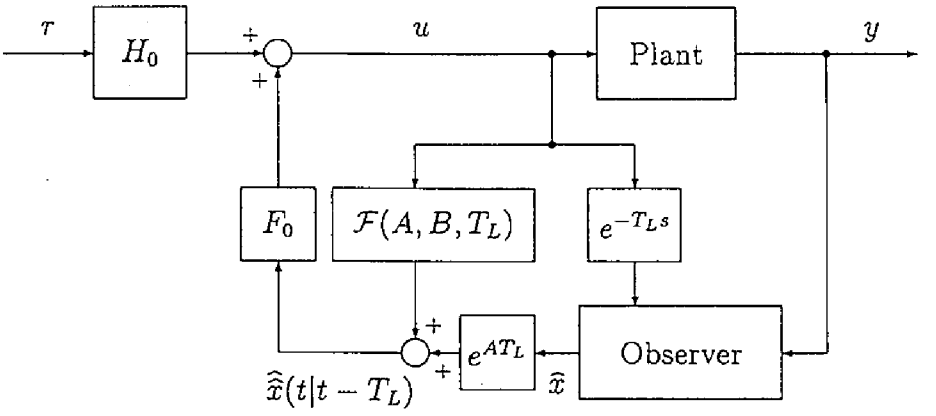

Fig. 3.2: State-predictive LQ servo system incorporating an observer (State-predictive LQ-obs servo system)

where x_f is a state variable of finite interval integration.

The resulting closed-loop system is shown in Fig. 3.2. We call this system a state-predictive LQ servo system incorporating an observer, or simply a *state-predictive LQ-obs servo system.* Since the observer (3.13) and the state prediction mechanism (3.15) do not affect the transfer characteristics from r to y, this servo system has the same tracking ability for step references as the above LQ servo system by state feedback, and attains the optimal transient responses to step references under the performance index (3.6) (this optimality is called *plant-variable-optimality* (PV-optimality) [17], [19], since (3.6) includes only the plant variables). However, it does not possess robust tracking ability against step disturbances and the modeling errors of the plant.

3.1.2 Introduction of integral compensation

In this subsection, according to internal model principle [10], an integral compensator is added in order to endow the state-predictive LQ-obs servo system of the preceding subsection with robust tracking ability. To this end, we introduce the *augmented state-predictive LQ-obs servo system* of Fig. 3.3. As shown in the figure, it includes the state-predictive LQ-obs servo system and the integral compensator

$$w(t) = \int_0^t e(\tau)\, d\tau + w_0 \tag{3.20}$$

where

$$e(t) := r(t) - y(t)\,(= r(t) - Cx(t - T_L)) \tag{3.21}$$

is the tracking error of the output $y(t)$ and w_0 is the initial value of $w(t)$. While the above integral $w(t)$ includes the information up to time t about the reference r, it

includes only the information up to time $t - T_L$ about the state x. For this reason, we equip the augmented state-predictive LQ-obs servo system with another prediction mechanism for the integral compensation, which yields an estimate $\widehat{\widetilde{w}}(t)$ of the integral of the 'delay-free error' $r(t) - Cx(t)$ given by

$$\widehat{\widetilde{w}}(t) := w(t) - \int_{t-T_L}^{t} C\widehat{\widetilde{x}}(\tau|t-T_L)d\tau, \tag{3.22}$$

where $\widehat{\widetilde{x}}(\tau|t-T_L)$ is given by (3.15). Defining the estimation error $\varepsilon(t)$ of the observer and the prediction error $\varepsilon_f(t)$ of the plant state associated with the finite interval integration by

$$\varepsilon(t) := q(t) - Mx(t-T_L), \tag{3.23}$$

$$\varepsilon_f(t) := y_f(t) - x(t) + e^{AT_L}x(t-T_L), \tag{3.24}$$

the closed-loop system is described from (3.1), (3.20), (3.13) and (3.19) by

$$\begin{bmatrix} \dot{x}(t) \\ \dot{\widehat{\widetilde{w}}}(t) \\ \dot{\varepsilon}(t) \\ \dot{\varepsilon}_f(t) \end{bmatrix} = \begin{bmatrix} A+BF_0 & 0 & BF_0e^{AT_L}D & BF_0 \\ -C & 0 & -C\int_0^{T_L} e^{A\sigma}d\sigma D\widehat{A} & -C \\ 0 & 0 & \widehat{A} & 0 \\ 0 & 0 & 0 & A \end{bmatrix} \begin{bmatrix} x(t) \\ \widehat{\widetilde{w}}(t) \\ \varepsilon(t) \\ \varepsilon_f(t) \end{bmatrix}$$

$$+ \begin{bmatrix} B \\ 0 \\ 0 \\ 0 \end{bmatrix} v(t) + \begin{bmatrix} BH_0 \\ I \\ 0 \\ 0 \end{bmatrix} r(t), \tag{3.25}$$

where $v(t)$ is a new input (see Fig. 3.3), and $\zeta(t)$ is a new output defined by

$$\zeta(t) := \Gamma\widehat{\widetilde{x}}(t|t-T_L) + \widehat{\widetilde{w}}(t) \tag{3.26}$$

with

$$\Gamma := C(A+BF_0)^{-1}. \tag{3.27}$$

By introducing a feedback gain G such that

$$v(t) = G\zeta(t) \tag{3.28}$$

(see Fig. 3.4), we can verify the following (in completely the same manner as in [11] and [20]). That is, in the nominal setting, the output $\widehat{\widetilde{w}}(t)$ of the 'predictive integral

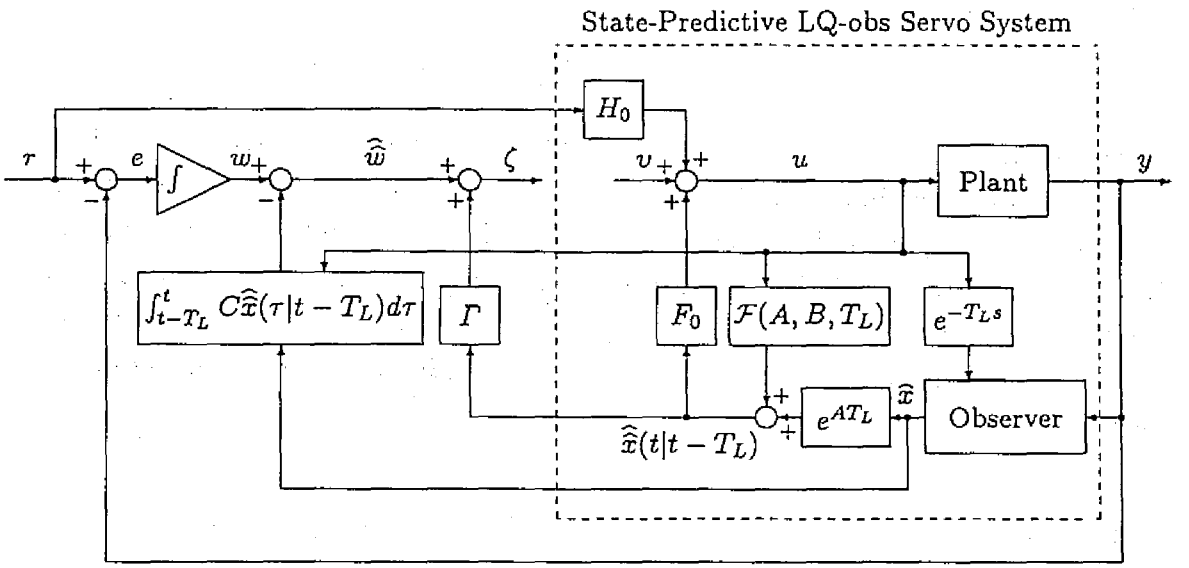

Fig. 3.3: Augmented state-predictive LQ-obs servo system

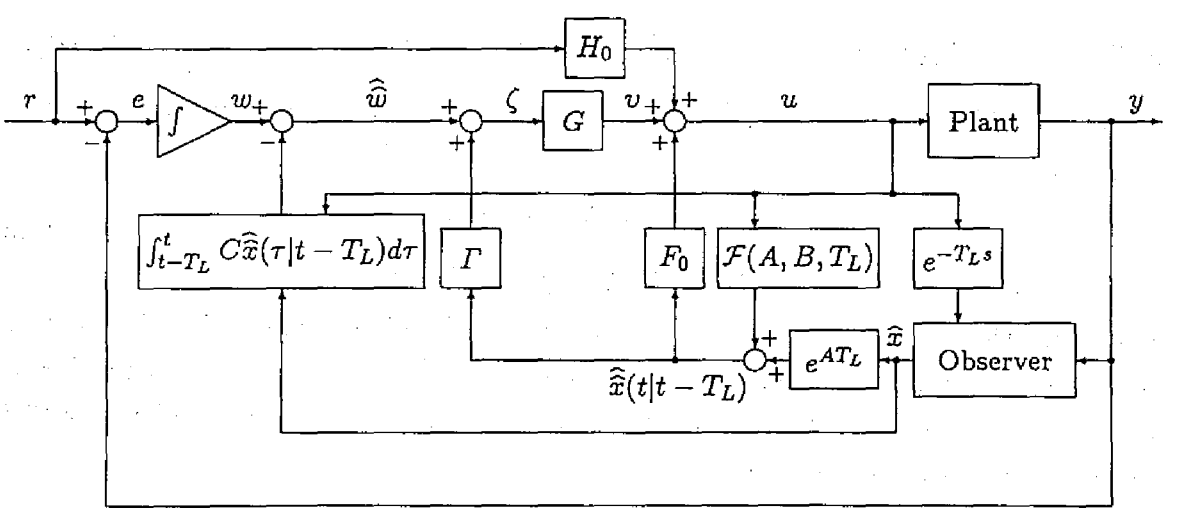

Fig. 3.4: State-predictive plant-variable-optimal LQI-obs servo system (State-predictive 2DOF-LQI-obs servo system)

compensator' (3.22) is canceled by the feedback $\Gamma\widehat{\widehat{x}}(t|t-T_L)$ (i.e., we have $\zeta \equiv 0$)[1], and, by (3.28), the plant input given by

$$u(t) = F_0\widehat{\widehat{x}}(t|t-T_L) + H_0 r(t) + v(t) \tag{3.29}$$

coincides with that of the state-predictive LQ-obs servo system given by (3.16), and so the performance index (3.6) is minimized. On the other hand, if there exist step disturbances and/or modeling errors, they would make v and ζ nonzero, in general. In such a case, the predictive integral compensator (3.22) will make the tracking error tend to zero provided that the closed-loop system is stable. In view of these properties, we call the closed-loop system of Fig. 3.4 a *state-predictive PV-optimal LQI-obs servo system.*

3.2 Optimal G for disturbance rejection

In the preceding section, we introduced a feedback gain G. This gain can be chosen arbitrarily as long as it stabilizes the closed-loop system, and the nominal responses for step references remain the same regardless of the choice of G. In this section, we regard G as the feedback gain which adjusts disturbance rejection characteristics, and study how to determine G in order to obtain the optimal disturbance responses. This leads us to a two-degree-of-freedom optimal design of state-predictive servo systems.

3.2.1 Disturbances and the disturbance compensation input

We consider the case where the plant (3.1) is subject to the step disturbances d_x and d_y as

$$\begin{aligned} \frac{dx(t)}{dt} &= Ax(t) + Bu(t) + d_x(t), \\ y(t) &= Cx(t-T_L) + d_y(t-T_L). \end{aligned} \tag{3.30}$$

Note that the step disturbance d_y is added not to the plant output directly but to the output of the lumped parameter part of the plant. In the following, we consider only the case of $r = 0$ in view of linearity of the system. Then, since the observer (3.13) produces the estimate $\widehat{x}(t-T_L)$ given by

$$\widehat{x}(t-T_L) = x(t-T_L) + D\varepsilon(t) - Ld_y(t-T_L) \tag{3.31}$$

[1]Here, we assumed that the initial values of x, w, q, x_f and the initial function of the pure delay are all zero for simplicity. If this is not the case, the above argument is subject to some modification [11], [12], but this point is not crucial since we deal with transfer characteristics in this chapter.

under the presence of the above disturbances, the part of the state-predictive LQ-obs servo system in Fig. 3.3 is described by

$$\left\{\begin{array}{rcl} \dfrac{dx(t)}{dt} &=& (A+BF_0)x(t)+BF_0e^{AT_L}D\varepsilon(t)+BF_0\varepsilon_f(t) \\ & & +Bv(t)+d_x(t)-BF_0e^{AT_L}Ld_y(t-T_L) \\ y(t) &=& Cx(t-T_L)+d_y(t-T_L) \\ \dfrac{d\varepsilon(t)}{dt} &=& \widehat{A}\varepsilon(t)-Md_x(t-T_L)-Kd_y(t-T_L) \\ \dfrac{d\varepsilon_f(t)}{dt} &=& A\varepsilon_f(t)-d_x(t)+e^{AT_L}d_x(t-T_L). \end{array}\right. \tag{3.32}$$

Let $v_{d\infty}^{\rm obs}$ be the (constant) value of v that achieves $y \equiv r\ (=0)$ under the above disturbances, and let $x_{d\infty}$, $\varepsilon_{d\infty}$ and $\varepsilon_{fd\infty}$ be the steady-state values of x, ε and ε_f, respectively, for the input $v \equiv v_{d\infty}^{\rm obs}$ (the superscript '$^{\rm obs}$' stands for the value for the system incorporating an observer, by which we make distinction from the value for the system with state feedback to be discussed in Section 3.4, and the subscript '$_d$' stands for the value under the presence of the step disturbances d_x and d_y). We call $v_{d\infty}^{\rm obs}$ the steady-state *disturbance compensation input*. The values of $v_{d\infty}^{\rm obs}$, $x_{d\infty}$, $\varepsilon_{d\infty}$ and $\varepsilon_{fd\infty}$ can be obtained from (3.32) as[2]

$$\begin{bmatrix} x_{d\infty} \\ v_{d\infty}^{\rm obs} \\ \varepsilon_{d\infty} \\ \varepsilon_{fd\infty} \end{bmatrix} = \begin{bmatrix} A+BF_0 & B & BF_0e^{AT_L}D & BF_0 \\ C & 0 & 0 & 0 \\ 0 & 0 & \widehat{A} & 0 \\ 0 & 0 & 0 & A \end{bmatrix}^{-1} \times \begin{bmatrix} -\{d_x-BF_0e^{AT_L}Ld_y\} \\ -d_y \\ Md_x+Kd_y \\ (I-e^{AT_L})d_x \end{bmatrix}$$

$$= \begin{bmatrix} -(A+BF_0)^{-1}\{(I+BH_0\Gamma)d_x-BH_0d_y\} \\ [\{H_0\Gamma+F_0\int_0^{T_L}e^{A\sigma}d\sigma-F_0e^{AT_L}D\widehat{A}^{-1}M\}d_x \\ \quad -(F_0e^{AT_L}D\widehat{A}^{-1}K-F_0e^{AT_L}L+H_0)d_y] \\ \widehat{A}^{-1}(Md_x+Kd_y) \\ -\int_0^{T_L}e^{A\sigma}d\sigma d_x \end{bmatrix}. \tag{3.33}$$

[2]Nonsingularity of A is assumed in (3.33) for simplicity. Even if A is singular, our key result (3.47) below can be justified by similar arguments, and so the results of this chapter remain true.

The state equation of the predictive integral compensator (3.22) is described by

$$\begin{aligned}\frac{d\widehat{\bar{w}}(t)}{dt} &= -Cx(t) - C\int_0^{T_L} e^{A\sigma}d\sigma D\widehat{A}\varepsilon(t) - C\varepsilon_f(t) \\ &\quad +C\int_0^{T_L} e^{A\sigma}d\sigma LCd_x(t-T_L) \\ &\quad -\{I - C\int_0^{T_L} e^{A\sigma}d\sigma DK\}d_y(t-T_L). \end{aligned} \tag{3.34}$$

Therefore, from (3.32) and (3.34), the state equation for the whole system of Fig. 3.3 with disturbances is given by

$$\begin{aligned}\frac{d}{dt}\begin{bmatrix} x(t) \\ \widehat{\bar{w}}(t) \\ \varepsilon(t) \\ \varepsilon_f(t) \end{bmatrix} &= \begin{bmatrix} A+BF_0 & 0 & BF_0e^{AT_L}D & BF_0 \\ -C & 0 & -C\int_0^{T_L} e^{A\sigma}d\sigma D\widehat{A} & -C \\ 0 & 0 & \widehat{A} & 0 \\ 0 & 0 & 0 & A \end{bmatrix}\begin{bmatrix} x(t) \\ \widehat{\bar{w}}(t) \\ \varepsilon(t) \\ \varepsilon_f(t) \end{bmatrix} \\ &\quad + \begin{bmatrix} B \\ 0 \\ 0 \\ 0 \end{bmatrix} v(t) \\ &\quad + \begin{bmatrix} d_x(t) - BF_0e^{AT_L}Ld_y(t-T_L) \\ [C\int_0^{T_L} e^{A\sigma}d\sigma LCd_x(t-T_L) \\ \quad -\{I - C\int_0^{T_L} e^{A\sigma}d\sigma DK\}d_y(t-T_L)] \\ -Md_x(t-T_L) - Kd_y(t-T_L) \\ -d_x(t) + e^{AT_L}d_x(t-T_L) \end{bmatrix}. \end{aligned} \tag{3.35}$$

From (3.17), (3.24) and (3.31), we have

$$\widehat{\bar{x}}(t|t-T_L) = x(t) + e^{AT_L}D\varepsilon(t) + \varepsilon_f(t) - e^{AT_L}Ld_y(t-T_L). \tag{3.36}$$

In view of this and (3.26), we apply the transformation

$$\begin{bmatrix} x(t) \\ \zeta(t) \\ \varepsilon(t) \\ \varepsilon_f(t) \end{bmatrix} = \begin{bmatrix} I & 0 & 0 & 0 \\ \Gamma & I & \Gamma e^{AT_L}D & \Gamma \\ 0 & 0 & I & 0 \\ 0 & 0 & 0 & I \end{bmatrix}\begin{bmatrix} x(t) \\ \widehat{\bar{w}}(t) \\ \varepsilon(t) \\ \varepsilon_f(t) \end{bmatrix} - \begin{bmatrix} 0 \\ \Gamma e^{AT_L}Ld_y(t-T_L) \\ 0 \\ 0 \end{bmatrix} \tag{3.37}$$

to the system (3.35). Then, we obtain

$$\begin{bmatrix} \dot{x}(t) \\ \dot{\zeta}(t) \\ \dot{\varepsilon}(t) \\ \dot{\varepsilon}_f(t) \end{bmatrix} = \begin{bmatrix} A+BF_0 & 0 & BF_0e^{AT_L}D & BF_0 \\ 0 & 0 & \Omega_{T_L} & 0 \\ 0 & 0 & \widehat{A} & 0 \\ 0 & 0 & 0 & A \end{bmatrix}\begin{bmatrix} x(t) \\ \zeta(t) \\ \varepsilon(t) \\ \varepsilon_f(t) \end{bmatrix} + \begin{bmatrix} B \\ \Psi \\ 0 \\ 0 \end{bmatrix} v(t)$$

$$+\begin{bmatrix} d_x(t) - BF_0 e^{AT_L} L d_y(t-T_L) \\ [\{-\Gamma e^{AT_L} + C\int_0^{T_L} e^{A\sigma}d\sigma\} LC d_x(t-T_L) \\ \quad +\{-\Psi F_0 e^{AT_L} L - I + C\int_0^{T_L} e^{A\sigma}d\sigma DK \\ \qquad -\Gamma e^{AT_L} DK\} d_y(t-T_L)] \\ -M d_x(t-T_L) - K d_y(t-T_L) \\ -d_x(t) + e^{AT_L} d_x(t-T_L) \end{bmatrix}, \tag{3.38}$$

where

$$\Psi := \Gamma B = -H_0^{-1}, \tag{3.39}$$

$$\Omega_{T_L} := \Psi F_0 e^{AT_L} D - C\int_0^{T_L} e^{A\sigma}d\sigma D\widehat{A} + \Gamma e^{AT_L} D\widehat{A}. \tag{3.40}$$

3.2.2 Evaluation of disturbance responses via the error system for disturbances

In the following, we assume that the closed-loop system had reached the steady state for the step disturbances d'_x and d'_y by $t = -0$, and that the disturbances changed into d_x and d_y at $t = 0$. Since the effect of the disturbances d_x and d_y can be observed from $y(t)$ only after $t = T_L$, the control action for these disturbances can be taken only after $t = T_L$. This implies that the behavior of the system for $0 \le t < T_L$ is completely the same as that of the state-predictive LQ-obs servo system with $v \equiv v^{\mathrm{obs}}_{d'\infty}$, where $v^{\mathrm{obs}}_{d'\infty}$ is defined as $v^{\mathrm{obs}}_{d\infty}$ with d_x, d_y given by (3.33) replaced by d'_x, d'_y (i.e., the behavior for $0 \le t < T_L$ is independent of the gain G). Hence, we consider only $t \ge T_L$, and we regard the initial time as $t = T_L$.

Now, we assume that the value of ζ in the steady state $y \equiv 0$ is $\zeta^{\mathrm{obs}}_{d\infty}$. Defining the errors of x, ζ, v, ε and ε_f from their steady-state values under the disturbances as

$$\begin{aligned} \tilde{x}_d(t) &= x(t) - x_{d\infty}, \\ \tilde{\zeta}_d(t) &= \zeta(t) - \zeta^{\mathrm{obs}}_{d\infty}, \\ \tilde{v}_d(t) &= v(t) - v^{\mathrm{obs}}_{d\infty}, \\ \tilde{\varepsilon}_d(t) &= \varepsilon(t) - \varepsilon_{d\infty}, \\ \tilde{\varepsilon}_{fd}(t) &= \varepsilon_f(t) - \varepsilon_{fd\infty}, \end{aligned} \tag{3.41}$$

they satisfy

$$\frac{d}{dt}\begin{bmatrix} \tilde{x}_d(t) \\ \tilde{\zeta}_d(t) \\ \tilde{\varepsilon}_d(t) \\ \tilde{\varepsilon}_{fd}(t) \end{bmatrix} = \begin{bmatrix} A+BF_0 & 0 & BF_0 e^{AT_L} D & BF_0 \\ 0 & 0 & \Omega_{T_L} & 0 \\ 0 & 0 & \widehat{A} & 0 \\ 0 & 0 & 0 & A \end{bmatrix} \begin{bmatrix} \tilde{x}_d(t) \\ \tilde{\zeta}_d(t) \\ \tilde{\varepsilon}_d(t) \\ \tilde{\varepsilon}_{fd}(t) \end{bmatrix}$$

$$+\begin{bmatrix} B \\ \Psi \\ 0 \\ 0 \end{bmatrix} \tilde{v}_d(t) \qquad (t \geq T_L) \tag{3.42}$$

from (3.33) and (3.38).

Here, we consider the behavior of $\tilde{\varepsilon}_{fd}(t)$. From (3.33) with d_x replaced by d'_x,

$$\varepsilon_f(0) = A^{-1}(I - e^{AT_L})d'_x. \tag{3.43}$$

Since the transition equation of ε_f during $0 \leq t < T_L$ is described by

$$\frac{d\varepsilon_f(t)}{dt} = A\varepsilon_f - d_x + e^{AT_L}d'_x, \tag{3.44}$$

we have

$$\begin{aligned} \varepsilon_f(T_L) &= e^{AT_L}\varepsilon_f(0) + \int_0^{T_L} e^{A(T_L-\tau)}(-d_x + e^{AT_L}d'_x)d\tau \\ &= A^{-1}(I - e^{AT_L})d_x. \end{aligned} \tag{3.45}$$

From (3.33) and (3.45), the value of $\tilde{\varepsilon}_{fd}(T_L)$ becomes

$$\tilde{\varepsilon}_{fd}(T_L) = 0. \tag{3.46}$$

Since the transition of $\tilde{\varepsilon}_{fd}$ after $t = T_L$ is described by

$$\frac{d\tilde{\varepsilon}_{fd}(t)}{dt} = A\tilde{\varepsilon}_{fd}(t),$$

$\tilde{\varepsilon}_{fd}(t) = 0$ is always satisfied after $t = T_L$. This justifies our employing the state equation (3.42) with $\tilde{\varepsilon}_{fd}$ omitted:

$$\frac{d}{dt}\begin{bmatrix} \tilde{x}_d(t) \\ \tilde{\zeta}_d(t) \\ \tilde{\varepsilon}_d(t) \end{bmatrix} = \begin{bmatrix} A+BF_0 & 0 & BF_0D \\ 0 & 0 & \Omega_{T_L} \\ 0 & 0 & \widehat{A} \end{bmatrix}\begin{bmatrix} \tilde{x}_d(t) \\ \tilde{\zeta}_d(t) \\ \tilde{\varepsilon}_d(t) \end{bmatrix} + \begin{bmatrix} B \\ \Psi \\ 0 \end{bmatrix}\tilde{v}_d(t) \quad (t \geq T_L). \tag{3.47}$$

Here,

$$\left(\begin{bmatrix} A+BF_0 & 0 & BF_0e^{AT_L}D \\ 0 & 0 & \Omega_{T_L} \\ 0 & 0 & \widehat{A} \end{bmatrix}, \begin{bmatrix} B \\ \Psi \\ 0 \end{bmatrix}\right) \tag{3.48}$$

is stabilizable from stability of $A + BF_0$ and $\widehat{A}$ and from nonsingularity of Ψ.

In order to suppress the effect of the disturbances as quickly as possible, it seems reasonable to apply an optimal feedback to the above system. Recalling that the

purpose of this design step is to obtain the feedback gain G from ζ to v, we pose the performance index of the restricted form

$$\int_{T_L}^{\infty} \left(\begin{bmatrix} \tilde{x}_d(t) \\ \tilde{\zeta}_d(t) \\ \tilde{\varepsilon}_d(t) \end{bmatrix}^T \begin{bmatrix} 0 & 0 & 0 \\ 0 & \Xi & \Xi_{12} \\ 0 & \Xi_{12}^T & \Xi_{22} \end{bmatrix} \begin{bmatrix} \tilde{x}_d(t) \\ \tilde{\zeta}_d(t) \\ \tilde{\varepsilon}_d(t) \end{bmatrix} + \tilde{v}_d(t)^T \Theta \tilde{v}_d(t) \right) dt \tag{3.49}$$

with

$$\Xi > 0, \begin{bmatrix} \Xi & \Xi_{12} \\ \Xi_{12}^T & \Xi_{22} \end{bmatrix} \geq 0, \Theta > 0, \tag{3.50}$$

so that such a feedback follows as the optimal solution[3].

From $\Xi > 0$,

$$\left(\begin{bmatrix} 0 & 0 & 0 \\ 0 & \Xi & \Xi_{12} \\ 0 & \Xi_{12}^T & \Xi_{22} \end{bmatrix}^{1/2}, \begin{bmatrix} A+BF_0 & 0 & BF_0 e^{AT_L} D \\ 0 & 0 & \Omega_{T_L} \\ 0 & 0 & \widehat{A} \end{bmatrix} \right) \tag{3.51}$$

is detectable, and therefore, the Riccati equation associated with the optimal control problem for the above performance index has a unique positive semidefinite solution.

3.2.3 Optimal G

Assuming that the solution is given by

$$\Pi_z := \begin{bmatrix} 0 & 0 & 0 \\ 0 & \Pi & 0 \\ 0 & 0 & \Pi_{22} \end{bmatrix}, \tag{3.52}$$

the Riccati equation can be written as

$$\begin{bmatrix} 0 & 0 & 0 \\ 0 & \Pi & 0 \\ 0 & 0 & \Pi_{22} \end{bmatrix} \begin{bmatrix} A+BF_0 & 0 & BF_0 e^{AT_L} D \\ 0 & 0 & \Omega_{T_L} \\ 0 & 0 & \widehat{A} \end{bmatrix}$$
$$+ \begin{bmatrix} A+BF_0 & 0 & BF_0 e^{AT_L} D \\ 0 & 0 & \Omega_{T_L} \\ 0 & 0 & \widehat{A} \end{bmatrix}^T \begin{bmatrix} 0 & 0 & 0 \\ 0 & \Pi & 0 \\ 0 & 0 & \Pi_{22} \end{bmatrix}$$

[3]As will be clear later, in the design step we do not have to introduce this performance index actually; the purpose of the 'design procedure' here is in fact to show that the optimal G in the state feedback case is still optimal in the output feedback case. Thus, although the form of (3.49) may look restrictive, it is enough for this purpose.

$$
-\begin{bmatrix} 0 & 0 & 0 \\ 0 & \Pi & 0 \\ 0 & 0 & \Pi_{22} \end{bmatrix}
\begin{bmatrix} B \\ \Psi \\ 0 \end{bmatrix} \Theta^{-1} \begin{bmatrix} B \\ \Psi \\ 0 \end{bmatrix}^T
\begin{bmatrix} 0 & 0 & 0 \\ 0 & \Pi & 0 \\ 0 & 0 & \Pi_{22} \end{bmatrix}
$$
$$
+\begin{bmatrix} 0 & 0 & 0 \\ 0 & \Xi & \Xi_{12} \\ 0 & \Xi_{12}^T & \Xi_{22} \end{bmatrix} = 0. \tag{3.53}
$$

This is equivalent to the following three equations:

$$
-\Pi\Psi\Theta^{-1}\Psi^T\Pi + \Xi = 0, \tag{3.54}
$$
$$
\Pi\Omega_{T_L} + \Xi_{12} = 0, \tag{3.55}
$$
$$
\Pi_{22}\widehat{A} + \widehat{A}^T\Pi_{22} + \Xi_{22} = 0. \tag{3.56}
$$

Assuming that Π is the unique positive definite solution of the Riccati equation (3.54), (3.55) is satisfied if the weighting matrix Ξ_{12} is chosen as

$$
\Xi_{12} = -\Pi\Omega_{T_L}. \tag{3.57}
$$

If, in addition, Ξ_{22} is chosen so that

$$
\Xi_{22} \geq \Omega_{T_L}^T H_0^T \Theta H_0 \Omega_{T_L}, \tag{3.58}
$$

the positive semidefiniteness condition of (3.50) is satisfied, and $\Pi_{22} \geq 0$ is obtained as the solution of the Lyapunov equation (3.56). Therefore, by employing the weighting matrices satisfying (3.57) and (3.58), the optimal control law that minimizes the performance index (3.49) (and, at the same time, stabilizes the closed-loop system) is given by

$$
\begin{aligned}
\tilde{v}_d(t) &= -\Theta^{-1} \begin{bmatrix} B \\ \Psi \\ 0 \end{bmatrix}^T \begin{bmatrix} 0 & 0 & 0 \\ 0 & \Pi & 0 \\ 0 & 0 & \Pi_{22} \end{bmatrix} \begin{bmatrix} \tilde{x}_d(t) \\ \tilde{\zeta}_d(t) \\ \tilde{\epsilon}_d(t) \end{bmatrix} \\
&= -\Theta^{-1}\Psi^T\Pi\tilde{\zeta}_d(t) \\
&= G\tilde{\zeta}_d(t)
\end{aligned} \tag{3.59}
$$

with

$$
G = -\Theta^{-1}\Psi^T\Pi, \tag{3.60}
$$

where Π is the unique positive definite solution of the Riccati equation (3.54). Note that the above G is nonsingular and its value is independent of $\zeta_{d\infty}^{\text{obs}}$. From (3.41), the optimal v is given by

$$
v(t) = G\zeta(t) + v_{\text{ext}}, \tag{3.61}
$$

where

$$v_{\rm ext} := v_{d\infty}^{\rm obs} - G\zeta_{d\infty}^{\rm obs}. \tag{3.62}$$

Here, since G is nonsingular, the steady-state value $\zeta_{d\infty}^{\rm obs}$ has a one-to-one correspondence with $v_{\rm ext}$, and is conversely determined from $v_{\rm ext}$ as

$$\zeta_{d\infty}^{\rm obs} = G^{-1}(v_{d\infty}^{\rm obs} - v_{\rm ext}). \tag{3.63}$$

In other words, whatever $v_{\rm ext}$ one may choose, the control law (3.61) will be optimal under the performance index (3.49) among all the control laws that achieve the same steady-state value of ζ as that given by (3.63). Furthermore, robust tracking is ensured for any value of $v_{\rm ext}$. Therefore, any constant value may be assigned to $v_{\rm ext}$, but, for simplicity, we assume $v_{\rm ext} = 0$ in the following[4]. Then, the optimal v is given by

$$v(t) = G\zeta(t) \tag{3.64}$$

and thus we obtain the state-predictive PV-optimal LQI-obs servo system of the structure shown in Fig. 3.4. In this case, $\zeta_{d\infty}^{\rm obs}$ is given from (3.63) as

$$\zeta_{d\infty}^{\rm obs} = G^{-1}v_{d\infty}^{\rm obs}. \tag{3.65}$$

Note that the resulting G of (3.60) coincides with the optimal gain in the delay-free, state feedback case [19] (and the delay-free, output feedback case [20]). This implies that the optimal gain G (from the viewpoint of disturbance rejection) for the plant with no delay in state feedback case is also optimal for the plant with a pure delay incorporating an observer and a state prediction mechanism; the performance index (3.49) need not be introduced actually in the design procedure, and we may design the gains F_0, H_0 and G as the delay-free, state feedback case [19]. This fact itself is not surprising, but the argument given in this section is very important when we study an asymptotic property of disturbance responses in the following section.

We now summarize the features of the state-predictive PV-optimal LQI-obs servo system obtained in this section. Namely, in its design procedure, tracking characteristics for step references can be determined optimally by F_0 and H_0, and feedback characteristics for step disturbances (and modeling errors) can be determined also optimally by G without changing tracking characteristics. From this reason, it is called a state-predictive two-degree-of-freedom LQI servo system incorporating an observer, or simply a *state-predictive 2DOF-LQI-obs servo system*. Note that the structure of this system is nothing but the 2DOF-LQI-obs servo system in the delay-free, state feedback case [19] plus an observer and a prediction mechanism.

[4]The optimal value of $\zeta_{d\infty}^{\rm obs}$ (and therefore the optimal value of $v_{\rm ext}$) depends on the disturbances d_x and d_y. If no information about the disturbances is available, a suboptimal choice is $v_{\rm ext} = 0$. See [19] for details.

3.3 Structure of the state-predictive two-degree-of-freedom LQI servo system

Next, we show that the state-predictive 2DOF-LQI-obs servo system studied in the preceding section can be transformed into the state-predictive 2DOF servo system of Fig. 3.5. To show this, using (3.17), (3.28), (3.26), (3.15) and (3.22), we rewrite $u(t)$ of Fig. 3.4 given by (3.29) as

$$\begin{aligned}
u(t) &= (F_0+G\Gamma)\hat{\bar{x}}(t|t-T_L)+G\hat{\bar{w}}(t)+H_0r(t)\\
&= (F_0+G\Gamma)\{e^{AT_L}\hat{x}(t-T_L)+\int_{t-T_L}^{t}e^{A(t-\tau)}Bu(\tau)d\tau\}\\
&\quad +G\{w(t)-\int_{t-T_L}^{t}C\hat{\bar{x}}(\tau|t-T_L)d\tau\}+H_0r(t)\\
&= (F_0+G\Gamma)\{e^{AT_L}\hat{x}(t-T_L)+\int_{t-T_L}^{t}e^{A(t-\tau)}Bu(\tau)d\tau\}\\
&\quad +G[w(t)-\int_{t-T_L}^{t}C\{e^{A(\tau-t+T_L)}\hat{x}(t-T_L)\\
&\quad +\int_{t-T_L}^{\tau}e^{A(\tau-\sigma)}Bu(\sigma)d\sigma\}d\tau]+H_0r(t)\\
&= [G \quad F_0+G\Gamma]\left\{\begin{bmatrix} I & -\int_{t-T_L}^{t}Ce^{A(\tau-t+T_L)}d\tau \\ 0 & e^{AT_L}\end{bmatrix}\begin{bmatrix} w(t)\\ \hat{x}(t-T_L)\end{bmatrix}\right.\\
&\quad \left.+\begin{bmatrix} -\int_{t-T_L}^{t}C\int_{t-T_L}^{\tau}e^{A(\tau-\sigma)}Bu(\sigma)d\sigma d\tau \\ \int_{t-T_L}^{t}e^{A(t-\tau)}Bu(\tau)d\tau\end{bmatrix}\right\}+H_0r(t). \qquad (3.66)
\end{aligned}$$

As shown in Section 3.7, this equation can be further rewritten as

$$u(t)=F_a\left\{e^{A_aT_L}\begin{bmatrix} w(t)\\ \hat{x}(t-T_L)\end{bmatrix}+\int_{t-T_L}^{t}e^{A_a(t-\sigma)}B_au(\sigma)d\sigma\right\}+H_0r(t) \qquad (3.67)$$

with

$$\begin{aligned}
A_a &= \begin{bmatrix} 0 & -C\\ 0 & A\end{bmatrix},\\
B_a &= \begin{bmatrix} 0\\ B\end{bmatrix}, \qquad (3.68)\\
F_a &= \begin{bmatrix} G & F_0+G\Gamma\end{bmatrix}.
\end{aligned}$$

This implies that the state-predictive 2DOF-LQI-obs servo system of Fig. 3.4 is equivalent to the state-predictive servo system of Fig. 3.5 where

$$I_{\mathrm{I}} = \begin{bmatrix} I_m\\ 0\end{bmatrix},$$

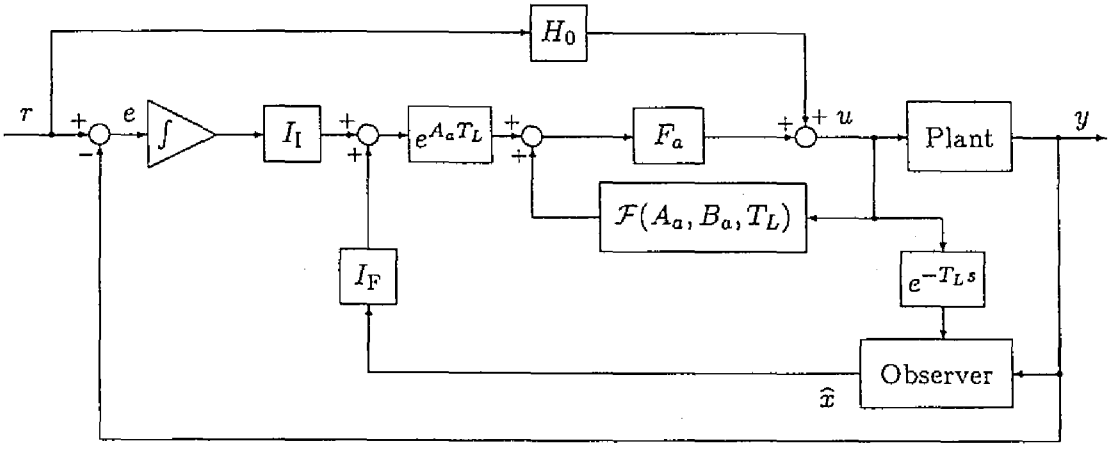

Fig. 3.5: Equivalent state-predictive servo system

$$I_{\rm F} = \begin{bmatrix} 0 \\ I_n \end{bmatrix}. \tag{3.69}$$

Note that the system of Fig. 3.5 with the feedforward path removed is nothing but the state-predictive servo system given in Chapter 2 (Fig. 2.4) with a particular form of F_a. This equivalent form might be easier to implement. Furthermore, in this equivalent form, we can directly apply the robust stability analysis method for state-predictive control systems, which will be given in Chapter 4, to analyze robust stability of our 2DOF-LQI-obs servo systems if the plant is an SISO system.

3.4 Relationship between the weighting matrices and disturbance rejection

It is shown in [19] and [20] that, in the delay-free case, disturbance rejection becomes quicker as the weighting matrix Ξ becomes larger (if Θ is fixed). In this section, we show that this is also the case in state-predictive 2DOF-LQI-obs servo systems, and, what is more important, that the asymptotic disturbance response for $\Xi \to \infty$ coincides with the response of the system shown in Fig. 3.6 for $t \geq T_L$. Note that the system of Fig. 3.6 is similar to the corresponding system in the delay-free, output feedback case [20] plus a prediction mechanism, but is actually slightly different. Also, recall that the response for $0 \leq t < T_L$ is independent of G, and thus is independent of Ξ. The latter fact is related to the optimal design of an observer discussed in the next section.

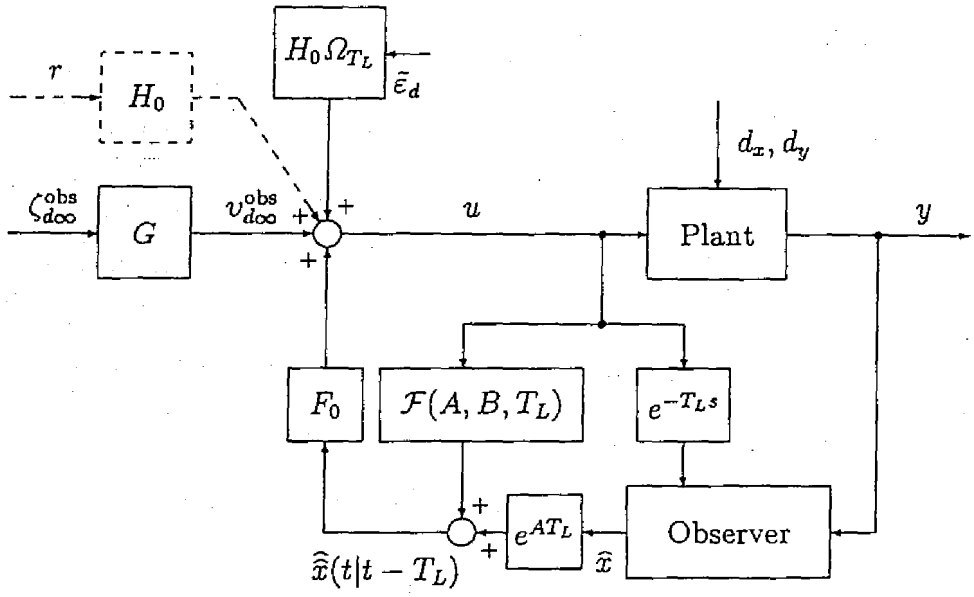

Fig. 3.6: State-predictive LQ-obs servo system with disturbance compensation input

3.4.1 Candidate for the asymptotic disturbance response and a fundamental relation

Now, as in (3.30), we consider the case where the plant is subject to the step disturbances d_x and d_y. Again, we assume that the closed-loop system had reached the steady state for the step disturbances d'_x and d'_y by $t = -0$, and that the disturbances changed to d_x and d_y at $t = 0$. Furthermore, by the reason stated in the preceding section, we regard the initial time as $t = T_L$ and consider the behavior of the system only after $t = T_L$. (Note that the behavior for $0 \leq t < T_L$ is affected neither by the observer parameters nor the gain G, and is the same as the state feedback case (with a delay) [13].) Then, for $t \geq T_L$, the state-predictive 2DOF-LQI-obs servo system

satisfies

$$\left\{\begin{array}{rcl}
\dfrac{dx_{\mathrm{LQI}}(t)}{dt} &=& Ax_{\mathrm{LQI}}(t)+Bu_{\mathrm{LQI}}(t)+d_x(t)\\
\dfrac{d\zeta(t)}{dt} &=& \Gamma\dfrac{dx_{\mathrm{LQI}}(t)}{dt}+\Gamma e^{AT_L}D\dfrac{d\varepsilon(t)}{dt}+\Gamma\dfrac{d\varepsilon_f(t)}{dt}\\
&& -Cx_{\mathrm{LQI}}(t)-C\int_0^{T_L}e^{A\sigma}d\sigma D\hat{A}\varepsilon(t)\\
&& -C\varepsilon_f(t)+C\int_0^{T_L}e^{A\sigma}d\sigma LCd_x(t-T_L)\\
&& -\{I-C\int_0^{T_L}e^{A\sigma}d\sigma DK\}d_y(t-T_L)\\
\dfrac{d\varepsilon(t)}{dt} &=& \hat{A}\varepsilon(t)-\{Md_x(t-T_L)+Kd_y(t-T_L)\}\\
\dfrac{d\varepsilon_f(t)}{dt} &=& A\varepsilon_f(t)-d_x(t)+e^{AT_L}d_x(t-T_L)\\
u_{\mathrm{LQI}}(t) &=& F_0x_{\mathrm{LQI}}(t)+F_0e^{AT_L}D\varepsilon(t)+F_0\varepsilon_f(t)\\
&& +G\zeta(t)-F_0e^{AT_L}Ld_y(t-T_L)\\
y_{\mathrm{LQI}}(t) &=& Cx_{\mathrm{LQI}}(t-T_L)+d_y(t-T_L),
\end{array}\right. \tag{3.70}$$

where the initial conditions are

$$\begin{aligned}
x_{\mathrm{LQI},T_L} &= x_{d'\infty}+\varepsilon_{fd'\infty}-\varepsilon_{fd\infty},\\
\varepsilon_{T_L} &= \varepsilon_{d'\infty},\\
\varepsilon_{f,T_L} &= \varepsilon_{fd\infty},\\
\zeta_{T_L} &= \zeta^{\mathrm{obs}}_{d'\infty}.
\end{aligned} \tag{3.71}$$

Here, $x_{d'\infty}$, $\varepsilon_{d'\infty}$, $\varepsilon_{fd'\infty}$ and $\zeta^{\mathrm{obs}}_{d'\infty}$ are respectively the steady-state values of x, ε, ε_f and ζ for d'_x and d'_y (defined as $x_{d\infty}$, $\varepsilon_{d\infty}$, $\varepsilon_{fd\infty}$ and $\zeta^{\mathrm{obs}}_{d\infty}$ of (3.33) and (3.65), respectively, with d_x, d_y replaced by d'_x, d'_y).

Remark 3.1 In general, from (3.26), (3.17) and (3.31), ζ is discontinuous at $t=T_L$, and we have $\zeta_{T_L}=\zeta^{\mathrm{obs}}_{d'\infty}-\Gamma e^{AT_L}L(d_y-d'_y)$. For full-order observers, however, $L=0$ is true and we have $\zeta_{T_L}=\zeta^{\mathrm{obs}}_{d'\infty}$. Furthermore, assuming that an observer with $L\neq 0$ is employed only when $d_y=d'_y$ is always true (i.e., the disturbance added to the plant output does not change at all), we again have $\zeta_{T_L}=\zeta^{\mathrm{obs}}_{d'\infty}$ and thus ζ becomes continuous at $t=T_L$. Disturbances are suppressed basically with high gain feedback, and therefore, the plant input u would exhibit an extremely large undesirable jump if ζ is discontinuous. In view of this fact, the above-mentioned assumption can be validated from practical point of view.

Extracting the part of the state-predictive LQ-obs servo system from this system (recall Fig. 3.3), and letting v be the sum of the constant value $v^{\mathrm{obs}}_{d\infty}$ $(=G\zeta^{\mathrm{obs}}_{d\infty})$ given by (3.33) and $H_0\Omega_{T_L}\tilde{\varepsilon}_d$ ($\tilde{\varepsilon}_d$ is defined by (3.41)), we obtain the following fictitious system

(see Fig. 3.6):

$$\left\{\begin{array}{rcl} \dfrac{dx_{\mathrm{LQ}}(t)}{dt} &=& Ax_{\mathrm{LQ}}(t)+Bu_{\mathrm{LQ}}(t)+d_x(t) \\ \dfrac{d\varepsilon(t)}{dt} &=& \widehat{A}\varepsilon(t)-\{Md_x(t-T_L)+Kd_y(t-T_L)\} \\ \dfrac{d\varepsilon_f(t)}{dt} &=& A\varepsilon_f(t)-d_x(t)+e^{AT_L}d_x(t-T_L) \\ u_{\mathrm{LQ}}(t) &=& F_0x_{\mathrm{LQ}}(t)+F_0e^{AT_L}D\varepsilon(t)+F_0\varepsilon_f(t)+G\zeta_{d\infty}^{\mathrm{obs}} \\ && -F_0e^{AT_L}Ld_y(t-T_L)+H_0\Omega_{T_L}\tilde{\varepsilon}_d(t) \\ y_{\mathrm{LQ}}(t) &=& Cx_{\mathrm{LQ}}(t-T_L)+d_y(t-T_L). \end{array}\right. \tag{3.72}$$

Here, in accordance with the assumptions that the system of Fig. 3.4 had reached the steady state by $t=-0$ and the fact that the change of the disturbances cannot be observed before $t=T_L$, we assume that the disturbance compensation input $v \equiv v_{d'\infty}^{\mathrm{obs}}$ had been applied for $t<T_L$. By this assumption, $u_{\mathrm{LQI}}(t)$ and $u_{\mathrm{LQ}}(t)$ coincide for $0 \le t < T_L$, and the initial condition for (3.72) is given by

$$\begin{array}{rcl} x_{\mathrm{LQ},T_L} &=& x_{d'\infty}+\varepsilon_{fd'\infty}-\varepsilon_{fd\infty}, \\ \varepsilon_{T_L} &=& \varepsilon_{d'\infty}, \\ \varepsilon_{f,T_L} &=& \varepsilon_{fd\infty}. \end{array} \tag{3.73}$$

Basically, what we show in this section is that, as the weighting matrix Ξ becomes larger, the disturbance responses of our state-predictive 2DOF-LQI-obs servo system monotonically tend to the responses of the (3.72). We call this system the *state-predictive LQ-obs servo system with disturbance compensation input*, whose implication is explained below.

First, observe that $H_0\Omega_{T_L}\tilde{\varepsilon}_d$ vanishes eventually. The remaining constant term of v, i.e. $v_{d\infty}^{\mathrm{obs}}$, is the input to cancel the disturbances d_x and d_y for $t \ge 0$ in the steady state. For quick disturbance rejection, it would be desirable if v tends to $v_{d\infty}^{\mathrm{obs}}$ instantaneously (and hence ζ tends to a constant value instantaneously, too). In the output feedback case, however, this cannot occur, in general, because of the estimation delay of an observer. Actually, as implied by the arguments of [11], 'inevitable transient terms' reflecting the estimation delay arise in v and ζ (regardless of G) for almost all disturbances d_x and d_y, unless the observer is such that $\Omega_{T_L}=0$[5]. As seen from this,

[5]In the delay-free case, Fujisaki and Ikeda [11] studied only a full-order observer, but their arguments can be extended readily to the general observer (3.13), and to the case with a delay. Based on this consideration, they proposed to employ an observer such that $\Omega_{T_L}=0$, if it exists. However, this is not such a choice that minimizes the performance deterioration *compared with the state feedback case*, because the *total* effect of the observer is not taken into account. See Subsection 3.4.4 for details.

the term $H_0\Omega_{T_L}\tilde{\varepsilon}_d$ represents the inevitable transient term in v caused by an observer. Combining the above considerations, we can see that the state-predictive LQ-obs servo system with disturbance compensation input (3.72) represents the system that gives the *best possible disturbance responses under output feedback.*

From the above equations and from (3.27), (3.33), (3.39) and (3.28), the signals

$$\begin{aligned} \bar{x}_d(t) &:= x_{\mathrm{LQI}}(t) - x_{\mathrm{LQ}}(t), \\ \bar{\zeta}_d^{\mathrm{temp}}(t) &:= \zeta(t) - \zeta_{d\infty}^{\mathrm{obs}}, \\ \bar{u}_d(t) &:= u_{\mathrm{LQI}}(t) - u_{\mathrm{LQ}}(t), \\ \bar{y}_d(t) &:= y_{\mathrm{LQI}}(t) - y_{\mathrm{LQ}}(t) \end{aligned} \tag{3.74}$$

satisfy the following equations (here, the symbol '$-$' stands for the difference between the two corresponding signals in the systems (3.70) and (3.72)):

$$\left\{ \begin{aligned} \frac{d}{dt}\begin{bmatrix} \bar{x}_d \\ \bar{\zeta}_d^{\mathrm{temp}} \\ \tilde{\varepsilon}_d \\ \tilde{\varepsilon}_{fd} \end{bmatrix} &= \begin{bmatrix} A & 0 & 0 & 0 \\ -\Psi F_0 & 0 & 0 & 0 \\ 0 & 0 & \widehat{A} & 0 \\ 0 & 0 & 0 & A \end{bmatrix} \begin{bmatrix} \bar{x}_d \\ \bar{\zeta}_d^{\mathrm{temp}} \\ \tilde{\varepsilon}_d \\ \tilde{\varepsilon}_{fd} \end{bmatrix} + \begin{bmatrix} B \\ \Psi \\ 0 \\ 0 \end{bmatrix} \bar{u}_d(t) \\ \bar{y}_d(t) &= C\bar{x}_d(t), \end{aligned} \right. \tag{3.75}$$

$$\bar{u}_d(t) = F_0\bar{x}_d(t) + G\bar{\zeta}_d^{\mathrm{temp}}(t) - H_0\Omega_{T_L}\tilde{\varepsilon}_d(t). \tag{3.76}$$

From (3.71) and (3.73), the initial conditions are

$$\begin{aligned} \bar{x}_{d,T_L} &= 0, \\ \tilde{\varepsilon}_{d,T_L} &= \varepsilon_{d'\infty} - \varepsilon_{d\infty}, \\ \tilde{\varepsilon}_{fd,T_L} &= 0, \\ \bar{\zeta}_{d,T_L}^{\mathrm{temp}} &= \zeta_{d'\infty}^{\mathrm{obs}} - \zeta_{d\infty}^{\mathrm{obs}}. \end{aligned} \tag{3.77}$$

It should be noted here that in the argument of disturbance rejection, we may assume that the matrix F_0 has already been determined. Therefore, (3.75) represents a fixed system, which, together with the 'control law' (3.76) describes the fundamental relation that $\bar{x}_d$, $\bar{\zeta}_d^{\mathrm{temp}}$, $\tilde{\varepsilon}_d$, $\tilde{\varepsilon}_{fd}$, $\bar{u}_d$ and $\bar{y}_d$ satisfy.

From $\tilde{\varepsilon}_{fd,T_L} = 0$ in (3.77),

$$\tilde{\varepsilon}_{fd}(t) = 0 \tag{3.78}$$

is always satisfied after $t = T_L$ as in the preceding section. This also justifies our employing the state equation (3.75) with $\tilde{\varepsilon}_{fd}(t)$ omitted:

$$\frac{d}{dt}\begin{bmatrix} \bar{x}_d \\ \bar{\zeta}_d^{\mathrm{temp}} \\ \tilde{\varepsilon}_d \end{bmatrix} = \begin{bmatrix} A & 0 & 0 \\ -\Psi F_0 & 0 & 0 \\ 0 & 0 & \widehat{A} \end{bmatrix} \begin{bmatrix} \bar{x}_d \\ \bar{\zeta}_d^{\mathrm{temp}} \\ \tilde{\varepsilon}_d \end{bmatrix} + \begin{bmatrix} B \\ \Psi \\ 0 \end{bmatrix} \bar{u}_d(t). \tag{3.79}$$

3.4.2 Evaluation of the difference of the signals via an interpretation of the fundamental relation

As shown in Section 3.7, we can interpret the 'control law' (3.76) as the optimal control input for the 'plant' (3.75) with respect to the performance index

$$
\begin{aligned}
J \;=\; \int_{T_L}^{\infty} \Bigg(& \begin{bmatrix} \bar{x}_d \\ \bar{\zeta}_d^{\mathrm{temp}} \\ \tilde{\varepsilon}_d \end{bmatrix}^T \begin{bmatrix} I & 0 & 0 \\ 0 & I & -G^{-1}H_0\Omega_{T_L} \\ 0 & 0 & I \end{bmatrix}^T \\
& \times \begin{bmatrix} Q & 0 & 0 \\ 0 & \Xi & \bar{\Xi}'_{12} \\ 0 & \bar{\Xi}'^{T}_{12} & \bar{\Xi}'_{22} \end{bmatrix} \begin{bmatrix} I & 0 & 0 \\ 0 & I & -G^{-1}H_0\Omega_{T_L} \\ 0 & 0 & I \end{bmatrix} \begin{bmatrix} \bar{x}_d \\ \bar{\zeta}_d^{\mathrm{temp}} \\ \tilde{\varepsilon}_d \end{bmatrix} + \bar{u}_d^T \Theta \bar{u}_d \Bigg) dt,
\end{aligned}
\tag{3.80}
$$

where $\bar{\Xi}'_{12}$ and $\bar{\Xi}'_{22}$ are the weighting matrices given by (3.168) and (3.175) in Subsection 3.7.2. (Here, we assumed $\Theta = R$ for the sake of simplicity in the description. The following discussion can be extended to the case of $\Theta \geq R$ as in [19].) The positive semidefinite stabilizing solution of the Riccati equation associated with the above optimal control problem is given by

$$
\begin{bmatrix} I & 0 & 0 \\ 0 & I & -G^{-1}H_0\Omega_{T_L} \\ 0 & 0 & I \end{bmatrix}^T \begin{bmatrix} P & 0 & 0 \\ 0 & \Pi & 0 \\ 0 & 0 & \bar{\Pi}'_{22} \end{bmatrix} \begin{bmatrix} I & 0 & 0 \\ 0 & I & -G^{-1}H_0\Omega_{T_L} \\ 0 & 0 & I \end{bmatrix}, \tag{3.81}
$$

where $\bar{\Pi}'_{22}$ is the positive semidefinite solution of the Lyapunov equation (3.172) in Subsection 3.7.2. Therefore, the optimal value of the performance index (3.80) is given from (3.77) and (3.81) as

$$
\begin{aligned}
J \;=\; & \begin{bmatrix} \bar{x}_{d0} \\ \bar{\zeta}_{d0}^{\mathrm{temp}} \\ \tilde{\varepsilon}_{d0} \end{bmatrix}^T \begin{bmatrix} I & 0 & 0 \\ 0 & I & -G^{-1}H_0\Omega_{T_L} \\ 0 & 0 & I \end{bmatrix}^T \begin{bmatrix} P & 0 & 0 \\ 0 & \Pi & 0 \\ 0 & 0 & \bar{\Pi}'_{22} \end{bmatrix} \\
& \times \begin{bmatrix} I & 0 & 0 \\ 0 & I & -G^{-1}H_0\Omega_{T_L} \\ 0 & 0 & I \end{bmatrix} \begin{bmatrix} \bar{x}_{d0} \\ \bar{\zeta}_{d0}^{\mathrm{temp}} \\ \tilde{\varepsilon}_{d0} \end{bmatrix} \\
= \; & \{(\zeta_{d'\infty}^{\mathrm{obs}} - \zeta_{d\infty}^{\mathrm{obs}}) - G^{-1}H_0\Omega_{T_L}(\varepsilon_{d'\infty} - \varepsilon_{d\infty})\}^T \\
& \times \Pi \{(\zeta_{d'\infty}^{\mathrm{obs}} - \zeta_{d\infty}^{\mathrm{obs}}) - G^{-1}H_0\Omega_{T_L}(\varepsilon_{d'\infty} - \varepsilon_{d\infty})\} \\
& + (\varepsilon_{d'\infty} - \varepsilon_{d\infty})^T \bar{\Pi}'_{22}(\varepsilon_{d'\infty} - \varepsilon_{d\infty}).
\end{aligned}
\tag{3.82}
$$

From (3.33), (3.39), (3.60) and (3.65), we have

$$\begin{aligned}
&\varepsilon_{d'\infty} - \varepsilon_{d\infty} = \widehat{A}^{-1}\{M(d'_x - d_x) + K(d'_y - d_y)\}, \\
&\zeta^{\rm obs}_{d'\infty} - \zeta^{\rm obs}_{d\infty} - G^{-1}H_0\Omega_{T_L}(\varepsilon_{d'\infty} - \varepsilon_{d\infty}) = \Pi^{-1}\delta_{T_L},
\end{aligned} \tag{3.83}$$

where

$$\begin{aligned}
\delta_{T_L} \;:=\; & H_0^T\Theta[-H_0(\Gamma e^{AT_L} - C\int_0^{T_L} e^{A\sigma}d\sigma)LC(d'_x - d_x) \\
& -\{H_0(\Gamma e^{AT_L} - C\int_0^{T_L} e^{A\sigma}d\sigma)DK + H_0 - F_0e^{AT_L}L\}(d'_y - d_y)],
\end{aligned} \tag{3.84}$$

is independent of the weighting matrices $\Xi, \bar{\Xi}'_{12}, \bar{\Xi}'_{22}$, and therefore, the optimal value of the performance index (3.80) is given by

$$J = \delta_{T_L}^T\Pi^{-1}\delta_{T_L} + (\varepsilon_{d'\infty} - \varepsilon_{d\infty})^T\bar{\Pi}'_{22}(\varepsilon_{d'\infty} - \varepsilon_{d\infty}). \tag{3.85}$$

Note that (3.85) is the sum of a term proportional to Π^{-1} and a term proportional to $\bar{\Pi}'_{22}$.

From the above arguments, we can conclude that the responses of the systems (3.70) and (3.72) are closer if the value of (3.85) is smaller. This is the key in the arguments of the following subsection.

3.4.3 Role of the weighting matrix Ξ

In this subsection, we show that the response of the state-predictive 2DOF-LQI-obs servo system tends to that of the state-predictive LQ-obs servo system with disturbance compensation input as Ξ becomes larger. To this end, suppose that one designs the state-predictive 2DOF-LQI-obs servo systems using two different weighting matrices satisfying $\Xi_a < \Xi_b$, while Θ is fixed. From (3.54), the solutions for the corresponding Riccati equations satisfy $\Pi_a < \Pi_b$ [31]. Assuming $\bar{\Xi}'_{22}$ is fixed, $\bar{\Pi}'_{22}$ is also fixed (see (3.172) in Subsection 3.7.2[6]). From these inequalities, we obtain the following relations (the inequality sign between (3.87) and (3.88) comes from (3.80), (3.85) and $\Pi_a < \Pi_b$, and the inequality signs between (3.86) and (3.87), and between (3.88) and (3.89) come from $\Xi_b > \Xi_a$).

$$\int_{T_L}^{\infty}\left(\begin{bmatrix}\bar{x}_{da}\\ \bar{\zeta}_{da}\\ \tilde{\varepsilon}_d\end{bmatrix}^T\begin{bmatrix}Q & 0 & 0\\ 0 & \Xi_b & \bar{\Xi}'_{12}\\ 0 & \bar{\Xi}'^{\,T}_{12} & \bar{\Xi}'_{22}\end{bmatrix}\begin{bmatrix}\bar{x}_{da}\\ \bar{\zeta}_{da}\\ \tilde{\varepsilon}_d\end{bmatrix} + \bar{u}_{da}^T\Theta\bar{u}_{da}\right)dt \tag{3.86}$$

[6]The condition (3.175) for $\bar{\Xi}'_{22}$ is dependent on Ξ, but if this condition is satisfied for $\Xi = \Xi_a$, then this is also satisfied for $\Xi = \Xi_b$. Therefore, it is assumed that $\bar{\Xi}'_{22}$ is fixed to a matrix which satisfies the condition (3.175) for $\Xi = \Xi_a$.

$$> \int_{T_L}^{\infty} \left(\begin{bmatrix} \bar{x}_{da} \\ \bar{\zeta}_{da} \\ \tilde{\varepsilon}_d \end{bmatrix}^T \begin{bmatrix} Q & 0 & 0 \\ 0 & \Xi_a & \bar{\Xi}'_{12} \\ 0 & \bar{\Xi}'^T_{12} & \bar{\Xi}'_{22} \end{bmatrix} \begin{bmatrix} \bar{x}_{da} \\ \bar{\zeta}_{da} \\ \tilde{\varepsilon}_d \end{bmatrix} + \bar{u}_{da}^T \Theta \bar{u}_{da} \right) dt \qquad (3.87)$$

$$> \int_{T_L}^{\infty} \left(\begin{bmatrix} \bar{x}_{db} \\ \bar{\zeta}_{db} \\ \tilde{\varepsilon}_d \end{bmatrix}^T \begin{bmatrix} Q & 0 & 0 \\ 0 & \Xi_b & \bar{\Xi}'_{12} \\ 0 & \bar{\Xi}'^T_{12} & \bar{\Xi}'_{22} \end{bmatrix} \begin{bmatrix} \bar{x}_{db} \\ \bar{\zeta}_{db} \\ \tilde{\varepsilon}_d \end{bmatrix} + \bar{u}_{db}^T \Theta \bar{u}_{db} \right) dt \qquad (3.88)$$

$$> \int_{T_L}^{\infty} \left(\begin{bmatrix} \bar{x}_{db} \\ \bar{\zeta}_{db} \\ \tilde{\varepsilon}_d \end{bmatrix}^T \begin{bmatrix} Q & 0 & 0 \\ 0 & \Xi_a & \bar{\Xi}'_{12} \\ 0 & \bar{\Xi}'^T_{12} & \bar{\Xi}'_{22} \end{bmatrix} \begin{bmatrix} \bar{x}_{db} \\ \bar{\zeta}_{db} \\ \tilde{\varepsilon}_d \end{bmatrix} + \bar{u}_{db}^T \Theta \bar{u}_{db} \right) dt \qquad (3.89)$$

In the above, $\bar{x}_{da}$, $\bar{\zeta}_{da}$, $\bar{u}_{da}$, $\bar{x}_{db}$, $\bar{\zeta}_{db}$, $\bar{u}_{db}$, respectively, denote $\bar{x}_d$, $\bar{\zeta}_d$, which is defined by

$$\begin{aligned} \bar{\zeta}_d &:= \bar{\zeta}_d^{\text{temp}} - G^{-1} H_0 \Omega_{T_L} \tilde{\varepsilon}_d \\ &= \zeta - \zeta_{\text{LQ}} \quad (\zeta_{\text{LQ}} := \zeta_{d\infty}^{\text{obs}} + G^{-1} H_0 \Omega_{T_L} \tilde{\varepsilon}_d), \end{aligned} \qquad (3.90)$$

and $\bar{u}_d$ for the case where Ξ_a and Ξ_b are employed in the design procedure (note that the behavior of $\tilde{\varepsilon}_d$ is independent of the weighting matrices Ξ_a and Ξ_b). The implication of the ζ_{LQ} in the above equation would be clear if we look at Fig. 3.6.

It follows from (3.86) and (3.88), or from (3.87) and (3.89), that the quadratic-integral of $\bar{x}_d$, $\bar{\zeta}_d$, $\tilde{\varepsilon}_d$ and $\bar{u}_d$ becomes smaller under the same performance index (and so disturbance rejection becomes quicker) as Ξ becomes larger. As a special case, let us consider the case where the solutions of the Riccati equations satisfy $\Pi_b = \alpha \Pi_a$ ($\alpha > 1$). The corresponding weighting matrices Ξ_a and Ξ_b are related by

$$\Xi_b = \alpha^2 \Xi_a \ (> \Xi_a), \qquad (3.91)$$

and therefore (3.86)–(3.89) are satisfied. This means that if we determine Π as the solution of the Riccati equation (3.54) for some Ξ and then multiply it by a scalar $\alpha (> 1)$ and determine G from (3.60) (this is equivalent to simply multiplying the original gain G by α), disturbance rejection becomes quicker. Moreover, by letting α tend to infinity, the first term of the right hand side of (3.85) tends to 0 with the order of α^{-1}. On the other hand, we can choose $\bar{\Xi}'_{22}$, which was fixed in the above argument, proportionally to α^{-2} (see (3.175) in Subsection 3.7.2). Therefore, it follows that $\bar{\Pi}'_{22}$ can be made small proportionally to α^{-2} (see (3.172) in Subsection 3.7.2). Since $\tilde{\varepsilon}_{d0} = \varepsilon_{d'\infty} - \varepsilon_{d\infty}$ is independent of the weighting matrix Ξ, the second term of the right hand side of (3.85) also tends to 0 with the order of α^{-2} by letting α tend to infinity.

The above arguments can be summarized as follows. Regardless of the observer parameters, disturbance rejection of the state-predictive 2DOF-LQI-obs servo system becomes quicker as the weighting matrix Ξ becomes larger, and the responses of x_{LQI}, ζ, u_{LQI} and y_{LQI} tend to the responses of x_{LQ}, ζ_{LQ} (this signal in turn tends to the step signal $\zeta_{d\infty}^{\mathrm{obs}}$ because G becomes larger as Ξ becomes larger), u_{LQ} and y_{LQ} of the state-predictive LQ-obs servo system with the disturbance compensation input. The scalar α retains the function as a tuning parameter as in the delay-free, state feedback case [19].

3.4.4 Performance deterioration by an observer

Now, let us consider the implication of the state-predictive LQ-obs servo system with disturbance compensation input (Fig. 3.6). In view of (3.33), (3.31), (3.40) and (3.41), it can be transformed into the system of Fig. 3.7, where

$$v_{d\infty}^{\mathrm{state}} = (H_0\Gamma - F_0\int_0^{T_L} e^{A\sigma}d\sigma)d_x - H_0 d_y \tag{3.92}$$

is the disturbance compensation input for the state-predictive LQ servo system with state feedback. In the state feedback case, the asymptotic response of the state-predictive 2DOF-LQI servo system for $\Xi \to \infty$ tends to the response of the system of Fig. 3.7 with the signal $H_0(\Gamma e^{AT_L} - C\int_0^{T_L} e^{A\sigma}d\sigma)D\widehat{A}\tilde{\varepsilon}_d$ removed, as in the delay-free, output feedback case [20]. Therefore, we can conclude that the deterioration of disturbance rejection ability caused by the introduction of an observer is represented by the arising of the additional signal $H_0(\Gamma e^{AT_L} - C\int_0^{T_L} e^{A\sigma}d\sigma)D\widehat{A}\tilde{\varepsilon}_d$. Based on this interpretation, the problem of designing the optimal observer that minimizes this deterioration under a suitable measure is studied in the next section.

3.5 Optimal observer for state-predictive two-degree-of-freedom LQI servo systems

3.5.1 Problem formulation

From the interpretations given at the end of the preceding section, we can conclude the following (see Subsection 3.7.3 for details). Namely, if we evaluate the response of the system of Fig. 3.6 under the performance index (3.6), the evaluation is larger than its optimal value (which is attained by the system of Fig. 3.7, as mentioned above) by

$$\Delta J = \int_{T_L}^{\infty} \eta(t)^{\mathrm{T}} R\eta(t)\, dt, \tag{3.93}$$

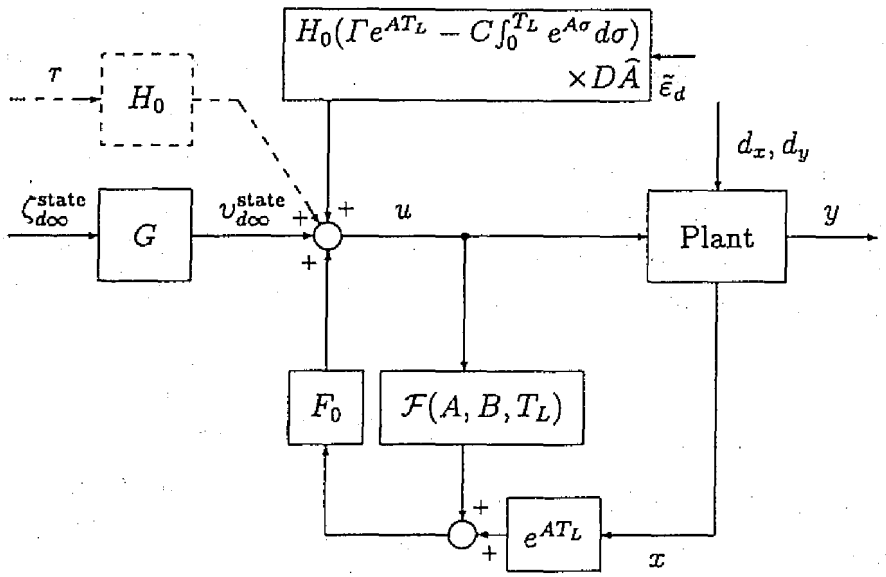

Fig. 3.7: Equivalent system to state-predictive LQ-obs servo system with disturbance compensation input

where

$$\eta(t) := H_0(\Gamma e^{AT_L} - C\int_0^{T_L} e^{A\sigma}d\sigma)D\widehat{A}\tilde{\varepsilon}_d(t) \tag{3.94}$$

In other words, the performance deterioration under the performance index (3.6) due to the introduction of an observer and the existence of step disturbances is given by this ΔJ, where η is given by (3.94). Clearly, the value of ΔJ is dependent on the observer parameters. In this section, assuming that statistical properties of the step disturbances d_x and d_y are known, we derive an optimal observer that minimizes the expectation of the performance deterioration ΔJ.

To formulate our problem, let us define

$$\delta_x := d_x - d_x', \quad \delta_y := d_y - d_y'. \tag{3.95}$$

Then, from (3.38) and (3.94), we can rewrite (3.93) as

$$\begin{aligned}\Delta J &= \int_{T_L}^{\infty} \left(H_0(\Gamma e^{AT_L} - C\int_0^{T_L} e^{A\sigma}d\sigma)De^{\widehat{A}t}(M\delta_x + K\delta_y)\right)^T \\ &\quad \times R\left(H_0(\Gamma e^{AT_L} - C\int_0^{T_L} e^{A\sigma}d\sigma)De^{\widehat{A}t}(M\delta_x + K\delta_y)\right)dt \\ &= (M\delta_x + K\delta_y)^T \int_{T_L}^{\infty} e^{\widehat{A}^T t}Ve^{\widehat{A}t}\,dt\,(M\delta_x + K\delta_y),\end{aligned} \tag{3.96}$$

where

$$V := D^T(\Gamma e^{AT_L} - C\int_0^{T_L} e^{A\sigma}d\sigma)^T H_0^T R H_0(\Gamma e^{AT_L} - C\int_0^{T_L} e^{A\sigma}d\sigma)D\ (\geq 0). \tag{3.97}$$

Therefore, letting X be the solution to the Lyapunov equation

$$X\widehat{A} + \widehat{A}^T X + V = 0, \tag{3.98}$$

we obtain

$$\Delta J = \begin{bmatrix} \delta_x \\ \delta_y \end{bmatrix}^T \begin{bmatrix} M & K \end{bmatrix}^T X \begin{bmatrix} M & K \end{bmatrix} \begin{bmatrix} \delta_x \\ \delta_y \end{bmatrix}. \tag{3.99}$$

Thus, the expectation of ΔJ is given by

$$E[\Delta J] = \text{trace}\left(X \begin{bmatrix} M & K \end{bmatrix} W \begin{bmatrix} M & K \end{bmatrix}^T \right) \tag{3.100}$$

where W is given by

$$W := E\left[\begin{bmatrix} \delta_x \\ \delta_y \end{bmatrix} \begin{bmatrix} \delta_x \\ \delta_y \end{bmatrix}^T \right]. \tag{3.101}$$

We assume in this section that

$$W =: \begin{bmatrix} W_{xx} & W_{xy} \\ W_{xy}^T & W_{yy} \end{bmatrix} \tag{3.102}$$

is known[7]. Thus, our problem is to design an optimal observer that minimizes (3.100) for given W.

Note that (3.100) could be rewritten from (3.96) in a different form as

$$\begin{aligned} & E[\Delta J] \\ &= E\left[\text{trace}\left(V \int_{T_L}^{\infty} e^{\widehat{A}t} (M\delta_x + K\delta_y)(M\delta_x + K\delta_y)^T e^{\widehat{A}^T t}\, dt \right) \right] \\ &= \text{trace}\left(V \int_{T_L}^{\infty} e^{\widehat{A}t} \begin{bmatrix} M & K \end{bmatrix} W \begin{bmatrix} M & K \end{bmatrix}^T e^{\widehat{A}^T t}\, dt \right). \end{aligned} \tag{3.103}$$

3.5.2 Optimal full-order observer

For simplicity, we first consider the case of full-order observers. In this case, without loss of generality, we may assume

$$\widehat{A} = A + KC,$$

[7]Assuming that $[d_x^T\ d_y^T]^T$ and $[d_x'^T\ d_y'^T]^T$ are independent and have the identical statistical property, W is given by

$$W = 2E\left[\begin{bmatrix} d_x \\ d_y \end{bmatrix} \begin{bmatrix} d_x \\ d_y \end{bmatrix}^T \right].$$

$$\begin{aligned} \hat{B} &= B, \\ D &= I, \\ L &= 0, \\ M &= I. \end{aligned} \tag{3.104}$$

Therefore, our problem reduces to the following.

Problem 3.1 Given W, minimize

$$J_{\text{obs}} = \text{trace}\left(X \begin{bmatrix} I & K \end{bmatrix} W \begin{bmatrix} I & K \end{bmatrix}^T\right) \tag{3.105}$$

with respect to K subject to the stability constraint of $\hat{A} = A + KC$, where X is the solution of the Lyapunov equation

$$X(A+KC) + (A+KC)^T X + V = 0 \tag{3.106}$$

with

$$V = \left(\Gamma e^{AT_L} - C\int_0^{T_L} e^{A\sigma}d\sigma\right)^T H_0^T R H_0 \left(\Gamma e^{AT_L} - C\int_0^{T_L} e^{A\sigma}d\sigma\right). \tag{3.107}$$

This problem can be solved by a technique similar to that of [28] and [25] using the matrix minimum principle [5] in the following way.

We first introduce the Lagrange function

$$\begin{aligned} \phi(K,X,Y) &= \text{trace}\Big(X \begin{bmatrix} I & K \end{bmatrix} W \begin{bmatrix} I & K \end{bmatrix}^T \\ &\qquad +Y^T\{X(A+KC) + (A+KC)^T X + V\}\Big) \\ &= \text{trace}\Big(X\{W_{xx} + KW_{xy}^T + W_{xy}K^T + KW_{yy}K^T\} \\ &\qquad +Y^T\{X(A+KC) + (A+KC)^T X + V\}\Big) \end{aligned} \tag{3.108}$$

where $Y \in \mathbf{R}^{n\times n}$ is the Lagrange multiplier. Therefore, using the formulas given in [5], we obtain

$$\frac{\partial \phi}{\partial K} = X(2W_{xy} + 2KW_{yy} + YC^T + Y^T C^T), \tag{3.109}$$

$$\begin{aligned} \frac{\partial \phi}{\partial X} &= W_{xx} + W_{xy}K^T + KW_{xy}^T + KW_{yy}K^T \\ &\qquad +Y(A+KC)^T + (A+KC)Y, \end{aligned} \tag{3.110}$$

$$\frac{\partial \phi}{\partial Y} = X(A+KC) + (A+KC)^T X + V. \tag{3.111}$$

Therefore, we obtain the necessary conditions

$$X(2W_{xy} + 2KW_{yy} + YC^T + Y^T C^T) = 0, \tag{3.112}$$

$$W_{xx} + W_{xy}K^T + KW_{xy}^T + KW_{yy}K^T + Y(A+KC)^T + (A+KC)Y = 0, \tag{3.113}$$

$$X(A+KC) + (A+KC)^T X + V = 0. \tag{3.114}$$

(Naturally, (3.114) is nothing but (3.106).)

Now, we can derive the following theorem.

Theorem 3.1 Suppose that $W_{yy} > 0$ and $\left(A - W_{xy}W_{yy}^{-1}C, (W_{xx} - W_{xy}W_{yy}^{-1}W_{xy}^T)^{1/2}\right)$ is stabilizable. Define K_0 by

$$K_0 = -(YC^T + W_{xy})W_{yy}^{-1} \tag{3.115}$$

where Y is the unique positive semidefinite solution of the Riccati equation

$$YA^T + AY - (YC^T + W_{xy})W_{yy}^{-1}(CY + W_{xy}^T) + W_{xx} = 0. \tag{3.116}$$

Then,

(a) K_0 is an optimal observer gain.

(b) If $(V^{1/2}, A + K_0C)$ is observable, then K_0 is the unique optimal observer gain.

(c) The optimal value of J_{obs} is given by

$$J_{\text{obs},0} = \text{trace}(VY). \tag{3.117}$$

Remark 3.2 Needless to say, the resulting optimal observer is a Kalman filter.

Proof. Since (3.113) is a Lyapunov equation and since $W_{xx} + W_{xy}K^T + KW_{xy}^T + KW_{yy}K^T$ is symmetric, we have $Y = Y^T$. Therefore, (3.112) reduces to

$$X(W_{xy} + KW_{yy} + YC^T) = 0. \tag{3.118}$$

Here, assuming $\det X \neq 0$, we can solve the above equation for K uniquely as

$$K = -(YC^T + W_{xy})W_{yy}^{-1}. \tag{3.119}$$

Substituting this into (3.113), we obtain the Riccati equation (3.116). By the assumption of the theorem, this equation has a unique stabilizing solution, which is given as the unique positive semidefinite solution. Substituting this Y into (3.119), we obtain the observer gain (3.115). Let us denote by X_0 the solution of the Lyapunov equation (3.114) with K replaced by K_0:

$$X_0(A + K_0C) + (A + K_0C)^T X_0 + V = 0. \tag{3.120}$$

Note that $A+K_0C$ is stable by the assumptions of the theorem, and hence the solution X_0 is unique.

To show (a) (i.e., to show that K_0 is optimal), let K be any observer gain such that $A + KC$ is stable, and let

$$\Delta K := K - K_0. \tag{3.121}$$

A positive semidefinite solution X of the Lyapunov equation (3.106) corresponds to this K. Letting

$$\Delta X := X - X_0, \tag{3.122}$$

ΔX is symmetric and the Lyapunov equation (3.106) can be rewritten as

$$(X_0 + \Delta X)\{A + (K_0 + \Delta K)C\} + \{A + (K_0 + \Delta K)C\}^T(X_0 + \Delta X) + V = 0. \tag{3.123}$$

Subtracting the Lyapunov equation (3.120) from the above Lyapunov equation, we obtain

$$\begin{aligned} &\Delta X \Delta K C + C^T \Delta K^T \Delta X \\ &\quad = -\{\Delta X(A + K_0C) + X_0 \Delta K C + (A + K_0C)^T \Delta X + C^T \Delta K^T X_0\}. \end{aligned} \tag{3.124}$$

In a similar fashion, we can derive

$$\begin{aligned} J_{\text{obs}} - J_{\text{obs},0} \;=\; \text{trace}\,\big(&X_0\{-YC^T\Delta K^T - \Delta K C Y + \Delta K W_{yy} \Delta K^T\} \\ &+\Delta X\{W_{xx} + K_0 W_{xy}^T - YC^T K_0^T\} \\ &-Y\{\Delta X \Delta K C + C^T \Delta K^T \Delta X\} \\ &+\Delta X \Delta K W_{yy} \Delta K^T\big), \end{aligned} \tag{3.125}$$

where J_{obs} and $J_{\text{obs},0}$ respectively denote the values of (3.105) for K and K_0.

Substituting (3.124) into the above equation and rearranging the result using a property of a matrix trace and (3.116), we have

$$\begin{aligned} J_{\text{obs}} - J_{\text{obs},0} &= \text{trace}(X \Delta K W_{yy} \Delta K^T) \\ &= \text{trace}\,\big((X^{1/2}\Delta K) W_{yy} (X^{1/2}\Delta K)^T\big) \\ &\geq 0. \end{aligned} \tag{3.126}$$

This completes the proof of (a).

Next, let us prove (b). Suppose $J_{\rm obs} = J_{\rm obs,0}$. Then, from (3.126), we have

$$X\Delta K = 0. \tag{3.127}$$

Substituting this into (3.123), we readily obtain

$$X(A + K_0C) + (A + K_0C)^T X + V = 0. \tag{3.128}$$

Hence we have $X = X_0$ by (3.120), so that $X_0\Delta K = 0$ by (3.127). Now, if $(V^{1/2}, A + K_0C)$ is observable, then $X_0 > 0$ from (3.120). Thus, $\delta K = 0$ follows. This completes the proof of (b).

To prove (c), note that

$$Y\widehat{A}^T + \widehat{A}Y + \begin{bmatrix} I & K_0 \end{bmatrix} W \begin{bmatrix} I & K_0 \end{bmatrix}^T = 0 \quad (\widehat{A} = A + K_0C) \tag{3.129}$$

is true from (3.115) and (3.116). This implies

$$\int_{T_L}^{\infty} e^{\widehat{A}t} \begin{bmatrix} I & K_0 \end{bmatrix} W \begin{bmatrix} I & K_0 \end{bmatrix} e^{\widehat{A}^T t}\, dt = Y, \tag{3.130}$$

and hence we obtain (3.117) from (3.103). Q.E.D.

From the above theorem, the optimal observer gain K_0 is determined only by the plant (A and C) and the statistical property of disturbances (W_{xx}, W_{xy} and W_{yy}), and is independent of V. This means that K_0 is independent of the feedback gain F_0. In other words, it is independent of the weighting matrices Q and R that determine the nominal responses for step references, even though we formulated our problem as that of minimizing the deviations of the responses under the presence of disturbances from this nominal responses. Thus, separation property holds in our two-degree-of-freedom servo problem, as well as in the one-degree-of-freedom regulator problems such as the stochastic LQG problem [34] and the deterministic regulator problems [35], [30].

As for the one-degree-of-freedom deterministic problems dealt with in [35], [30] (i.e., the problems of designing full-order/reduced-order observers that are optimal with respect to the distribution of the initial state of the plant), one might wonder if the problem studied in this section were equivalent to their problems. However, this is not the case, because no optimal solution exists as a Kalman filter for their problems [30], which is in sharp contrast with our problem. Some more comments will be given about this point also in the following subsection.

3.5.3 Optimal reduced-order observer

In this subsection, we consider the case of reduced-order observers. Since $L \neq 0$, in general, for reduced-order observers, we assume the disturbances satisfy $\delta_y = d_y - d'_y = 0$ in this subsection for the reason mentioned in Remark 3.1 in Subsection 3.4.1. Note that

$$W_{xy} = 0, \quad W_{yy} = 0 \tag{3.131}$$

in this case.

For simplicity, let us consider the case of minimal-order observers. Also, without loss of generality, assume that

$$A = \begin{bmatrix} A_{11} & A_{12} \\ A_{21} & A_{22} \end{bmatrix}, \; B = \begin{bmatrix} B_1 \\ B_2 \end{bmatrix}, \; C = \begin{bmatrix} 0 & I_m \end{bmatrix}. \tag{3.132}$$

Note that (A_{21}, A_{11}) is detectable by the assumption that (C, A) is detectable. Now, by the canonical form of observers [30], minimal-order observers can be parameterized as

$$\begin{gathered} \hat{A} = A_{11} + NA_{21}, \quad \hat{B} = B_1 + NB_2, \\ K = -(A_{12} + NA_{22}) + (A_{11} + NA_{21})N, \\ D = \begin{bmatrix} I_{n-m} \\ 0 \end{bmatrix}, \quad L = \begin{bmatrix} -N \\ I_m \end{bmatrix}, \quad M = \begin{bmatrix} I_{n-m} & N \end{bmatrix}, \end{gathered} \tag{3.133}$$

where $N \in \mathbf{R}^{(n-m)\times m}$ is an arbitrary matrix such that $\hat{A}$ becomes stable. Thus, by (3.131), our problem reduces as follows.

Problem 3.2 Given W_{xx}, minimize

$$J_{\text{obs}} = \text{trace}\left(XMW_{xx}M^T\right) \tag{3.134}$$

with respect to N subject to the stability constraint of $\hat{A} = A_{11} + NA_{21}$, where X is the solution of the Lyapunov equation

$$X(A_{11} + NA_{21}) + (A_{11} + NA_{21})^T X + V = 0 \tag{3.135}$$

with V given by (3.97).

Now, let us partition W_{xx} in a compatible form with (3.132) as

$$W_{xx} =: \begin{bmatrix} W_{xx}^{11} & W_{xx}^{12} \\ W_{xx}^{12T} & W_{xx}^{22} \end{bmatrix}. \tag{3.136}$$

Then, in view of the form of M in (3.133), the following theorem follows readily from Theorem 3.1 by inspection of (3.105), (3.106) and (3.134), (3.135).

Theorem 3.2 Suppose that $W_{xx}^{22} > 0$ and $\left(A_{11} - W_{xx}^{12}(W_{xx}^{22})^{-1}A_{21}, \left(W_{xx}^{11} - W_{xx}^{12}(W_{xx}^{22})^{-1}W_{xx}^{12T}\right)^{1/2}\right)$ is stabilizable. Define N_0 by

$$N_0 = -\left(YA_{21}^T + W_{xx}^{12}\right)\left(W_{xx}^{22}\right)^{-1} \tag{3.137}$$

where Y is the unique positive semidefinite solution of the Riccati equation

$$YA_{11}^T + A_{11}Y - \left(YA_{21}^T + W_{xx}^{12}\right)\left(W_{xx}^{22}\right)^{-1}\left(A_{21}Y + W_{xx}^{12T}\right) + W_{xx}^{11} = 0. \tag{3.138}$$

Then,

(a) N_0 is an optimal solution.

(b) If $(V^{1/2}, A_{11} + N_0A_{21})$ is observable, then N_0 is the unique optimal solution.

(c) The optimal value of J_{obs} is given by

$$J_{\text{obs},0} = \text{trace}(VY). \tag{3.139}$$

The above theorem shows the design method of a minimal-order observer that is optimal with respect to disturbance rejection, under the assumption that the step disturbance d_y does not change at all (i.e., $d_y = d_y'$). Comparing this design method with that of the optimal minimal-order observer with respect to the distribution of the initial state of the plant [35], [30], we can see that our design method is nothing but theirs with the covariance matrix of the initial state of the plant set to $W_{xx} = E[\delta_x\delta_x^T]$. One might intuitively regard this as a natural consequence from the fact that step disturbances could be dealt with as deviations of the initial state of the plant (by shifting the equilibrium point of the plant in accordance with the step disturbances). However, the situation is not that simple. The following facts demonstrate the intrinsic difference between our problem and theirs.

(a) The covariance matrix associated with the equivalent initial state of the plant that corresponds to the step disturbance d_x does not coincide with $E[d_xd_x^T]$.

(b) In the optimal observer with respect to the distribution of the initial state of the plant, the initial state $q(T_L)$ of the observer can be set to an arbitrary value, and is actually a design parameter. However, in our optimal observer design with respect to disturbance rejection, $q(T_L)$ depends on the observer parameters to be determined, and cannot be adjusted. (Cf. (3.38).)

As explained above, our problem is essentially different from the problems studied in [35], [30], but a similar argument to that of [30] can be applied to show that the optimal value (3.139) is actually the optimal value that is attainable by a full-order/ reduced-order observer (rather than merely by a minimal-order observer), and that the optimal value (3.117) for the full-order observer case tends to (3.139) as $W_{yy} \to 0$.

3.5.4 Loop transfer recovery and perfect suppression of disturbances

In this subsection, we consider the special case where the step disturbances satisfy the matching condition $d_x, d'_x \in \mathrm{Im}(B)$, $d_y = d'_y = 0$, and show that the optimal observers of this case have a close connection with the technique of loop transfer recovery [9], [43]. Also, we discuss the possibility of perfect suppression of such step disturbances. Note that the matching condition implies

$$W_{xx} = B\widehat{W}_x B^T,\ W_{xy} = 0,\ W_{yy} = 0, \tag{3.140}$$

where $\widehat{W}_x$ is a positive semidefinite matrix. In the following, we assume $\widehat{W}_x > 0$ for simplicity.

Full-order observer case In the full-order observer case, we assumed $W_{yy} > 0$ in Subsection 3.5.2. However, (3.140) does not satisfy this requirement. To avoid this difficulty, instead of (3.140), we employ

$$W_{xx} = B\widehat{W}_x B^T,\ W_{xy} = 0,\ W_{yy} = \widehat{W}_y/\rho^2, \tag{3.141}$$

where $\widehat{W}_y$ is an arbitrary positive definite matrix and ρ (> 0) is a scalar. By letting $\rho \to \infty$, we can recover (3.140). When the plant is a minimum phase system, letting $\rho \to \infty$ has been studied in [1] in a different context, and from their results, we can conclude that our optimal observer achieves loop transfer recovery asymptotically as $\rho \to \infty$ at the plant input u. At the same time, the limiting observer for $\rho \to \infty$ enables us to achieve perfect suppression of the step disturbances by letting $\Xi \to \infty$ (which results $G \to \infty$). This can be shown as follows.

Under (3.141), the Riccati equation (3.116) reduces to

$$YA^T + AY - YC^T(\widehat{W}_y/\rho^2)^{-1}CY + B\widehat{W}_x B^T = 0. \tag{3.142}$$

From the well-know result about cheap control [27], [23], $Y \to 0$ as $\rho \to \infty$ if and only if the plant (C, A, B) is a minimum phase system. By (3.117), $J_{\mathrm{obs},0} \to 0$ follows

from $Y \to 0$, which implies that the deterioration of disturbance rejection ability can be made arbitrarily small by making ρ large enough. Since perfect suppression of step disturbances is achieved in the state feedback case by letting $\Xi \to \infty$ if the matching condition is satisfied [19], we can conclude that perfect suppression of step disturbances (in the sense of expectation) is possible also in the output feedback case if and only if the plant is a minimum phase system.

Minimal-order observer case In the minimal-order observer case, W_{xx} can be expressed as

$$W_{xx} = \begin{bmatrix} W_{xx}^{11} & W_{xx}^{12} \\ W_{xx}^{12T} & W_{xx}^{22} \end{bmatrix} = \begin{bmatrix} B_1 \widehat{W}_x B_1^T & B_1 \widehat{W}_x B_2^T \\ B_2 \widehat{W}_x B_1^T & B_2 \widehat{W}_x B_2^T \end{bmatrix}. \tag{3.143}$$

We assume $\det B_2 \neq 0$ so that the assumption $W_{xx}^{22} > 0$ is satisfied. Then, we can easily verify

$$W_{xx}^{11} - W_{xx}^{12} \left(W_{xx}^{22}\right)^{-1} W_{xx}^{12T} = 0. \tag{3.144}$$

From this, it is easy to see that the Riccati equation (3.138) has a solution $Y = 0$. In order for this to be a stabilizing solution, $A_{11} - W_{xx}^{12} (W_{xx}^{22})^{-1} A_{21}$ should be stable. This happens to be the case if and only if the plant is a minimum phase system. To show this, note that

$$W_{xx}^{12} \left(W_{xx}^{22}\right)^{-1} = B_1 B_2^{-1} \tag{3.145}$$

from (3.143). Therefore, we have

$$\det \left(sI - \left(A_{11} - W_{xx}^{12} \left(W_{xx}^{22}\right)^{-1} A_{21} \right) \right) \neq 0 \quad (\mathrm{Re}(s) \geq 0) \tag{3.146}$$

if and only if

$$\det \left(sI - \left(A_{11} - B_1 B_2^{-1} A_{21} \right) \right) \neq 0 \quad (\mathrm{Re}(s) \geq 0) \tag{3.147}$$

if and only if

$$\det \left[\begin{array}{c:c} sI - \begin{bmatrix} A_{11} & A_{12} \\ A_{21} & A_{22} \end{bmatrix} & \begin{bmatrix} B_1 \\ B_2 \end{bmatrix} \\ \hdashline \begin{bmatrix} 0 & I \end{bmatrix} & 0 \end{array} \right] \neq 0 \quad (\mathrm{Re}(s) \geq 0). \tag{3.148}$$

Now, when $Y = 0$ is a stabilizing solution, the optimal N_0 is given by

$$\begin{aligned} N_0 &= -W_{xx}^{12} \left(W_{xx}^{22}\right)^{-1} \\ &= -B_1 B_2^{-1}. \end{aligned} \tag{3.149}$$

This implies that the optimal minimal-order observer has the parameter

$$\hat{B} = 0, \tag{3.150}$$

or in other words, the optimal minimal-order observer is an unknown-input observer [26]. Therefore, by a well-known property of unknown-input observers, it achieves loop transfer recovery at the plant input completely (rather than asymptotically). At the same time, since $Y = 0$, we have $J_{\mathrm{obs},0} = 0$ from (3.139). This means that perfect suppression of step disturbances (in the sense of expectation) is possible by letting $\Xi \to \infty$ if and only if the plant is a minimum phase system with $\det B_2 \neq 0$. Note that the condition $\det B_2 \neq 0$ is equivalent to the condition that the plant has the maximum number of zeros (i.e., $n - m$ zeros) [7].

3.6 Example

In this section, we give a numerical example to illustrate the results of this chapter. All the simulations in this section were done under zero initial conditions of state variables.

Example 3.1 We consider the unstable plant given by

$$A = \begin{bmatrix} 0 & 2 \\ 1 & -1 \end{bmatrix}, \quad B = \begin{bmatrix} 1 \\ 1 \end{bmatrix}, \quad C = \begin{bmatrix} 0 & 1 \end{bmatrix}, \quad T_L = 1.$$

For this plant, we design a state-predictive 2DOF-LQI-obs servo system with a full-order observer using the weighting matrices

$$Q = \mathrm{diag}\,(0, 1), \quad R = 0.3,$$

for the response for step references, and

$$\Xi = 15\alpha^2, \quad \Theta = R,$$

where $\alpha(\geq 1)$ is a scalar, whose nominal value is 1, for the response for step disturbances.

We consider the case with the step disturbances

$$d_x = \begin{bmatrix} 0.4 \\ 0.2 \end{bmatrix}, \quad d_y = 0.1.$$

We choose the following observer gain:

$$K = \begin{bmatrix} -12.5 \\ -5.5 \end{bmatrix}.$$

K is determined to set the poles of the observer at -3, -3.5 so that the real part of the observer poles are smaller than the real part of the poles of the closed-loop system with state feedback (-1, -2.61, -2.71).

The response for the step reference of the state-predictive 2DOF-LQI-obs servo system is as shown in Fig. 3.8. (Note that the response for the step reference does not depend on either the feedback gain G (or α) nor the parameters of the observer.) The disturbance response of the state-predictive 2DOF-LQI-obs servo system for the nominal value of α is as shown in Fig. 3.9(a) with a solid line, while a dashed line shows the response of the state-predictive LQ-obs servo system with disturbance compensation input. In this case, by making the tuning parameter α larger, disturbance responses become quicker as shown in Fig. 3.9(b) and (c), and the disturbance response of our state-predictive 2DOF-LQI-obs servo system tends to that of the state-predictive LQ-obs servo system with disturbance compensation input.

Example 3.2 Next, we consider the stable, minimum phase plant given by

$$A = \begin{bmatrix} 0 & -2 \\ 1 & -3 \end{bmatrix}, \quad B = \begin{bmatrix} 1.2 \\ 1 \end{bmatrix}, \quad C = \begin{bmatrix} 0 & 1 \end{bmatrix}, \quad T_L = 1.$$

For this plant, we design a state-predictive 2DOF-LQI-obs servo system with a minimal-order observer using the weighting matrices

$$Q = \mathrm{diag}\,(0, 1), \quad R = 0.3,$$

for the response for step references, and

$$\Xi = 15\alpha^2, \quad \Theta = R,$$

where $\alpha(\geq 1)$ is a scalar, whose nominal value is 1, for the response for step disturbances.

We consider the case with the step disturbances

$$d_x = \begin{bmatrix} 0.6 \\ 0.5 \end{bmatrix}, \quad d_y = 0.$$

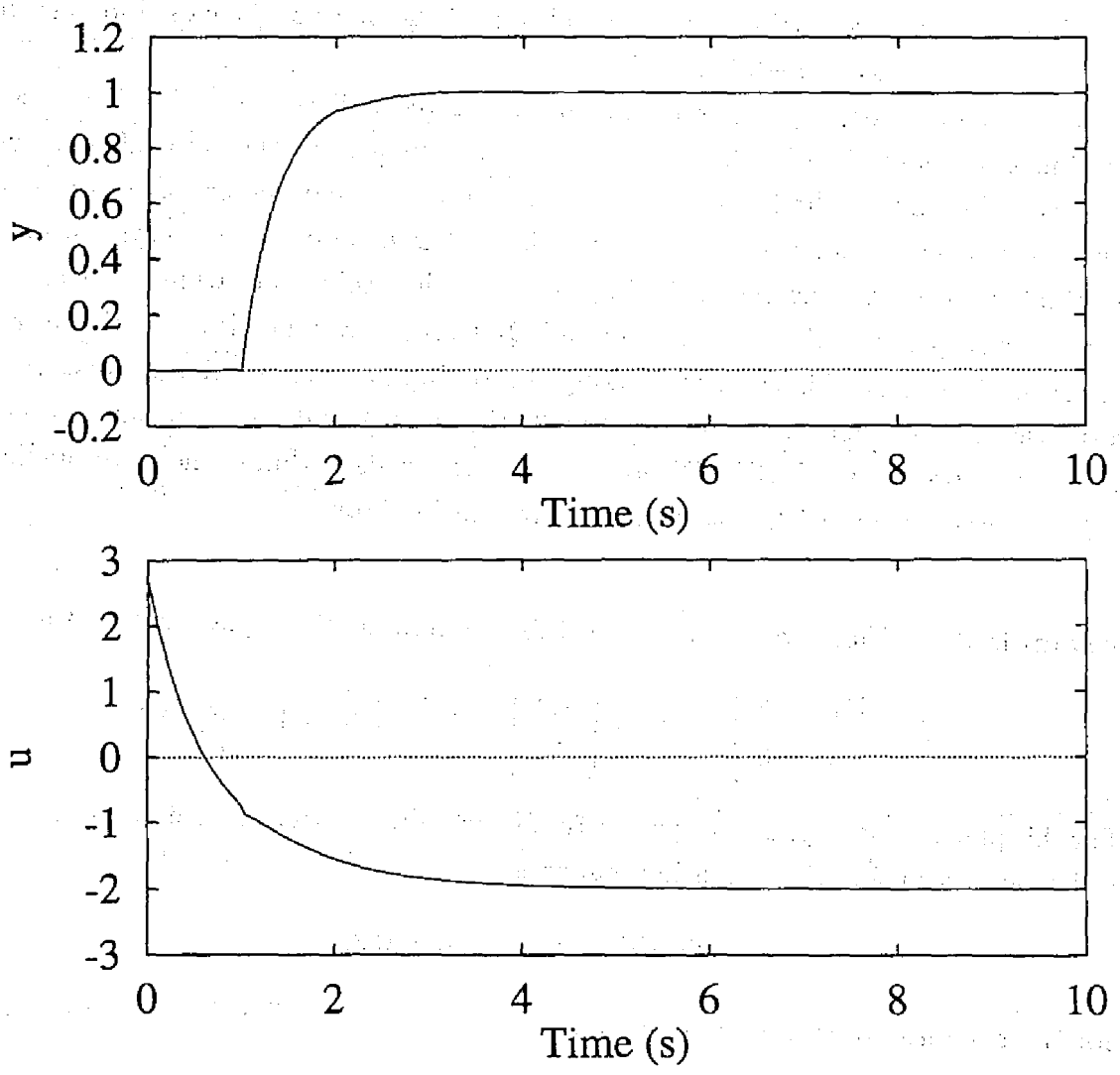

Fig. 3.8: Responses of the state-predictive 2DOF-LQI-obs servo systems for a step reference

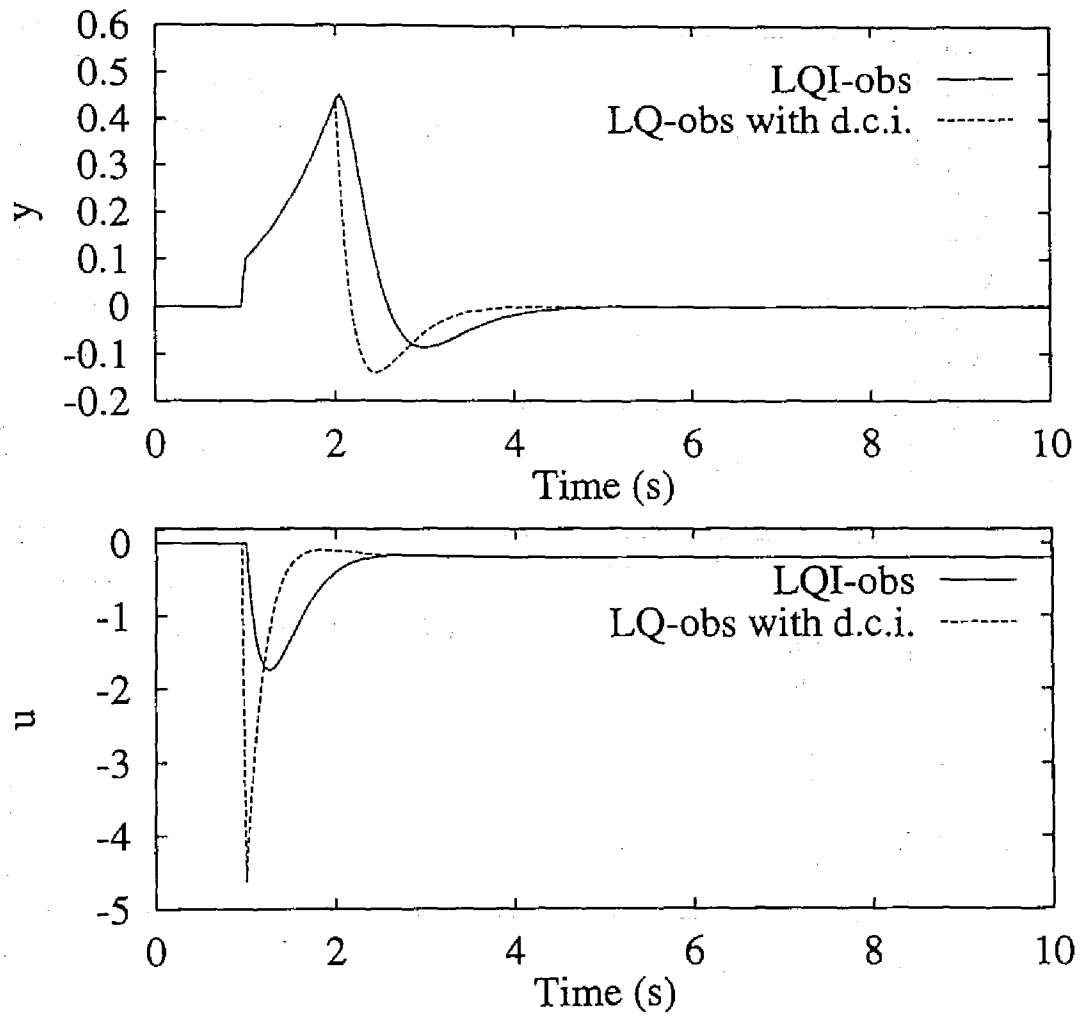
0.6
0.5
0.4
0.3
0.2
0.1
0
-0.1
-0.2
y
LQI-obs
LQ-obs with d.c.i.
0
2
4
6
8
10
Time (s)
0
-1
-2
-3
-4
-5
u
LQI-obs
LQ-obs with d.c.i.
0
2
4
6
8
10
Time (s)

(a) $\alpha^2 = 1$

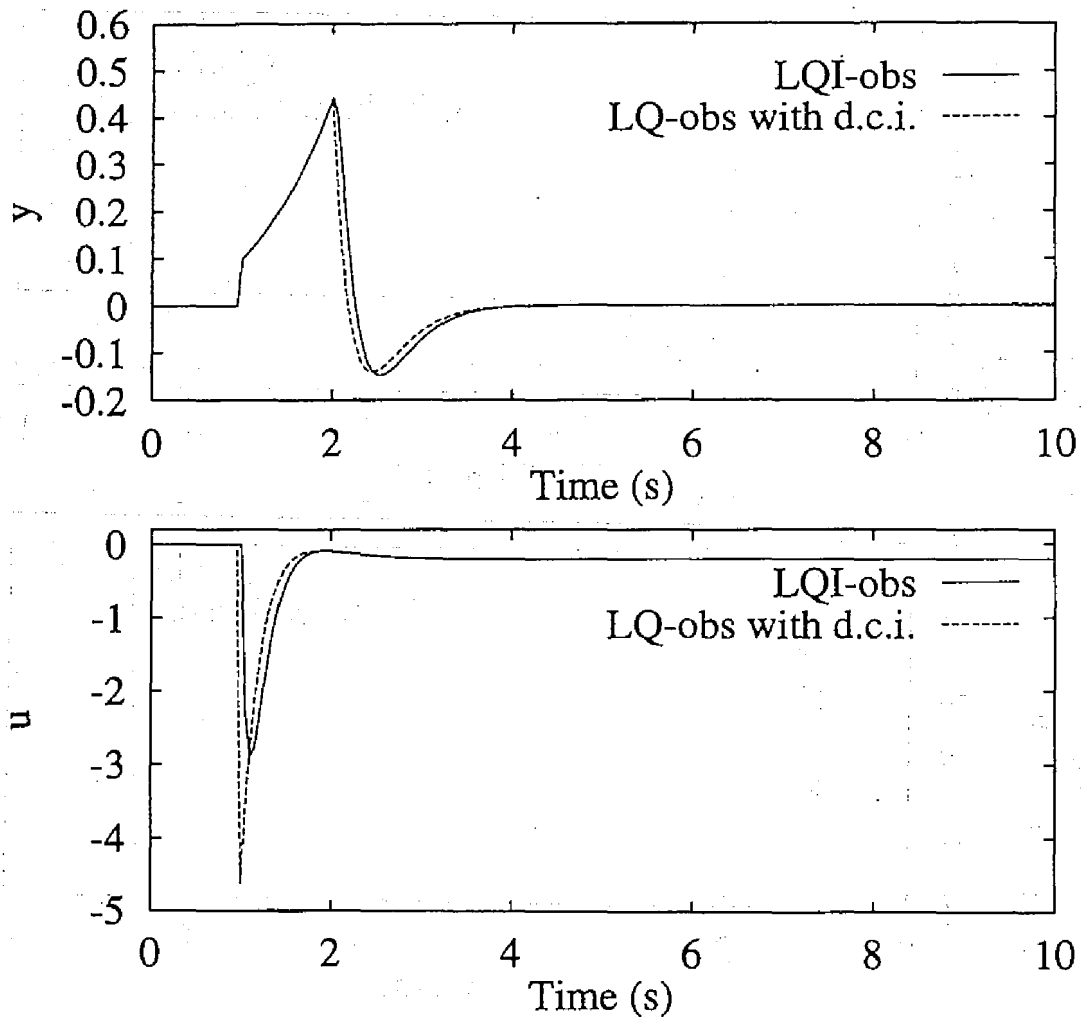
0.6
0.5
0.4
0.3
0.2
0.1
0
-0.1
-0.2
y
LQI-obs
LQ-obs with d.c.i.
0
2
4
6
8
10
Time (s)
0
-1
-2
-3
-4
-5
u
LQI-obs
LQ-obs with d.c.i.
0
2
4
6
8
10
Time (s)

(b) $\alpha^2 = 30$

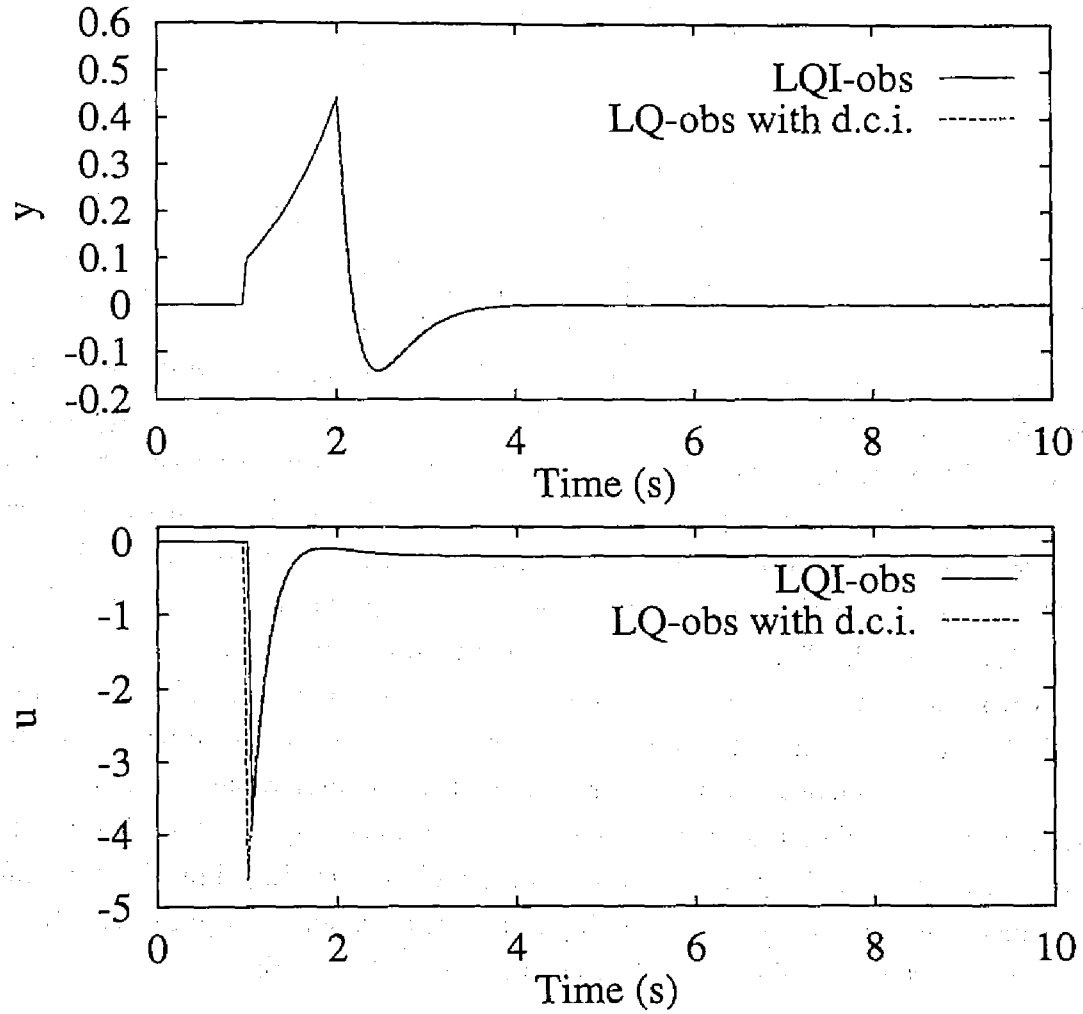

(c) $\alpha^2 = 1000$

Fig. 3.9: Disturbance responses of the state-predictive 2DOF-LQI-obs servo systems ($\alpha^2 = 1, 30, 1000$)

Note that these disturbances satisfy the matching condition. We choose the following two observers:

Observer 1:

$$\widehat{A}_1 = -1.2, \quad \widehat{B}_1 = 0, \quad K_1 = -0.16$$
$$D_1 = \begin{bmatrix} 1 \\ 0 \end{bmatrix}, \quad L_1 = \begin{bmatrix} 1.2 \\ 1 \end{bmatrix}.$$

and

Observer 2:

$$\widehat{A}_2 = -3, \quad \widehat{B}_2 = -1.8, \quad K_2 = 2$$
$$D_2 = \begin{bmatrix} 1 \\ 0 \end{bmatrix}, \quad L_2 = \begin{bmatrix} 3 \\ 1 \end{bmatrix}$$

The parameters of Observer 1 are determined by the design method described in Section 3.5, i.e., Observer 1 is an optimal minimal-order observer for the above disturbances, and the parameters of Observer 2 are determined to set the pole of the observer at $s = -3$, so that the real part of the observer pole is smaller than the real part of the poles of the closed-loop system with state feedback $(-1.11, -2.66, -2.86)$.

The response for the step reference of the state-predictive 2DOF-LQI-obs servo system is as shown in Fig. 3.10. The disturbance response of the state-predictive 2DOF-LQI servo system incorporating Observer 1 for the nominal value of α is as shown in Fig. 3.11 with a solid line, while the disturbance response of the state-predictive 2DOF-LQI servo system incorporating Observer 2 for the nominal value of α is as shown in Fig. 3.11 with a dashed line. Comparing the disturbance response for Observer 1 with that for Observer 2, the peak of the output y and the settling time are not different very much, but the maximum of the input u of the system incorporating Observer 1 is suppressed down to about two thirds as large as that of the system incorporating Observer 2.

Furthermore, the disturbance response of our system with Observer 1 coincides with that of 2DOF-LQI servo system with state feedback shown in Fig. 3.12, namely, it achieves loop transfer recovery at the plant input as mentioned in Section 3.5.

3.7 Details of derivations

3.7.1 Derivation of (3.67)

In this subsection, (3.67) will be derived from (3.66).

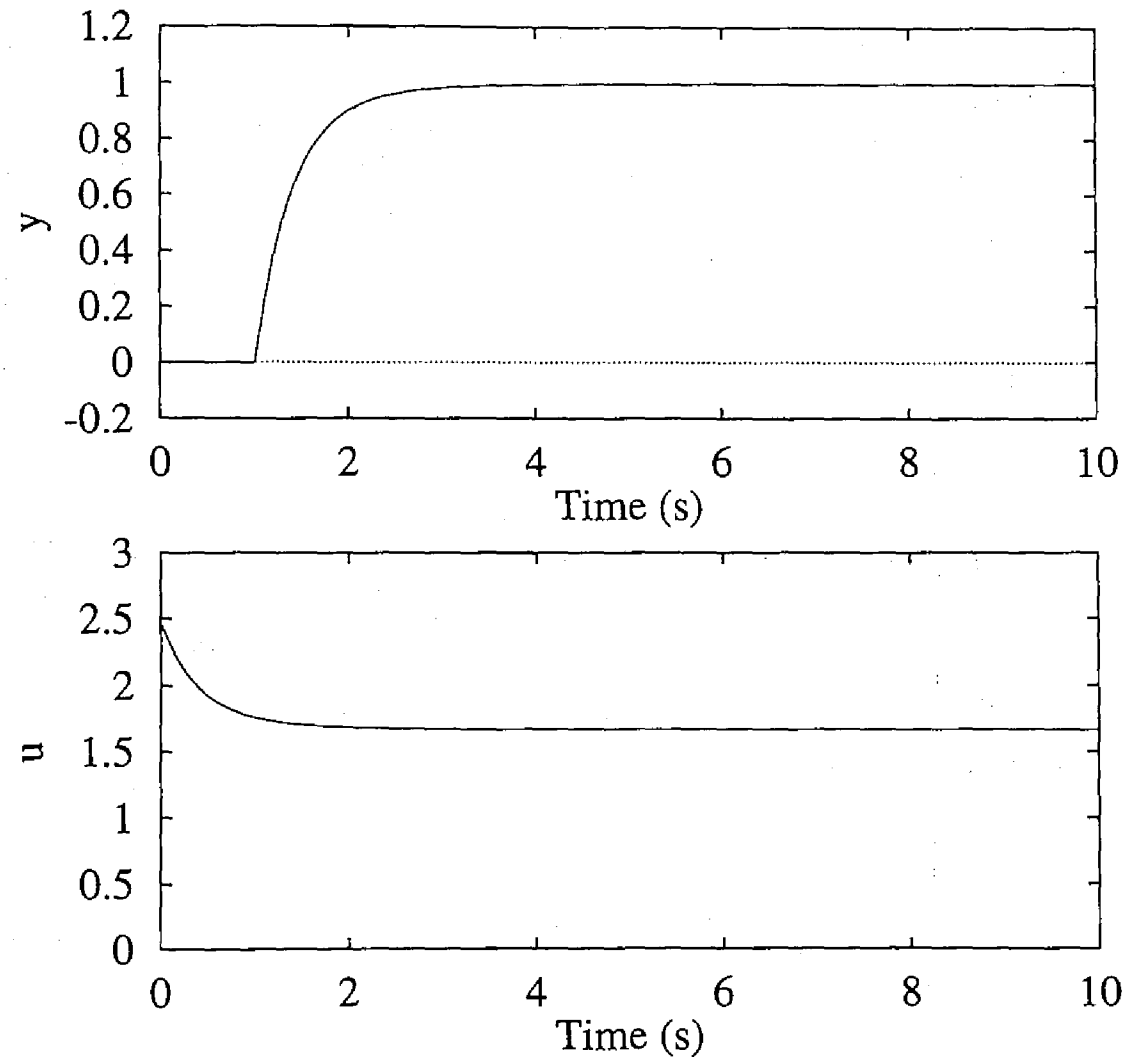

Fig. 3.10: Response of the state-predictive 2DOF-LQI-obs servo system for step reference

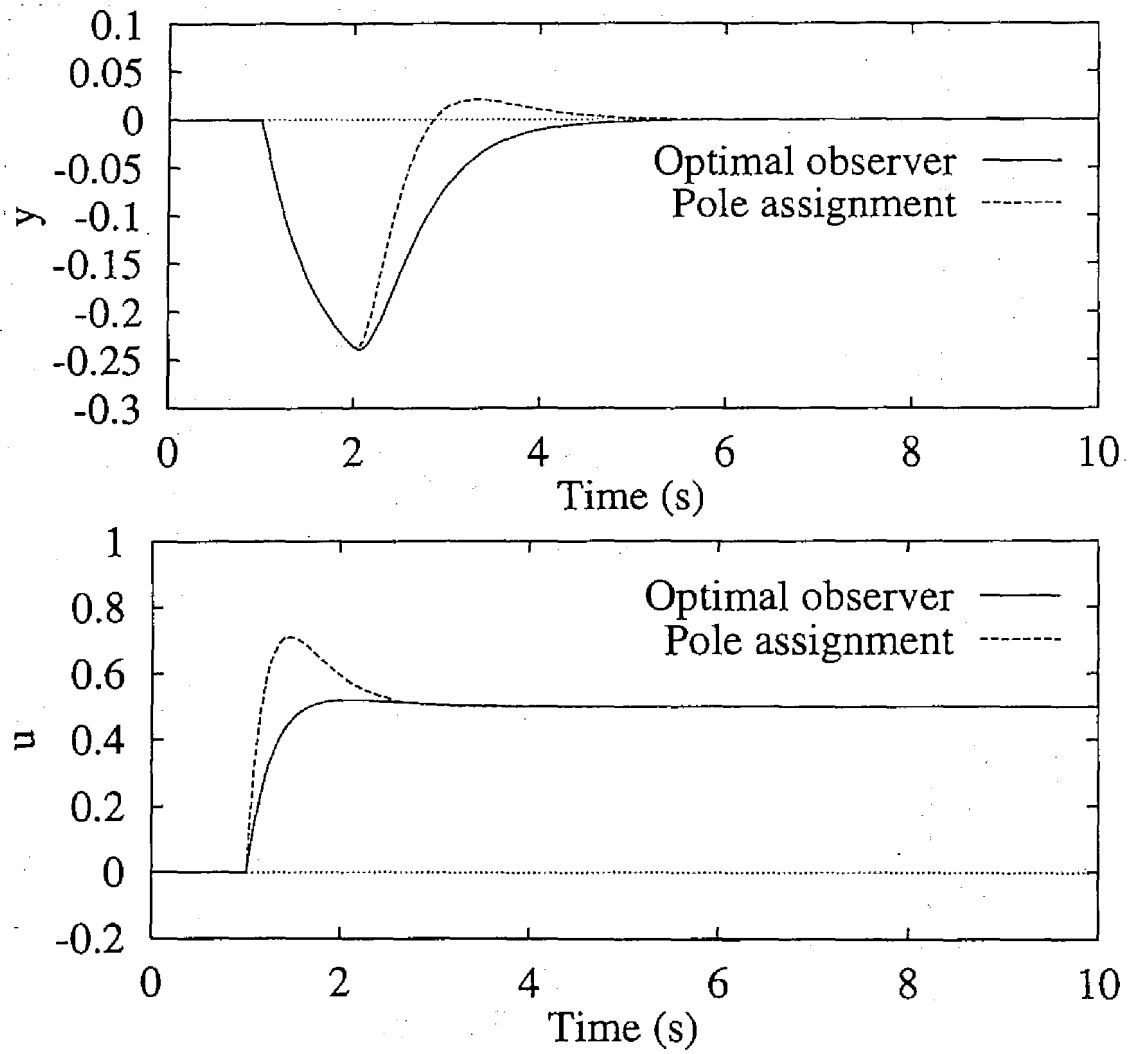

Fig. 3.11: Disturbance responses of the state-predictive 2DOF-LQI-obs servo system with optimal observer and with the observer determined by pole assignment ($\alpha^2 = 1$)

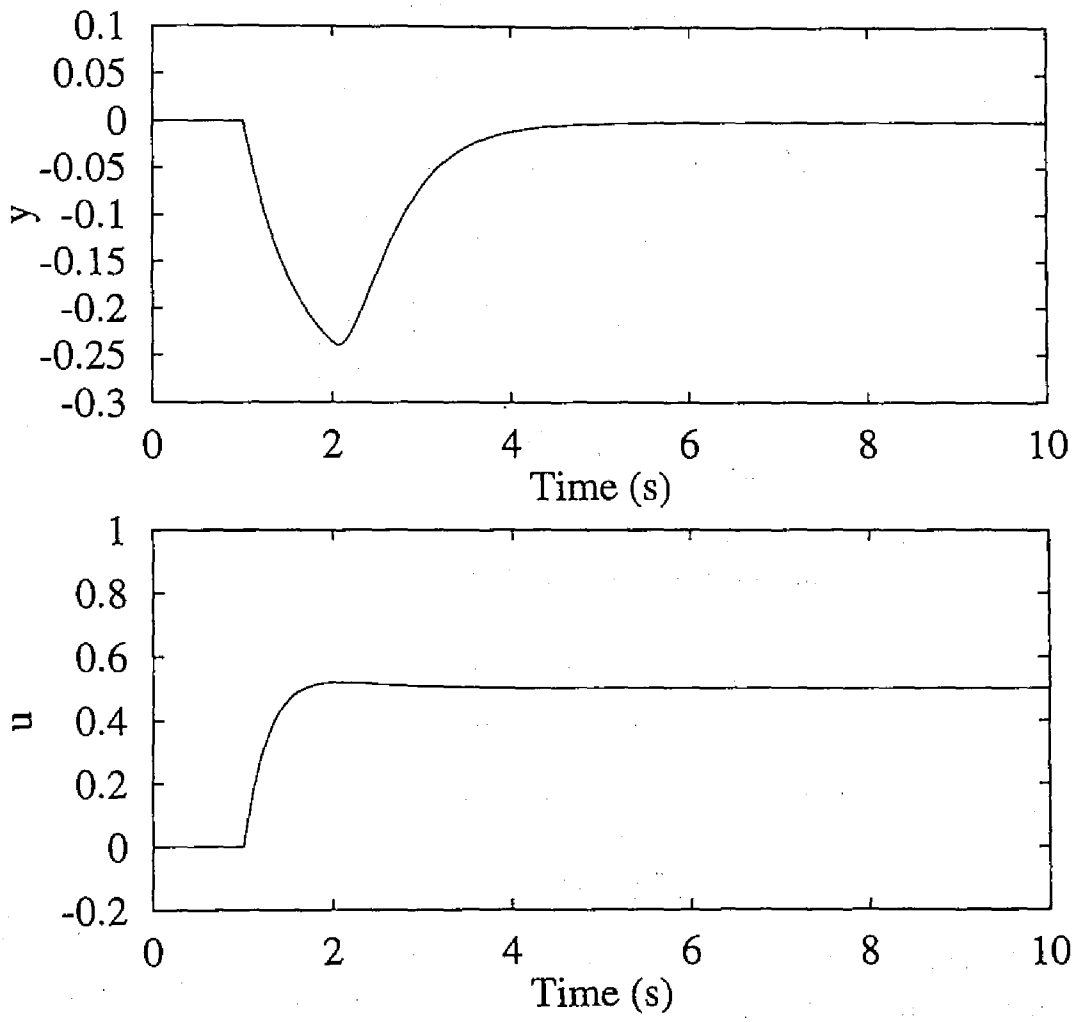

Fig. 3.12: Disturbance responses of the state-predictive 2DOF-LQI servo systems with state feedback ($\alpha^2 = 1$)

Interchanging the order of the integrals, we obtain

$$\begin{aligned} & -C\int_{t-T_L}^{t}\int_{t-T_L}^{\tau} e^{A(\tau-\sigma)}Bu(\sigma)d\sigma d\tau \\ &= -C\int_{t-T_L}^{t}\int_{\sigma}^{t} e^{A(\tau-\sigma)}d\tau Bu(\sigma)d\sigma \\ &= -C\int_{t-T_L}^{t}\int_{0}^{t-\sigma} e^{A\tau}d\tau Bu(\sigma)d\sigma. \end{aligned} \tag{3.151}$$

Then, the second term in the braces of (3.66) can be rewritten as

$$\begin{aligned} & \begin{bmatrix} -\int_{t-T_L}^{t} C\int_{t-T_L}^{\tau} e^{A(\tau-\sigma)}Bu(\sigma)d\sigma d\tau \\ \int_{t-T_L}^{t} e^{A(t-\tau)}Bu(\tau)d\tau \end{bmatrix} \\ &= \int_{t-T_L}^{t} \begin{bmatrix} I & -C\int_{0}^{t-\sigma} e^{A\tau}d\tau \\ 0 & e^{A(t-\sigma)} \end{bmatrix} \begin{bmatrix} 0 \\ B \end{bmatrix} u(\sigma)d\sigma \\ &= \int_{t-T_L}^{t} e^{A_a(t-\sigma)}B_a u(\sigma)d\sigma, \end{aligned} \tag{3.152}$$

where A_a and B_a are given by (2.11).

Furthermore, by simple calculation, we obtain

$$e^{A_a T_L} = \begin{bmatrix} I & -\int_{t-T_L}^{t} Ce^{A(\tau-t+T_L)}d\tau \\ 0 & e^{AT_L} \end{bmatrix},$$

and therefore, (3.66) can be rewritten as (3.67).

3.7.2 Interpretation of (3.76)

In this subsection, we show that the Riccati equation associated with the optimal control problem for the 'plant' (3.75) under the performance index (3.80) has a unique positive semidefinite stabilizing solution (3.81), and that the optimal 'control law' is given by (3.76).

To show this, we first interpret the control law (3.76) as consisting of two feedback control laws; this control law is equivalent to applying the control law

$$\bar{v}_d = F_2 \begin{bmatrix} \bar{x}_d \\ \bar{\zeta}_d^{\text{temp}} \\ \bar{\varepsilon}_d \end{bmatrix} \quad \left(F_2 := \begin{bmatrix} 0 & G & -H_0\Omega_{T_L} \end{bmatrix} \right) \tag{3.153}$$

to the system

$$\frac{d}{dt}\begin{bmatrix} \bar{x}_d \\ \bar{\zeta}_d^{\text{temp}} \\ \tilde{\varepsilon}_d \end{bmatrix} = \begin{bmatrix} A+BF_0 & 0 & 0 \\ 0 & 0 & 0 \\ 0 & 0 & \widehat{A} \end{bmatrix}\begin{bmatrix} \bar{x}_d \\ \bar{\zeta}_d^{\text{temp}} \\ \tilde{\varepsilon}_d \end{bmatrix} + \begin{bmatrix} B \\ \Psi \\ 0 \end{bmatrix}\bar{v}_d \tag{3.154}$$

which is obtained by applying the control law

$$\bar{u}_d = F_1\begin{bmatrix} \bar{x}_d \\ \bar{\zeta}_d^{\text{temp}} \\ \tilde{\varepsilon}_d \end{bmatrix} + \bar{v}_d \quad \left(F_1 := \begin{bmatrix} F_0 & 0 & 0 \end{bmatrix}\right) \tag{3.155}$$

to the system (3.75), where $\bar{v}_d$ is a new external input. Here, noting that F_0 is the optimal gain determined by (3.9) from the positive semidefinite solution P of the Riccati equation (3.10), it is easy to see that the Riccati equation

$$\begin{aligned} &P_1\begin{bmatrix} A & 0 & 0 \\ -\Psi F_0 & 0 & 0 \\ 0 & 0 & \widehat{A} \end{bmatrix} + \begin{bmatrix} A & 0 & 0 \\ -\Psi F_0 & 0 & 0 \\ 0 & 0 & \widehat{A} \end{bmatrix}^T P_1 \\ &\quad -P_1\begin{bmatrix} B \\ \Psi \\ 0 \end{bmatrix} R^{-1}\begin{bmatrix} B \\ \Psi \\ 0 \end{bmatrix}^T P_1 + \begin{bmatrix} Q & 0 & 0 \\ 0 & 0 & 0 \\ 0 & 0 & 0 \end{bmatrix} = 0 \end{aligned} \tag{3.156}$$

has a positive semidefinite solution

$$P_1 = \begin{bmatrix} P & 0 & 0 \\ 0 & 0 & 0 \\ 0 & 0 & 0 \end{bmatrix} \tag{3.157}$$

and that F_1 given by (3.155) can be expressed as

$$F_1 = -R^{-1}\begin{bmatrix} B \\ \Psi \\ 0 \end{bmatrix}^T \begin{bmatrix} P & 0 & 0 \\ 0 & 0 & 0 \\ 0 & 0 & 0 \end{bmatrix}. \tag{3.158}$$

As shown later, F_2 in (3.153) can be expressed as

$$F_2 = -\Theta^{-1}\begin{bmatrix} B \\ \Psi \\ 0 \end{bmatrix}^T \begin{bmatrix} 0 & 0 & 0 \\ 0 & \Pi & \bar{\Pi}_{12} \\ 0 & \bar{\Pi}_{12}^T & \bar{\Pi}_{22} \end{bmatrix} \tag{3.159}$$

where P_2 given by

$$P_2 = \begin{bmatrix} 0 & 0 & 0 \\ 0 & \Pi & \bar{\Pi}_{12} \\ 0 & \bar{\Pi}_{12}^T & \bar{\Pi}_{22} \end{bmatrix} \tag{3.160}$$

is the unique positive semidefinite solution of the Riccati equation associated with the optimal control problem for the system (3.154) under the performance index

$$J = \int_{T_L}^{\infty} \left(\begin{bmatrix} \bar{x}_d \\ \bar{\zeta}_d^{\text{temp}} \\ \tilde{\varepsilon}_d \end{bmatrix}^T \begin{bmatrix} 0 & 0 & 0 \\ 0 & \Xi & \bar{\Xi}_{12} \\ 0 & \bar{\Xi}_{12}^T & \bar{\Xi}_{22} \end{bmatrix} \begin{bmatrix} \bar{x}_d \\ \bar{\zeta}_d^{\text{temp}} \\ \tilde{\varepsilon}_d \end{bmatrix} + \bar{v}_d^T \Theta \bar{v}_d \right) dt \tag{3.161}$$

where

$$\bar{\Xi}_{12} = H_0^T \Theta H_0 \Omega_{T_L} \hat{A} - \Pi \Omega_{T_L} \tag{3.162}$$

and $\bar{\Xi}_{22}$ is an arbitrary positive semidefinite matrix satisfying

$$\begin{aligned} \bar{\Xi}_{22} \geq\ & \hat{A}^T \Omega_{T_L}^T H_0^T \Theta H_0 \Pi^{-1} H_0^T \Theta H_0 \Pi^{-1} H_0^T \Theta H_0 \Omega_{T_L} \hat{A} \\ & - \hat{A}^T \Omega_{T_L}^T H_0^T \Theta H_0 \Pi^{-1} H_0^T \Theta H_0 \Omega_{T_L} \\ & - \Omega_{T_L}^T H_0^T \Theta H_0 \Pi^{-1} H_0^T \Theta H_0 \Omega_{T_L} \hat{A} \\ & + \Omega_{T_L}^T H_0^T \Theta H_0 \Omega_{T_L}. \end{aligned} \tag{3.163}$$

Under (3.162) and (3.163), we have

$$\bar{\Xi}_z := \begin{bmatrix} 0 & 0 & 0 \\ 0 & \Xi & \bar{\Xi}_{12} \\ 0 & \bar{\Xi}_{12}^T & \bar{\Xi}_{22} \end{bmatrix} \geq 0.$$

From the above facts (and (3.166) and (3.167) below) and from Theorem 1 in [18], we can interpret the control law (3.76) as the optimal control law for the system (3.75) under the performance index (3.80) (we assumed $\Theta = R$ for simplicity, but similar results can be obtained even for $\Theta \geq R$ [19]). Furthermore, the same theorem shows that the positive semidefinite stabilizing solution of the Riccati equation associated with this optimal control problem is given by (3.81).

Now, what remains is to show that F_2 in (3.153) satisfies (3.159). We can show this as follows. The Riccati equation associated with the optimal control problem for the system (3.154) under the performance index (3.161) is given by

$$P_2 \begin{bmatrix} A + BF_0 & 0 & 0 \\ 0 & 0 & 0 \\ 0 & 0 & \hat{A} \end{bmatrix} + \begin{bmatrix} A + BF_0 & 0 & 0 \\ 0 & 0 & 0 \\ 0 & 0 & \hat{A} \end{bmatrix}^T P_2$$

$$-P_2\begin{bmatrix} B \\ \Psi \\ 0 \end{bmatrix}\Theta^{-1}\begin{bmatrix} B \\ \Psi \\ 0 \end{bmatrix}^T P_2 + \begin{bmatrix} 0 & 0 & 0 \\ 0 & \Xi & \bar{\Xi}_{12} \\ 0 & \bar{\Xi}_{12}^T & \bar{\Xi}_{22} \end{bmatrix} = 0. \qquad (3.164)$$

It is easy to see that the Riccati equation (3.164) has a unique positive semidefinite solution. Multiplying the Riccati equation (3.164) by

$$\begin{bmatrix} I & 0 & 0 \\ 0 & I & G^{-1}H_0\Omega_{T_L} \\ 0 & 0 & I \end{bmatrix}$$

from the right and by

$$\begin{bmatrix} I & 0 & 0 \\ 0 & I & G^{-1}H_0\Omega_{T_L} \\ 0 & 0 & I \end{bmatrix}^T$$

from the left, we have

$$\begin{aligned} P_2'\begin{bmatrix} A+BF_0 & 0 & 0 \\ 0 & 0 & -G^{-1}H_0\Omega_{T_L}\widehat{A} \\ 0 & 0 & \widehat{A} \end{bmatrix} \\ + \begin{bmatrix} A+BF_0 & 0 & 0 \\ 0 & 0 & -G^{-1}H_0\Omega_{T_L}\widehat{A} \\ 0 & 0 & \widehat{A} \end{bmatrix}^T P_2' \\ -P_2'\begin{bmatrix} B \\ \Psi \\ 0 \end{bmatrix}\Theta^{-1}\begin{bmatrix} B \\ \Psi \\ 0 \end{bmatrix}^T P_2' + \bar{\Xi}_z' = 0 \end{aligned} \qquad (3.165)$$

where

$$P_2' = \begin{bmatrix} I & 0 & 0 \\ 0 & I & G^{-1}H_0\Omega_{T_L} \\ 0 & 0 & I \end{bmatrix}^T P_2 \begin{bmatrix} I & 0 & 0 \\ 0 & I & G^{-1}H_0\Omega_{T_L} \\ 0 & 0 & I \end{bmatrix} \qquad (3.166)$$

$$\begin{aligned} \bar{\Xi}_z' &= \begin{bmatrix} 0 & 0 & 0 \\ 0 & \Xi & \bar{\Xi}_{12}' \\ 0 & \bar{\Xi}_{12}'^T & \bar{\Xi}_{22}' \end{bmatrix} \\ &:= \begin{bmatrix} I & 0 & 0 \\ 0 & I & G^{-1}H_0\Omega_{T_L} \\ 0 & 0 & I \end{bmatrix}^T \bar{\Xi}_z \begin{bmatrix} I & 0 & 0 \\ 0 & I & G^{-1}H_0\Omega_{T_L} \\ 0 & 0 & I \end{bmatrix} \end{aligned}$$

$$\geq 0, \tag{3.167}$$

$$\bar{\Xi}'_{12} = \Xi G^{-1} H_0 \Omega_{T_L} + \bar{\Xi}_{12} = H_0^T \Theta H_0 \Omega_{T_L} \widehat{A}, \tag{3.168}$$

$$\begin{aligned} \bar{\Xi}'_{22} &= \Omega_{T_L}^T H_0^T G^{-T} \Xi G^{-1} H_0 \Omega_{T_L} \\ &\quad + \bar{\Xi}_{12}^T G^{-1} H_0 \Omega_{T_L} + \Omega_{T_L}^T H_0^T G^{-T} \bar{\Xi}_{12} + \bar{\Xi}_{22}. \end{aligned} \tag{3.169}$$

Assuming that the unique positive semidefinite solution is given by

$$P'_2 = \begin{bmatrix} 0 & 0 & 0 \\ 0 & \Pi & 0 \\ 0 & 0 & \bar{\Pi}'_{22} \end{bmatrix}, \tag{3.170}$$

the Riccati equation (3.165) is equivalent to the following two equations:

$$-\Pi \Psi \Theta^{-1} \Psi^T \Pi + \Xi = 0, \tag{3.171}$$

$$\bar{\Pi}'_{22} \widehat{A} + \widehat{A}^T \bar{\Pi}'_{22} + \bar{\Xi}'_{22} = 0. \tag{3.172}$$

Since (3.171) coincides with (3.54), (3.171) is satisfied. On the other hand, since $\bar{\Xi}'_{22} \geq 0$ from (3.167), the Lyapunov equation (3.172) has a unique positive semidefinite solution $\bar{\Pi}'_{22}$. From the above, it follows that the Riccati equation (3.165) has a unique positive semidefinite solution of the form (3.170) (here, Π is the solution of (3.54) and $\bar{\Pi}'_{22}$ is the solution of (3.172)). From (3.166), the Riccati equation (3.164) has a unique positive semidefinite solution P_2 of the form (3.160). Therefore, the optimal gain for this optimal control problem is given by

$$-\Theta^{-1} \begin{bmatrix} B \\ \Psi \\ 0 \end{bmatrix}^T \begin{bmatrix} 0 & 0 & 0 \\ 0 & \Pi & \bar{\Pi}_{12} \\ 0 & \bar{\Pi}_{12}^T & \bar{\Pi}_{22} \end{bmatrix}, \tag{3.173}$$

and, by simple calculation, it can be rewritten as

$$\begin{bmatrix} 0 & G & -H_0 \Omega_{T_L} \end{bmatrix}. \tag{3.174}$$

This means that F_2 defined by (3.153) satisfies (3.159). This completes the proof of our assertion.

Note that from (3.162),(3.163) and (3.169), the positive semidefiniteness of (3.167) is equivalent to

$$\begin{aligned} \bar{\Xi}'_{22} &\geq \widehat{A}^T \Omega_{T_L}^T H_0^T \Theta H_0 \Pi^{-1} H_0^T \Theta H_0 \Pi^{-1} H_0^T \Theta H_0 \Omega_{T_L} \widehat{A} \\ &(= \widehat{A}^T \Omega_{T_L}^T H_0^T \Theta H_0 \Xi^{-1} H_0^T \Theta H_0 \Omega_{T_L} \widehat{A}). \end{aligned} \tag{3.175}$$

3.7.3 Derivation of (3.93)

In this subsection, we derive (3.93).

The system of Fig. 3.7 is described by

$$\begin{aligned}\frac{dx(t)}{dt} &= Ax(t) + Bu(t) + d_x,\\ u(t) &= F_0\{e^{AT_L}x(t-T_L) + \int_{t-T_L}^{t} e^{A(t-\tau)}Bu(\tau)d\tau\}\\ &\quad + H_0 r(t) + v_{d\infty}^{\text{state}} + \eta(t)\\ &= F_0 x(t) + H_0 r(t) + v_{d\infty}^{\text{state}} + \eta(t).\end{aligned} \tag{3.176}$$

By the definition (3.4), we can easily derive

$$\begin{aligned}\frac{d\tilde{x}(t)}{dt} &= A\tilde{x}(t) + B\tilde{u}(t),\\ \tilde{u}(t) &= F_0\tilde{x}(t) + \eta(t).\end{aligned} \tag{3.177}$$

Now, the integrand of (3.6) can be arranged as

$$\begin{aligned}&\tilde{x}^T Q\tilde{x} + \tilde{u}^T R\tilde{u}\\ &\quad = \tilde{x}^T Q\tilde{x} + (F_0\tilde{x} + \eta)^T R(F_0\tilde{x} + \eta)\\ &\quad = \tilde{x}^T(Q + F_0^T RF_0)\tilde{x} + \tilde{x}^T F_0^T R\eta + \eta^T RF_0\tilde{x} + \eta^T R\eta.\end{aligned} \tag{3.178}$$

Here, from (3.9) and (3.10), we have

$$Q + F_0^T RF_0 = -P(A + BF_0) - (A + BF_0)^T P. \tag{3.179}$$

Substituting this equation into (3.178) and arranging the result using (3.9) and (3.177), we obtain

$$\begin{aligned}&\tilde{x}^T Q\tilde{x} + \tilde{u}^T R\tilde{u}\\ &\quad = -\tilde{x}^T P\{(A + BF_0)x + B\eta\} - \{(A + BF_0)x + B\eta\}^T P\tilde{x} + \eta^T R\eta\\ &\quad = -\tilde{x}^T P\frac{d\tilde{x}}{dt} - \frac{d\tilde{x}}{dt}^T P\tilde{x} + \eta^T R\eta.\end{aligned} \tag{3.180}$$

Integrating the above equation over $[T_L, \infty)$ noting $\tilde{x}(\infty) = 0$, we have

$$J = \tilde{x}(T_L)^T P\tilde{x}(T_L) + \int_{T_L}^{\infty} \eta^T R\eta\, dt. \tag{3.181}$$

Since the first term of the right hand side is the optimal value that is attained by state feedback, (3.93) follows.

3.8 Concluding remarks

In this chapter, we studied a two-degree-of-freedom (2DOF) design method of robust servo systems for step references and disturbances, for the plant with a cascaded pure delay. Furthermore, we studied a design method of optimal observers to be used for this 2DOF servo systems.

The results obtained about a 2DOF design method of robust servo systems can be summarized as follows.

1. The tracking characteristics for step references and the feedback characteristics for step disturbances (and modeling errors) can be determined optimally using independent quadratic-integral performance indices. To attain such 2DOF optimality, we have only to introduce a state prediction mechanism into the 2DOF-LQI-obs servo system of the delay-free case [20]; the optimal feedback gains for the plant with a pure delay are the same as those for the plant with the delay removed.

2. An equivalent configuration of the above state-predictive servo system is given (Fig. 3.5), and a relationship between our design method and the existing design method [2], [16] is clarified.

3. As the weighting matrix Ξ becomes larger in the performance index for disturbance responses, disturbance rejection becomes quicker.

4. As Ξ tends to infinity uniformly, the response for a step disturbance tends to that of the state-predictive LQ-obs servo system with disturbance compensation input shown in Fig. 3.6.

5. Comparing the above response with the limiting response of the state feedback case, the deterioration of disturbance rejection ability caused by an observer is clarified quantitatively.

These results can be interpreted as theoretically proving our expectation that the fundamental characteristics of 2DOF-LQI-obs servo systems in the delay-free case are inherited to the state-predictive 2DOF-LQI-obs servo systems for plants with a delay.

In addition, we gave a design method of an optimal observer to be used for the state-predictive two-degree-of-freedom (2DOF) LQI servo system under output feedback. Specifically, we considered the presence of the step disturbances added to the plant, and gave the optimal full-order and minimal-order observers with respect to disturbance

rejection ability, assuming that the statistical properties of the disturbances are known. The obtained results can be summarized as follows.

6. Separation property holds also in the two-degree-of-freedom robust servo problem.

7. The optimal observers have a close connection with the technique of loop transfer recovery.

8. The optimal observers achieve perfect suppression of the step disturbances satisfying the matching condition if and only if the plant is a minimum phase system (and, in addition, has a maximum number of zeros, in the case of the optimal minimal-order observer).

Although our optimization argument was made under the limiting case of $\Xi \to \infty$ (or $G \to \infty$), it is easy to show that the optimal observers obtained by this limiting argument are optimal (in an appropriate sense) even with finite Ξ (or G). This is a direct consequence from the following facts (details are omitted):

(a) The 2DOF-LQI servo system (in the state feedback case) [19] is such that it minimizes a quadratic-integral performance index.

(b) The optimal observer obtained by the limiting argument does not depend on the matrix V.

From the above results, we obtained the complete solution to the optimal design problem of state-predictive two-degree-of-freedom LQI servo systems for step references and step disturbances.

Chapter 4

Robust stability analysis of state-predictive control systems

As described in Chapters 2 and 3, the present state of the lumped-parameter part of the plant is predicted in state-predictive controllers. As a matter of course, such prediction becomes possible only upon the knowledge of the plant dynamics. Actually, these controllers include dynamical models of the plant in themselves, and their performance much depends upon those models. This implies that the control systems can become very sensitive to modeling errors, especially when the response speed is raised excessively. Hence, in the design of these controllers, the robustness analysis is crucially important. The most important factor for the robust stability of the control systems with a pure delay is the mismatch of the delay time T_L. Actually, the error of T_L causes the error of the phase angle which increases in proportion to the angular frequency ω. Thus, the mismatch of the delay time produces a frequency-dependent error of the transfer function and even a small mismatch of the delay time produces a large effect on the transfer function in the high frequency range.

As for robust stability of the system with pure delay, Palmor [37] derived a basic result about the robust stability of the Smith controller. In [6], Bao and Araki deepened his idea and derived a graphical method to obtain the stability region on the gain–delay plane, which is applicable to the state-predictive controllers, too, and include Palmor's result as a special case. Their simulation suggested that their result is sharp for the cases with positive errors in the gain but is rather conservative for the cases with negative errors in the gain.

In this chapter, we study the robust stability of the state-predictive servo systems. To put it concretely, we consider the case where the plant has modeling errors in the delay time and in the gain, and we try to improve Bao-Araki's result and derive a robust stability criterion for the state-predictive and Smith control systems, which

gives necessary and sufficient boundaries. Throughout this chapter, we consider the case where $m = 1$, and assume that the control systems are all designed to be stable when there are no modeling errors.

4.1 Characteristic function of state-predictive servo systems with an observer

Consider the plant with a cascaded pure delay T_L on the output side, described by

$$\begin{aligned} \frac{dx(t)}{dt} &= Ax(t) + Bu(t), && (4.1)\\ y_{\rm A}(t) &= Cx(t), && (4.2)\\ y(t) &= y_{\rm A}(t - T_L), && (4.3) \end{aligned}$$

where $u(t)$ is a scalar input, $y(t)$ is a scalar output, $y_{\rm A}(t)$ is a scalar delay-free output, and $x(t)$ is an n-dimensional state, and (A, B) is controllable and (C, A) is observable. In this chapter, we deal with a state-predictive servo system of Fig. 4.1 designed for this plant. Here, the observer is given by

$$\begin{aligned} \frac{dq(t)}{dt} &= \widehat{A}q(t) + \widehat{B}u(t - T_L) - Ky(t),\\ \hat{x}(t - T_L) &= Dq(t) - Ly(t). \end{aligned} \qquad (4.4)$$

where $\widehat{A}$ is a stable matrix and $\widehat{A}$, $\widehat{B}$, K, D and L satisfy

$$\begin{aligned} \widehat{A}M &= MA + KC,\\ \widehat{B} &= MB,\\ I &= DM - LC \end{aligned} \qquad (4.5)$$

for a certain M [29], $\mathcal{F}(A_a, B_a, T_L)$ is a finite interval integration operator defined by

$$\mathcal{F}(A_a, B_a, T_L)u := \int_{-T_L}^{0} e^{A_a\tau} B_a u(t + \tau) d\tau, \qquad (4.6)$$

$I_{\rm I}$ and $I_{\rm F}$ are matrices defined by

$$I_{\rm I} = \begin{bmatrix} I_m \\ 0 \end{bmatrix}, \quad I_{\rm F} = \begin{bmatrix} 0 \\ I_n \end{bmatrix}, \qquad (4.7)$$

where I_i is an i-dimensional unit matrix, and the feedback gain F_a and the observer parameters are determined appropriately. In this chapter, since we consider only the feedback characteristics, we assume that $\tau = 0$.

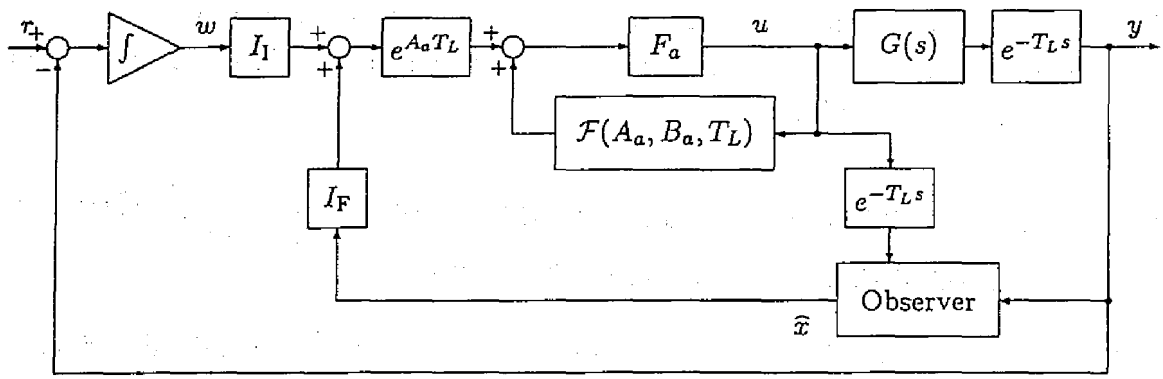

Fig. 4.1: State-predictive servo system

In our robust stability analysis, we only consider the parameter mismatches. Namely, we assume that the real plant is described by the following equations which have the same form with the plant model (4.1), (4.2) and (4.3), but the different parameters:

$$\frac{dx(t)}{dt} = A_r x(t) + B_r u(t), \tag{4.8}$$

$$y_A(t) = C_r x(t), \tag{4.9}$$

$$y(t) = y_A(t - T_{Lr}). \tag{4.10}$$

Now, we derive the characteristic function of the state-predictive servo system with an observer. The control law is given by

$$u(t) = F_a \left\{ e^{A_a T_L} \begin{bmatrix} w(t) \\ \widehat{x}(t - T_L) \end{bmatrix} + \int_{-T_L}^{0} e^{-A_a \tau} B_a u(t + \tau) d\tau \right\}, \tag{4.11}$$

with

$$A_a = \begin{bmatrix} 0 & -C \\ 0 & A \end{bmatrix},$$

$$B_a = \begin{bmatrix} 0 \\ B \end{bmatrix},$$

and F_a is the feedback gain such that the closed-loop coefficient matrix $A_a + B_a F_a$ is stable (note that $F_a = [G \quad G\Gamma]$ in the state-predictive two-degree-of-freedom LQI servo system dealt in the preceding chapter), and the integral compensator is given by

$$w(t) = \int_0^t e(\tau)\, d\tau + w_0 \tag{4.12}$$

If we apply Laplace transformation to (4.8), (4.4) and (4.11) under the initial conditions:

$$
\begin{aligned}
x(\theta) &= x_0(\theta), \qquad -\max(T_L, T_{L\mathrm{r}}) \le \theta \le 0, && (4.13)\\
u(\theta) &= u_0(\theta), \qquad -\max(T_L, T_{L\mathrm{r}}) \le \theta \le 0, && (4.14)\\
q(0) &= q_0, && (4.15)\\
w(0) &= w_0, && (4.16)
\end{aligned}
$$

and rearrange the terms, we obtain

$$
\begin{aligned}
(sI - A_{\mathrm{r}})x(s) - B_{\mathrm{r}}u(s) &= x_0(0), && (4.17)\\
-KC_{\mathrm{r}}e^{-T_{L\mathrm{r}}s}x(s) + (sI - \widehat{A})q(s) - \widehat{B}e^{-T_L s}u(s) &= q_0 + J_1(s) + J_2(s), && (4.18)\\
\widehat{x}(s) - Dq(s) + LC_{\mathrm{r}}e^{-T_{L\mathrm{r}}s}x(s) &= J_3(s), && (4.19)\\
-F_a e^{A_a T_L}\begin{bmatrix} w(s) \\ \widehat{x}(s) \end{bmatrix} + \{I - F_a\beta(s)\}u(s) &= J_4(s), && (4.20)\\
sw(s) + C_{\mathrm{r}}e^{-T_{L\mathrm{r}}s}x(s) &= w_0 + J_5(s). && (4.21)
\end{aligned}
$$

Here, $x(s)$, $u(s)$, $q(s)$, $\widehat{x}(s)$ and $w(s)$ are Laplace transformations of $x(t)$, $u(t)$, $q(t)$, $\widehat{x}(t)$ and $w(t)$, respectively, $\beta(s)$ is Laplace transformation of the finite interval integration operator $\mathcal{F}$ in (4.11) given by

$$\beta(s) = (I - e^{A_a T_L}e^{-T_L s})(sI - A_a)^{-1}B_a, \tag{4.22}$$

and $J_1(s)$, $J_2(s)$, $J_3(s)$, $J_4(s)$ and $J_5(s)$ are regular functions of s determined by the initial conditions as

$$
\begin{aligned}
J_1(s) &= KC_{\mathrm{r}}e^{-T_{L\mathrm{r}}s}\int_{-T_{L\mathrm{r}}}^{0} x_0(\theta)e^{-s\theta}d\theta, && (4.23)\\
J_2(s) &= -\widehat{B}e^{-T_L s}\int_{-T_L}^{0} u_0(\theta)e^{-s\theta}d\theta, && (4.24)\\
J_3(s) &= LC_{\mathrm{r}}e^{-T_{L\mathrm{r}}s}\int_{-T_{L\mathrm{r}}}^{0} x_0(\theta)e^{-s\theta}d\theta, && (4.25)\\
J_4(s) &= F_a\int_{-T_L}^{0} e^{-A_a\theta}B_a e^{s\theta}\int_{\theta}^{0} u_0(\tau)e^{-s\tau}d\tau d\theta, && (4.26)\\
J_5(s) &= C_{\mathrm{r}}e^{-T_{L\mathrm{r}}s}\int_{-T_{L\mathrm{r}}}^{0} x_0(\theta)e^{-s\theta}d\theta. && (4.27)
\end{aligned}
$$

From (4.17)–(4.21), the characteristic function of the state-predictive servo system is

obtained by

$$f(s) = \det \left[\begin{array}{ccc:cc} sI - A_r & 0 & -B_r & 0 & 0 \\ KC_r e^{-T_{Lr}s} & sI - \widehat{A} & -\widehat{B}e^{-T_{Lr}s} & 0 & 0 \\ 0 & 0 & I - F_a\beta(s) & -F_a e^{A_a T_L} & \\ \hdashline C_r e^{-T_{Lr}s} & 0 & 0 & sI & 0 \\ LC_r e^{-T_{Lr}s} & -D & 0 & 0 & I \end{array} \right]. \tag{4.28}$$

4.2 Robust stability for gain and delay time mismatches

In the following, we consider the case where the modeling errors exist only in the estimates of the gain and the delay time. Namely, we assume

$$\begin{aligned} A_r &= A, \\ B_r &= B, \\ C_r &= (1+\gamma)C, \\ T_{Lr} &= T_L + \delta, \end{aligned} \tag{4.29}$$

where $\gamma(\geq -1)$ and $\delta(\geq -T_L)$ gives the relative error of the gain and the absolute error of the delay time, respectively. Formally speaking, the assumption on the modeling error made up to this point is very restrictive in the sense that the form of the equation is largely fixed; to be more specific, the structure that the lumped parameter part and the pure delay are cascaded is fixed, no parasitic dynamics for the lumped parameter part is introduced, and the parameters A_r and B_r are fixed to the nominal values. However, these formal restrictiveness does "never" mean that the treated problem is special and that the results are practically useless. In practical situation, the errors of the plant model are often recognized as the errors in the gain and the phase shift and, for instance, the parasitic dynamics is nothing but a "model of the modeling error." Hence, even though the assumption in the modeling errors is formally restrictive, the results can be practically useful if the assumed modeling errors cover general gain and phase deviation which are practically plausible. In our study, simultaneous variation of the gain and the delay-time are going to be considered. The variation of the delay-time usually causes severest effects on the phase shift. Thus, the modeling errors considered here cover the worst case in terms of the gain and phase shifts, and, hence, our method is expected to give safe enough results. On the other hand, the controllers studied here are supposed to be applied to plants with a pure delay, and, so, existence of

the modeling error in the delay-time is surely plausible. In this sense, our method is expected not to give too much conservative results. As a result, it could be claimed that our method gives "practically necessary-and-sufficient" result for robust stability which can be obtained within the range of "linear theory."

Under the assumption (4.29), $f(s)$ becomes

$$f(s) = \det[sI - A_a - B_a F_a] \cdot \det[sI - \widehat{A}] \cdot [1 + P(s)Q(s)], \tag{4.30}$$

where

$$\begin{aligned} P(s) &= e^{-T_L s} C_a (sI - A_a - B_a F_a)^{-1} B_a \\ &\quad \times F_a e^{A_a T_L} \{D_a (sI - \widehat{A}_a)^{-1} K_a - L_a\}, \qquad (4.31) \\ Q(s) &= (1+\gamma) e^{-\delta s} - 1, \qquad (4.32) \end{aligned}$$

with

$$\begin{aligned} C_a &= \begin{bmatrix} 0 & C \end{bmatrix}, \qquad (4.33) \\ \widehat{A}_a &= \begin{bmatrix} 0 & 0 \\ 0 & \widehat{A} \end{bmatrix}, \qquad (4.34) \\ D_a &= \begin{bmatrix} 1 & 0 \\ 0 & D \end{bmatrix}, \qquad (4.35) \\ K_a &= \begin{bmatrix} 1 \\ K \end{bmatrix}, \qquad (4.36) \\ L_a &= \begin{bmatrix} 0 \\ L \end{bmatrix}. \qquad (4.37) \end{aligned}$$

The first two factors of (4.30) are the characteristic function of the state feedback system consisting of (4.1) and (4.11) and that of the observer (4.4), respectively, which are designed to be stable. Therefore, the stability of the control system under the parameter errors given by (4.29) is determined by the roots of

$$1 + P(s)Q(s) = 0. \tag{4.38}$$

From (4.32), we can easily assure that $Q(s)$ represents the relative error of the transfer function of the plant[1]. We can also assure that $-P(s)$ is the complementary sensitivity

[1]This implies that $Q(s)$ becomes 0 and, consequently, $f(s)$ becomes $\det[sI - A_a - B_a F_a] \det[sI - \widehat{A}]$ if there are no modeling errors. This proves that the state-predictive servo controller stabilizes an unstable plant [32], [16].

function of the system of Fig. 2.4; i.e., the closed-loop transfer function of the nominal control system. Hence, (4.38) is nothing but the closed-loop characteristic equation of the positive feedback loop consisting of the relative error $Q(s)$ and the nominal control system $-P(s)$[2].

Since the poles of $P(s)$ are all stable, since $Q(s)$ is regular, and since

$$P(s)Q(s) \to 0 \quad \text{as } |s| \to \infty, \text{ Re } s \geq 0, \tag{4.39}$$

we can apply the Nyquist method to judge the stability of the roots of (4.38) and obtain the next stability criterion [6].

Theorem 4.1 The system of Fig. 2.4 remains stable for the parameter errors given by (4.29) if and only if the Nyquist locus of $P(s)Q(s)$ does not encircle nor pass the point -1.

4.3 Delay margin of the state-predictive control system

In this and the next sections, the stability limit of the state-predictive control system is studied where the case of no gain mismatch is treated in this section in detail, and the general case in the next section.

At the stability limit, the characteristic equation (4.38) should have a root (or roots) on the imaginary axis; namely

$$1 + P(j\omega)Q(j\omega) = 0 \tag{4.40}$$

must hold at some frequency ω. Rewrite the equation as

$$P(j\omega) = -1/Q(j\omega) \tag{4.41}$$

and consider the locus of $P(j\omega)$ for $\omega = 0 \sim \infty$ (which will be referred to as *P-locus*), and the locus

$$R(j\alpha, \gamma) := -1/Q(j\omega) = \{1 - (1+\gamma)e^{-j\alpha}\}^{-1} \tag{4.42}$$

for $\alpha = -2\pi \sim 2\pi$ (which will be referred to as *R[γ]-locus*). Satisfaction of (4.41) is equivalent to

[2]The fact that the robust stability is deduced from the stability of this positive feedback loop is the standard result used in recent researches about robust stability. Here, we derived this result based on the characteristic equation, because the expression (4.31) is much more convenient for our purpose, because the effect of the pure delays can be seen more clearly including the initial value problem, and because the stability of the nominal system can be assured at the same time.

1. the P-locus and the $R[\gamma]$-locus cross, and

2. the values of ω and α at the crossing point satisfy $\alpha = \delta\omega$.

In the above, note that γ is the relative error of the gain and δ is the absolute error of the delay-time (see (4.29)).

Now, consider the case of no gain mismatch (i.e., $\gamma = 0$). The $R[0]$-locus is the straight line parallel to the imaginary axis passing the point $1/2$ on the real axis (shown in Fig. 4.2), where

$$\begin{aligned}
&\mathrm{Im}\,[R(j\alpha,0)] \to -\infty \quad \text{for } \alpha \to +0 \qquad \text{and } \alpha \to -2\pi + 0,\\
&\mathrm{Im}\,[R(j\alpha,0)] = 0 \qquad \text{for } \alpha = \pi \qquad \text{and } \alpha = -\pi,\\
&\mathrm{Im}\,[R(j\alpha,0)] \to +\infty \quad \text{for } \alpha \to 2\pi - 0 \quad \text{and } \alpha \to -0.
\end{aligned}$$

Note that, when α changes from -2π to 2π, the point $R(j\alpha, 0)$ covers the whole straight line twice; that is to say, each point of the line corresponds to two values of α (one is positive and the other negative). From (4.31), we can know that the P-locus has the usual characteristics of the Nyquist locus of the finite-dimensional strictly proper stable linear system cascaded with a pure delay; i.e., the locus starts from a point on (usually the positive side of) the real axis, encircles the origin infinitely many times, and converges to the origin.

If we carefully analyze the relation of the behavior of the point $P(j\omega)Q(j\omega)$ to the location of the P-locus and the $R[0]$-locus, we can derive the next result [6].

Theorem 4.2 (The case of no gain mismatch: $\gamma = 0$.)

Consider the system of Fig. 2.4 with the parameter errors given by (4.29) with $\gamma = 0$.

(a) If the P-locus and the $R[0]$-locus do not cross, the system remains stable for any δ.

(b) Assume that $P(0) > 0$ and that the P-locus and the $R[0]$-locus cross at one point A_1, at which $\omega = \omega_1$ on the P-locus and $\alpha = \alpha_1 (> 0)$ and $\alpha_1' (< 0)$ on the $R[0]$-locus. Let

$$\begin{aligned}
\overline{\delta}(0) &= \alpha_1/\omega_1,\\
\underline{\delta}(0) &= \max(\alpha_1'/\omega_1, -T_L).
\end{aligned} \tag{4.43}$$

The system is stable for

$$\underline{\delta}(0) < \delta < \overline{\delta}(0), \tag{4.44}$$

and is unstable otherwise.

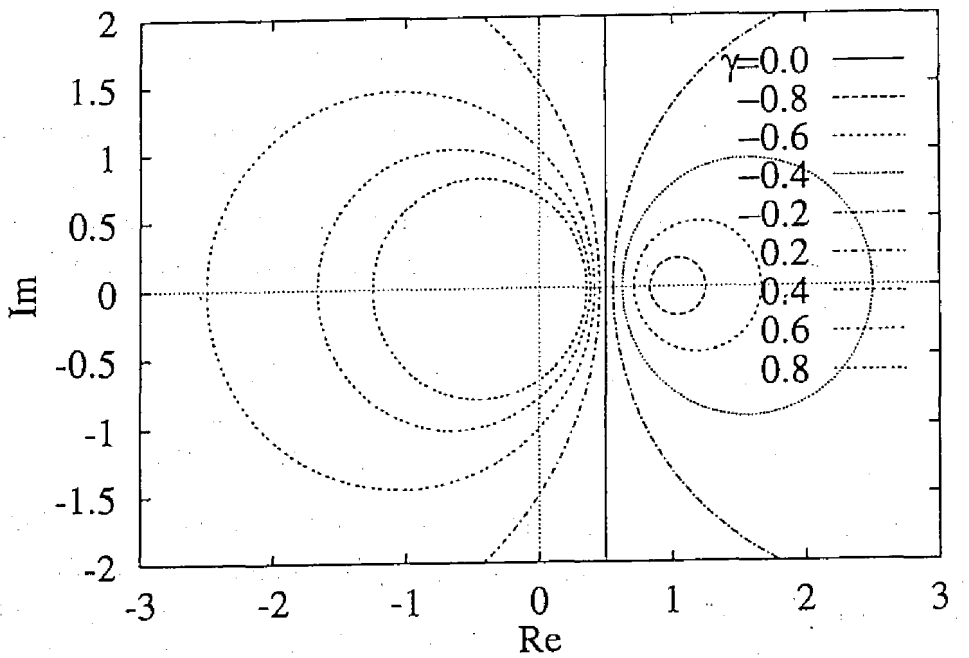

Fig. 4.2: $R[\gamma]$-loci

(c) Assume that $P(0) > 0$, and that the P-locus and the $R[0]$-locus cross at m points $A_1, \cdots, A_m$, and that, at the i-th point A_i, $\omega = \omega_i$ on the P-locus and $\alpha = \alpha_i (> 0)$ and $\alpha_i' (< 0)$ on the $R[0]$-locus. Let

$$\overline{\delta}(0) = \min(\alpha_1/\omega_1, \cdots, \alpha_m/\omega_m), \tag{4.45}$$

$$\underline{\delta}(0) = \max(\alpha_1'/\omega_1, \cdots, \alpha_m'/\omega_m, -T_L). \tag{4.46}$$

The system is stable for

$$\underline{\delta}(0) < \delta < \overline{\delta}(0). \tag{4.47}$$

In the case (c), it is not said that the system is unstable outside the interval (4.47). This means that there can be another interval (e.g., $\overline{\delta}(0) < \delta_1 < \delta < \delta_2$) in which the system becomes stable. But, the system is evidently unstable (to be exact oscillatory) at $\delta = \overline{\delta}(0)$ and $\delta = \underline{\delta}(0)$. Hence, $\overline{\delta}(0)$ and $\underline{\delta}(0)$ are actually the delay margins for $\gamma = 0$.

4.4 Robust stability condition for $\gamma \neq 0$

In this section, we consider the case where both gain and delay time mismatches exist.

When $\gamma > 0$ or $\gamma < 0$, the $R[\gamma]$-loci become circles as shown in Fig. 4.2. These circles are the mirror images of the equi-M lines of the Hall diagram. To state the robust stability condition for general values of γ, we need one more definition; i.e., the locus of $P(j\omega)$ for $\omega = -\infty \sim \infty$ is referred to as the *complete P-locus*. We focus upon the cases which correspond to (b) and (c) of Theorem 4.2. For this case, Bao and Araki derived the following theorem [6] (for simplicity, we show their theorem for $\gamma > 0$).

Theorem 4.3 (The mismatch of gain is positive ($\gamma > 0$).)

Consider the system of Fig. 2.4 with the parameter errors given by (4.29). Assume that $P(0) > 0$, $\arg P(j\omega)$ decreases monotonously and that the P-locus does not encircle nor intersect the point $-1/\gamma$. Assume that the P-locus and the $R[\gamma]$-locus cross at m points $\mathrm{A}_1,\cdots,\mathrm{A}_m$, and that, at the point A_i, $\omega = \omega_i$ ($\omega_1 < \omega_2 < \cdots < \omega_m$) on the P-locus and $\alpha = \alpha_i(> 0)$ and $\alpha_i'(< 0)$ on the $R[\gamma]$-locus. Let $\overline{\delta}(\gamma)$ and $\underline{\delta}(\gamma)$ be defined by

$$\overline{\delta}(\gamma) = \min(\alpha_i/\omega_m), \tag{4.48}$$

$$\underline{\delta}(\gamma) = \max(\alpha_i'/\omega_m, -\pi/\omega_m, -T_L). \tag{4.49}$$

Then, the system is stable for

$$\underline{\delta}(\gamma) < \delta < \overline{\delta}(\gamma). \tag{4.50}$$

This theorem gives necessary and sufficient boundaries only for the case in which the P-locus and $R[\gamma]$-locus cross at one point. Furthermore, their theorem for $\gamma < 0$ does not always give necessary and sufficient boundaries even for such a case.

On the other hand, we can derive the following theorem.

Theorem 4.4 Consider the system of Fig. 2.4 with the parameter errors given by (4.29). Assume that $P(0) > 0$ and that the complete P-locus does not encircle nor intersect the point $-1/\gamma$ when $\gamma \neq 0$. Assume that the P-locus and the $R[\gamma]$-locus cross at m points $\mathrm{A}_1,\cdots,\mathrm{A}_m$, and that, at the point A_i, $\omega = \omega_i$ on the P-locus and $\alpha = \alpha_i(> 0)$ and $\alpha_i'(< 0)$ on the $R[\gamma]$-locus. Let $\overline{\delta}(\gamma)$ and $\underline{\delta}(\gamma)$ be defined by

$$\overline{\delta}(\gamma) = \min(\alpha_1/\omega_1, \cdots, \alpha_m/\omega_m), \tag{4.51}$$

$$\underline{\delta}(\gamma) = \max(\alpha_1'/\omega_1, \cdots, \alpha_m'/\omega_m, -T_L). \tag{4.52}$$

Then, the system is stable for

$$\underline{\delta}(\gamma) < \delta < \overline{\delta}(\gamma). \tag{4.53}$$

Proof. When $\delta = 0$,

$$P(j\omega)Q(j\omega) = \gamma P(j\omega). \tag{4.54}$$

Therefore, by the first assumption and by Theorem 4.1, the system is stable when $\delta = 0$. Now, increase or decrease δ from 0. Since the Nyquist locus of $P(s)Q(s)$ continuously depends on δ, it does not encircle the point -1 until (4.40) is satisfied for the first time. Satisfaction of (4.40) is equivalent to the condition that the P-locus and the $R[\gamma]$-locus cross and, at the same time, the values of ω and α at the crossing point satisfy $\alpha = \delta\omega$. Therefore, the system reaches stability limits (i.e., the Nyquist locus of $P(s)Q(s)$ passes the point -1) for the first time if and only if $\delta = \min(\alpha_1/\omega_1, \cdots, \alpha_m/\omega_m)$ or $\delta = \max(\alpha'_1/\omega_1, \cdots, \alpha'_m/\omega_m)$. Noting that $\delta \geq -T_L$, we can conclude that the system is stable for δ satisfying (4.53).

Q.E.D.

In parallel to the case of Theorem 4.2, we can assure that $\overline{\delta}(\gamma)$ and $\underline{\delta}(\gamma)$ are the delay margins at γ. The above condition gives a sharper result than Theorems 5 and 6 in [6].

4.5 Example

Here, we discuss the robustness of the state-predictive 2DOF-LQI-obs servo system of Example 3.2 in Section 3.6.

First, we give an example to show the procedure to obtain the stability region of the state-predictive 2DOF-LQI-obs servo system using a minimal-order optimal observer of Example 3.2 by Theorem 4.4. The P-locus of the system for $\alpha^2 = 1$ and $R[\gamma]$-locus for $\gamma = 0.2$ are shown in Fig. 4.3. In this case, the P-locus and the $R[0.2]$-locus cross at three points, and the values of ω, α and α' at the crossing points are

$$\begin{aligned} \omega_1 &= 0.56, \quad \alpha_1 = 0.929, \quad \alpha'_1 = -5.35 \\ \omega_2 &= 2.59, \quad \alpha_2 = 5.24, \quad \alpha'_2 = -1.04 \\ \omega_3 &= 4.17, \quad \alpha_3 = 1.31, \quad \alpha'_3 = -4.98 \end{aligned}$$

Therefore, when $\gamma = 0.2$, the control systems remain stable for $-0.401 < \delta < 0.313$.

For the state-predictive 2DOF-LQI-obs servo systems with the optimal minimal-order observer for $\alpha^2 = 1$ and $\alpha^2 = 1000$, we calculated the delay margins at several values of γ and drew the stability regions around the origin on the γ–δ plane. The stability regions obtained by Theorem 4.4 for these systems are shown in Fig. 4.4.

From these regions, we can find that the state-predictive 2DOF-LQI-obs servo system for $\alpha^2 = 1$ is more robust than the system for $\alpha^2 = 1000$. The gains of the sensitivity function $S(s)$ and the complementary sensitivity function $T(s)$ at the plant input for our state-predictive 2DOF-LQI-obs servo system are shown in Fig. 4.5, where solid lines are for $\alpha^2 = 1$, and dashed lines are for $\alpha^2 = 1000$. This figure shows that the complementary function for $\alpha^2 = 1000$ is larger than that for $\alpha^2 = 1$ in the high frequency range. This agrees with the result of the stability regions for $\alpha^2 = 1$ and $\alpha^2 = 1000$.

Next, we compare the stability regions obtained by the condition derived by Bao and Araki [6] and by Theorems 4.2 and 4.3. The stability region obtained by Bao-Araki's condition is shown in Fig. 4.6 by the dotted line, while the stability region obtained by Theorem 4.4 by the solid line. This confirms that the stability region on the γ–δ plain obtained by Theorem 4.4 is larger than that by Bao-Araki's condition.

4.6 Concluding remarks

In this chapter, we studied robust stability of state-predictive servo systems for plants with a pure delay. We derived a robust stability condition in general case that the stability of the control system is determined by the roots of the characteristic equation (4.38) for the robust stability. In particular, in the case in which the modeling errors exist only in the estimates of the gain and the delay time, we gave a new robust stability criterion to obtain the stability region graphically. Using this criterion, we can test robust stability of the system by means of the Nyquist plots of the complementary sensitivity function and the error function, and obtain the "necessary and sufficient" stability region on the relative gain mismatch–delay time mismatch plane from the relation between the Nyquist plots.

In parallel to Sections 4.3 and 4.4, we can derive robust stability conditions for state-predictive regulators and the Smith control systems. Namely, if we replace the definition of $P(s)$ by those given in the following, Theorems 4.1, 4.2 and 4.4 hold for those control systems. The definitions of the matrices and transfer functions will be summarized below.

State-predictive regulator with an observer (Fig. 4.7):

$$P(s) = e^{-T_L s} C(sI - A - BF)^{-1} B \cdot F e^{AT_L} \{D(sI - \widehat{A})^{-1} K - L\} \qquad (4.55)$$

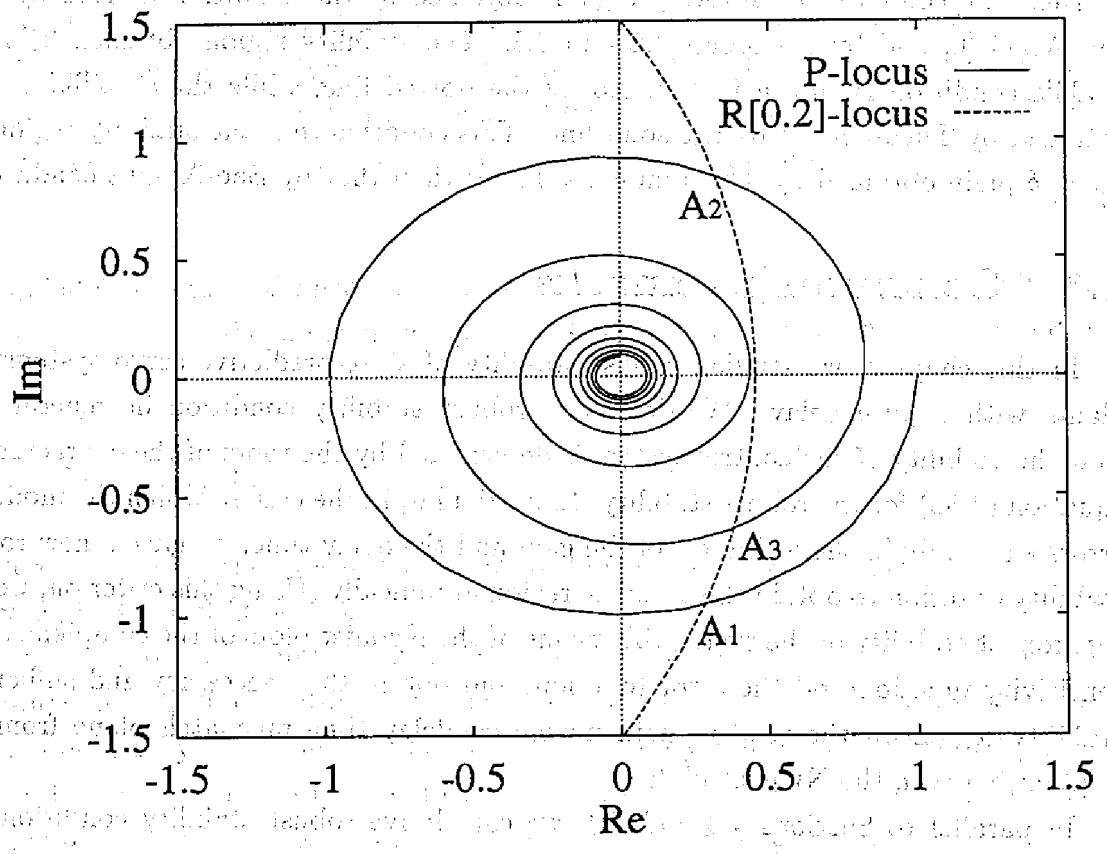

Fig. 4.3: P-loci and $R[\gamma]$-locus

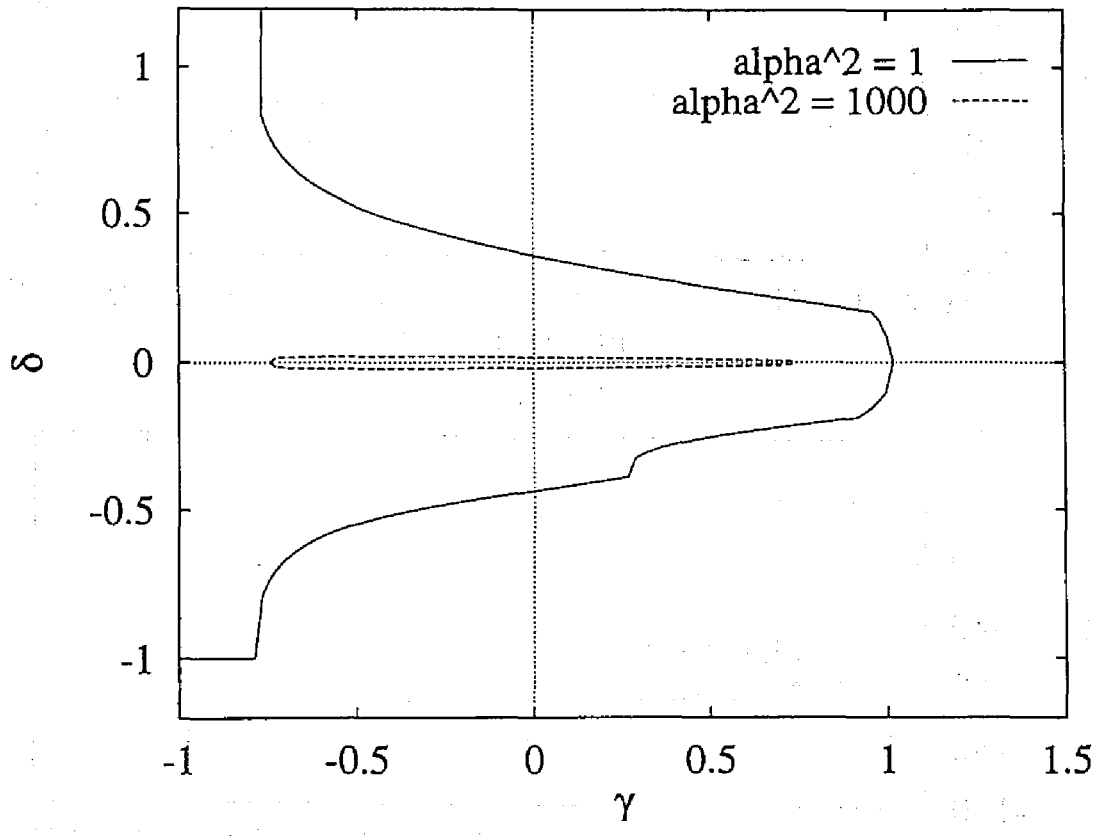

Fig. 4.4: Stability regions of the state-predictive servo system

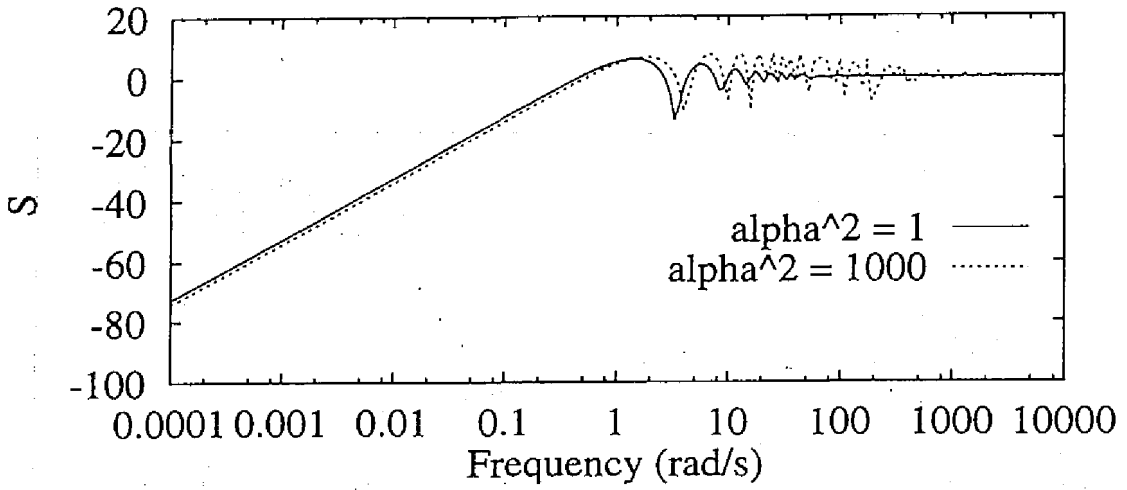

(a) $S(s)$

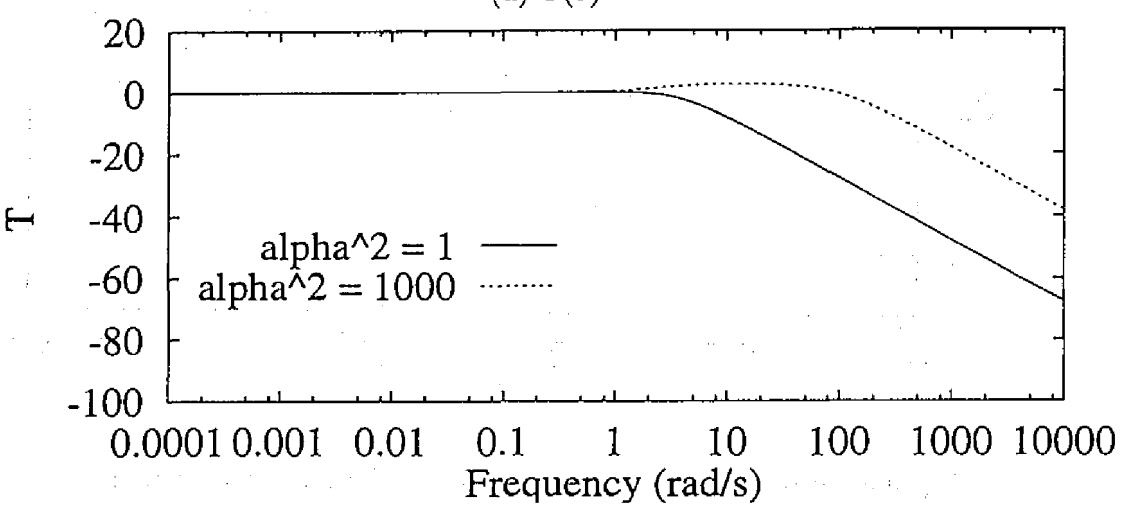

(b) $T(s)$

Fig. 4.5: Gains of $S(s)$ and $T(s)$ at the plant input

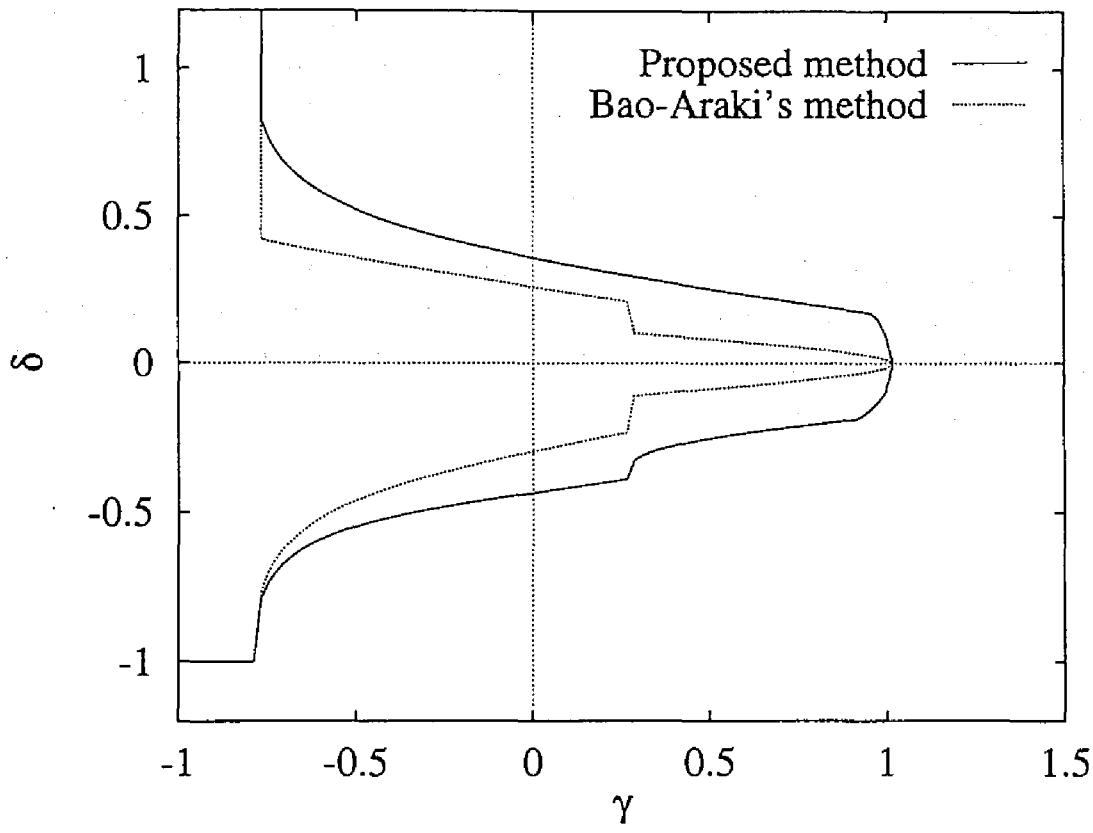

Fig. 4.6: Stability regions of the state-predictive servo system by our theorem and by Bao-Araki's theorem

Smith controller (Fig. 4.8):

$$P(s) = \frac{G(s)G_c(s)e^{-T_L s}}{1 + G(s)G_c(s)} \tag{4.56}$$

A, B, C and T_L are the parameters of the plant model (4.1), (4.2) and (4.3). F is the feedback gain such that the closed-loop coefficient matrix $A + BF$ has appropriate properties including stability. In (4.56), $G_c(s)$ is a controller designed for the lumped parameter part of the plant.

We could derive more general results from the viewpoint of complementary sensitivity function if the stability of the nominal system is guaranteed beforehand. Namely, assume that the modeling error of the transfer function of the plant is in the form

$$\text{Real Plant} = \{1 + Q(s)\}e^{-T_L s}G(s)$$

where $Q(s)$ is a general transfer function giving the relative error. Then, the stability of the control system can still be judged by the roots of the characteristic equation (4.38) for the robust stability. This can be proved from the consideration stated just above the equation (4.39).

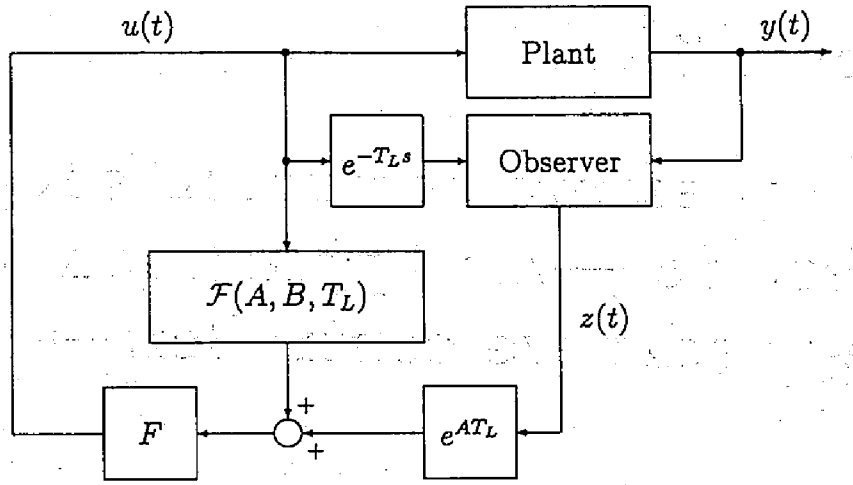

Fig. 4.7: State-predictive regulator

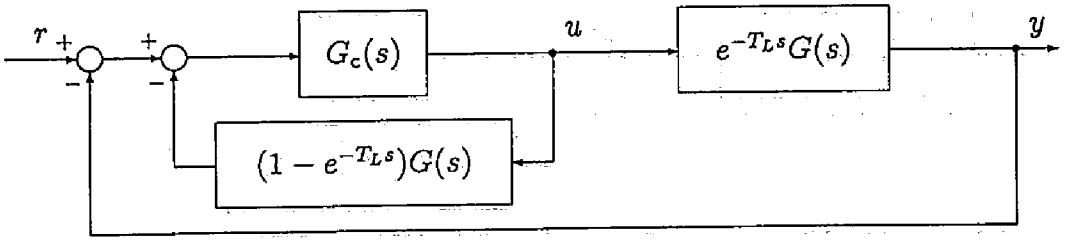

Fig. 4.8: The Smith control systems

Chapter 5

Blood pressure control in surgical operations —An application of state-predictive controllers—

Maintenance of blood pressure at a substantially low level has several advantages in surgery. It reduces intraoperative bleeding and clearly reveals detailed anatomical structures in the operative field which otherwise might be obscured by blood, thus facilitating a more accurate and speedy operation. Also, it may spare blood transfusion and prevent the side-effects such as increased risk of sepsis and organ failure. Despite these advantages, deliberate hypotension has not gained as widespread popularity as it deserves because it is difficult to manipulate the infusion rate of a hypotensive solution to keep the blood pressure at a sufficiently low level, while still above the critical limit.

Since the late 1970's, blood pressure control systems have been developed. The early researches chiefly aimed at cardiovascular surgery postoperative blood pressure management. Sheppard [40] used a modified PID controller, but this controller could not cope with individual differences of the response to hypotensive drugs. Adaptive control was applied by Widrow [47] and Arnsparger et al. [3], but these did not work well when disturbances existed. Koivo [24] developed a blood pressure control system based on optimal control which kept the blood pressure at a low level but the blood pressure range which could be set as the reference value was narrow. All of these were concerned with restoration of abnormal blood pressure to normal.

Researches were started recently to try to keep blood pressure at an abnormal level with the intention of facilitating surgical operations or medical treatments. Masuzawa and Fukui [33] applied optimal control using an impulse identification method, and developed a blood pressure control system to keep blood pressure at a low level, but the controlling time of each experiment was shorter than 70 minutes. Fukui and Masuzawa

[14] applied fuzzy logic to blood pressure control to keep blood pressure at a high level as a medical treatment for cancer, but oscillations could easily arise because the existence of the dead time in the response was not considered at the design stage.

Considering the above results of the former researches, we must take the dead time existing in the responses to drugs into account in developing a blood pressure control system. Then, we applied the state-predictive servo controller, which we dealt with in preceding chapters, to the blood pressure control, and developed a blood pressure control system which can cope with the dead time in the responses to drugs. This system monitors conditions (i.e., blood pressure, heart rate and blood loss) during surgical operations and keeps low blood pressure by changing the infusion rate of the hypotensive drug. In order to evaluate the accuracy and reliability of this system, we experimented on dogs.

In Section 5.1, the mean arterial pressure response of dogs to a hypotensive drug is modeled from the dose responses for the constant drug infusion. In Section 5.2, we design the blood pressure control system using the state-predictive servo controller for the model obtained in Section 5.1, and show the simulation results of the designed system with the modeling errors. In Section 5.3, we apply the controller designed in Section 5.2 to dogs, and show the results of the experiments on dogs.

5.1 Modeling of blood pressure response to hypotensive drug

The purpose of our study is to control the blood pressure by a hypotensive drug; namely, the controlled variable y is the mean arterial pressure (in the following, abbreviated to MAP) and the manipulating variable u is the infusion rate of the hypotensive drug. We made the dynamical model describing the relation of y to u based on the dose responses for the constant drug infusion. As the hypotensive drug, we used the trimethaphan camsilate. In this section, we report the modeling process.

The MAPs of two dogs infused with the hypotensive drug with constant rates were measured. The infusion rates for each dogs were set to 10.0, 20.0, 40.0 μg/kg/min and 40.0, 80.0, 160 μg/kg/min, respectively. Typical response curves are shown in Fig. 5.1. From those data, it was estimated that the system includes

(i) a pure delay,

(ii) some nonlinearity (or nonlinearities) of the saturating type, and

(iii) the dynamics in the non-saturating domain can be approximated by a first order delay.

The first estimation is made from the fact that every response is accompanied with a dead time at the beginning of infusion. The second estimation is made from the facts that the data can be classified into two groups depending upon whether the infusion rate exceeds a certain level, and that the responses corresponding to small infusion rates reach steady states which depend upon the infusion rates, while the responses corresponding to large infusion rates reach a steady state which does not depend on the infusion rate. The third estimation was made from the shapes of the response curves. Based on the first and third estimations we assumed the next dynamics for the non-saturating domain:

$$\begin{cases} \dfrac{dx(t)}{dt} &= -\dfrac{1}{T}x(t) + \dfrac{K_{\mathrm{m}}}{T}u(t), \\ y(t) &= x(t - T_L), \end{cases} \tag{5.1}$$

where $x(t)$ is a state variable, which corresponds to the MAP at $t + T_L$ in this case, T is a time-constant, K_{m} is a gain and T_L is a dead time.

From the second estimation, we assumed the next dynamics with a feedback with a dead zone for large infusion rates:

$$\begin{cases} \dfrac{dx(t)}{dt} &= -\dfrac{1}{T}x(t) + \dfrac{K_{\mathrm{m}}}{T}\{u(t) - w_{\mathrm{m}}(t)\}, \\ \dfrac{dw_{\mathrm{m}}(t)}{dt} &= x(t) - c, \qquad \text{for} \quad x(t) \geq c \\ y(t) &= x(t - T_L), \end{cases} \tag{5.2}$$

where $w_{\mathrm{m}}(t)$ is a state of an integrator in the feedback loop, c is the width of the dead zone, which corresponds to the steady state value of MAP for large infusion rates. These dynamics can be regarded as a simplified model of the renin-angiotensin system which is activated when the arterial blood pressure falls below a threshold level [41]. It should be noted that the value of the integrator in the feedback loop must be reset when the MAP becomes higher than the steady state value of MAP for large infusion rates. Therefore, we added the element for resetting the integrator

$$\frac{dw_{\mathrm{m}}(t)}{dt} = -kw_{\mathrm{m}}(t), \quad \text{for} \quad x(t) < c, \tag{5.3}$$

where k is a sufficiently large positive real number.

As we can find from the response curves of Fig. 5.1, the time-constant in decrease of MAP is different from the one in increase of MAP. So, we set

$$T = \begin{cases} T_1, & \text{when MAP is decreasing,} \\ T_2, & \text{when MAP is increasing.} \end{cases} \tag{5.4}$$

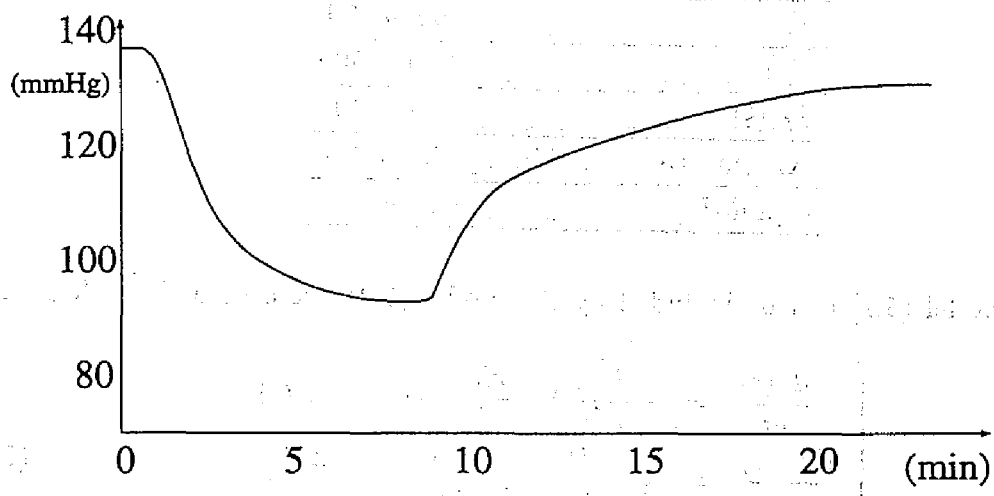

(a) For small infusion rate

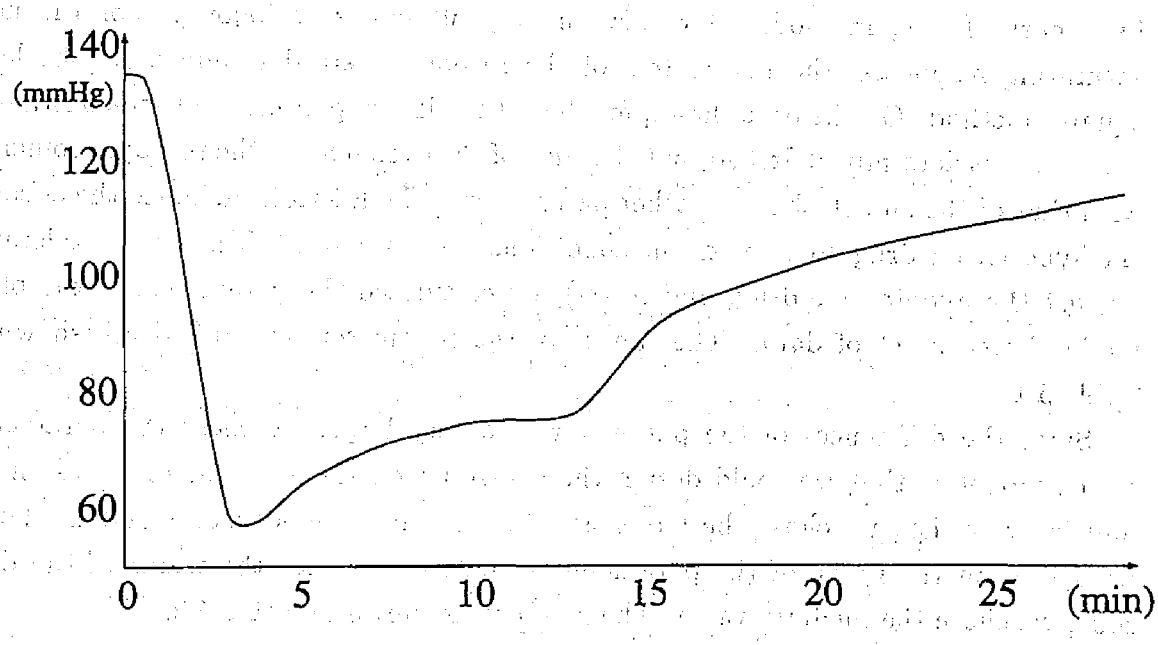

(b) For large infusion rate

Fig. 5.1: Dose response curves for trimethaphan camsilate

Table 5.1: The ranges of model parameters obtained from dose responses

T_1 (s)	$90 \sim 200$
T_2 (s)	$270 \sim 500$
T_L (s)	$30 \sim 40$
K_m (mmHg·kg·min/μg)	$2.0 \sim 4.5$
c (mmHg)	$52 \sim 57$

Since the model (5.1) can be included by the model (5.2), we obtained the following system:

$$\begin{cases} \dfrac{dx(t)}{dt} &= -\dfrac{1}{T}x(t) + \dfrac{K_\mathrm{m}}{T}\{u(t) - w_\mathrm{m}(t)\} \\ \dfrac{dw_\mathrm{m}(t)}{dt} &= \begin{cases} x(t) - c, & \text{for} \quad x(t) \geq c \\ -kw_\mathrm{m}(t), & \text{for} \quad x(t) < c \end{cases} \\ y(t) &= x(t - T_L). \end{cases} \tag{5.5}$$

Now, we determined the parameters of the model (i.e., the time-constant in decrease T_1, the time-constant in increase T_2, the dead time T_L, the gain of the first order delay K_m and the width of the dead zone c) from the responses of the MAP of two dogs by a curve fitting method. Our curve fitting method is as follows. For the non-saturating responses, the parameters of the response were determined by the least squares method. On the other hand, for the saturating responses, the time-constant in decrease was determined first so that the time of the overshoot of the response coincides with that of the model, then the other parameters were determined. Since the effect of the hypotensive drug differs with the conditions of dogs (depth of anesthesia, tolerance against the hypotensive drug, and so on), we calculated the parameters of the plant model for each set of data. The ranges of the parameters calculated are shown in Table 5.1.

Since the differences of the parameters are very large, we chose the parameters of the model so that we could design the controller on the safe side or to lessen the infusion rate, i.e., we chose the larger gain, the smaller time-constant and the larger dead time in the range of the parameters calculated. As for the width of the dead zone, we chose the medium value. The result is as shown in Table 5.2.

From the dose responses of this model, we found that the overshoots of the responses were larger than the real responses. So, we added a nonlinear function f to the model so that the overshoots matched the real responses. As a result, we obtained the model

Table 5.2: The determined values of model parameters

T_1 (s)	90
T_2 (s)	270
T_L (s)	40
K_m (mmHg·kg·min/μg)	4.5
c (mmHg)	54.5

shown in Fig. 5.2:

$$\begin{cases} \dfrac{dx(t)}{dt} &= -\dfrac{1}{T}x(t) + \dfrac{K_m}{T}\{u(t) - w_m(t)\} \\ \dfrac{dw_m(t)}{dt} &= \begin{cases} x(t) - c, & \text{for} \quad x(t) \geq c \\ -kw_m(t), & \text{for} \quad x(t) < c \end{cases} \\ y(t) &= f(x(t - T_L)), \end{cases} \tag{5.6}$$

where

$$f(x) = \begin{cases} x, & \text{for} \quad x \leq c \\ c\left\{\left(\dfrac{x}{c} - 1\right) + \left(\dfrac{1}{p}\right)^{\frac{p}{p-1}}\right\}^{\frac{1}{p}} - c\left\{1 - \left(\dfrac{1}{p}\right)^{\frac{1}{p-1}}\right\}, & \text{for} \quad x > c \end{cases} \tag{5.7}$$

with $p = 4$.

5.2 State-predictive blood pressure control system and simulation results

In this section, we design the blood pressure control system using the state-predictive servo controller (Fig. 2.4) for the model of the responses of dogs identified in Section 5.1, and show the simulation results of this system including the case where mismatches of the plant parameters exist.

We design a state-predictive servo system for the plant model without the feedback in Fig. 5.2 but with the dead zone (i.e., the model that consists of the first order delay with a nonlinear function f as shown in Fig. 5.3). Then, the infusion rate determined by the state-predictive servo controller is obtained by substituting

$$A = -\frac{1}{T_1}, \quad B = \frac{K_m}{T_1}, \quad C = 1 \tag{5.8}$$

into (4.11). Note that no observer is needed because the output of the plant is the state variable of the plant.

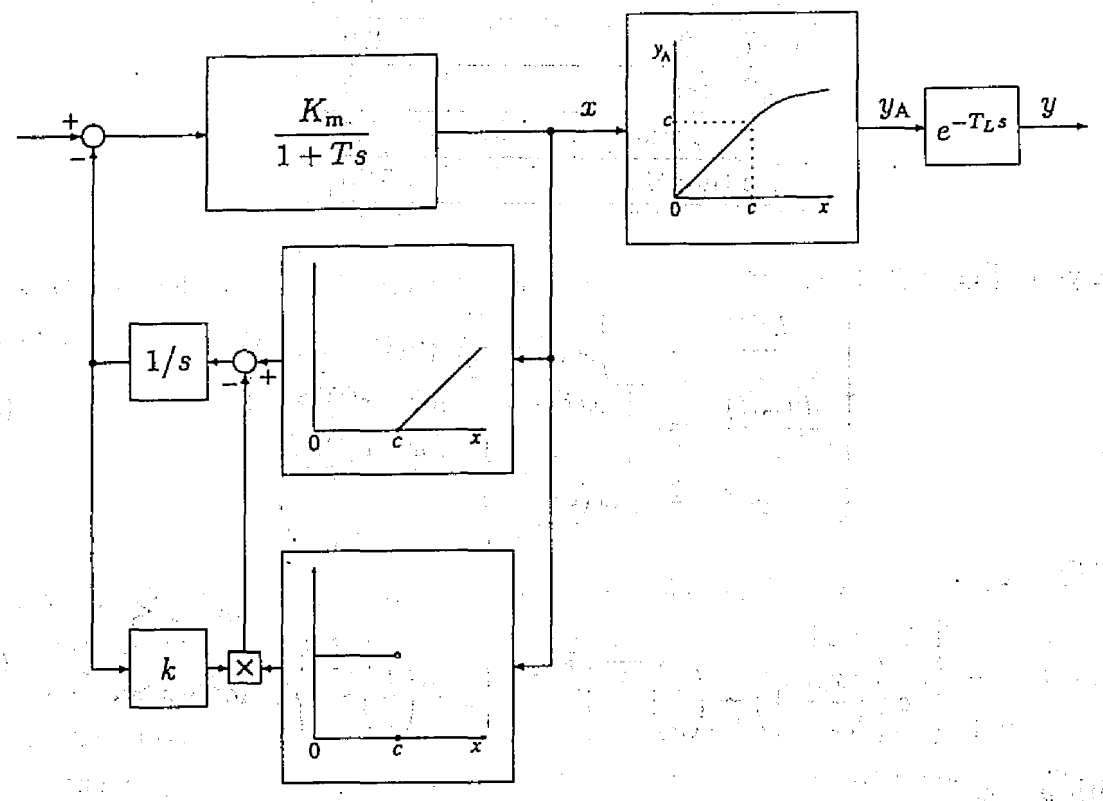

Fig. 5.2: Model obtained from dose responses

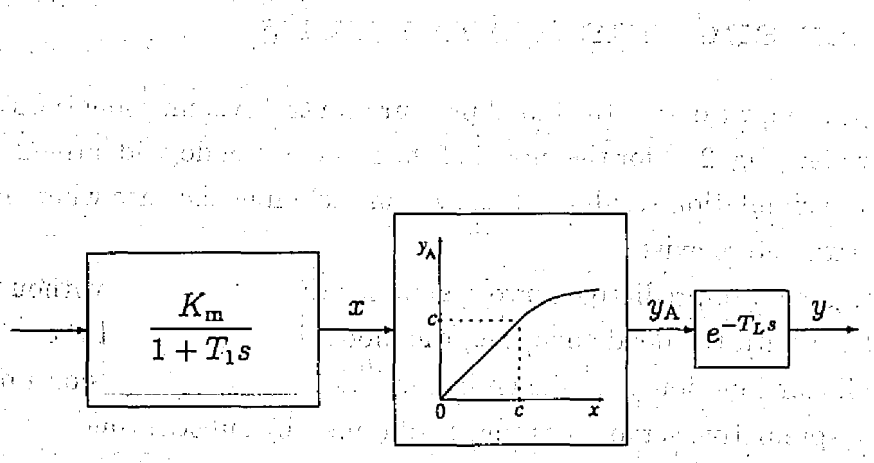

Fig. 5.3: Model for designing a state-predictive servo system

The specifications of the control system are as follows.

settling time T_s:	$300 \leq T_s \leq 1200$ s
overshoot A_o:	$A_o \leq 0.2r$
the steady state value of MAP y_∞:	$0.9r \leq y_\infty \leq 1.1r$

Here, r is the reference value for MAP.

We set the poles of the control system at -0.01 and -0.02 for the first order delay model, and simulated the step responses of this blood pressure control system.

The step response of the blood pressure control system without the modeling error (i.e., with no mismatches of the model) is shown in Fig. 5.4. From Fig. 5.4, we can find that the response settles to the reference by about 600 s with no overshoot and no steady state error. Next, we consider the case where the model has the parameter mismatches. Parameter mismatches are chosen in the ranges obtained in Section 5.1, i.e., between 2.0 and 4.5 mmHg·kg·min/μg for the gain K_m, between 90 and 200 s for the time-constant T_1, and between 30 and 40 s for the dead time T_L.

Case 1 (K_m has a modeling error)

The responses for $K_\mathrm{m} = 2.0$ and $K_\mathrm{m} = 3.0$ mmHg·kg·min/μg are shown in Fig. 5.5(a). Fig. 5.5(a) shows that as the mismatch becomes larger, the settling time becomes longer, but the system remains stable and satisfies the specifications.

Case 2 (T_1 has a modeling error)

The responses for $T_1 = 120$ and 200 s are shown in Fig. 5.5(b). Fig. 5.5(b) shows that as the mismatch becomes larger, the settling time becomes longer, and the responses turn to have small overshoots. But the system remains stable and satisfies the specifications.

Case 3 (T_L has a modeling error)

The response for $T_L = 30$ s is shown in Fig. 5.5(c). Fig. 5.5(c) shows that this mismatch has little effect on the settling time, the overshoot and the stability.

Case 4 (All parameters have the largest modeling errors in the ranges obtained in Section 5.1)

The response for $K_\mathrm{m} = 2.0$ mmHg·kg·min/μg, $T_1 = 120$ s and $T_L = 30$ s is shown in Fig. 5.5(d). The settling time is longer and the overshoot is larger than other cases, but the system remains stable and satisfies the specifications.

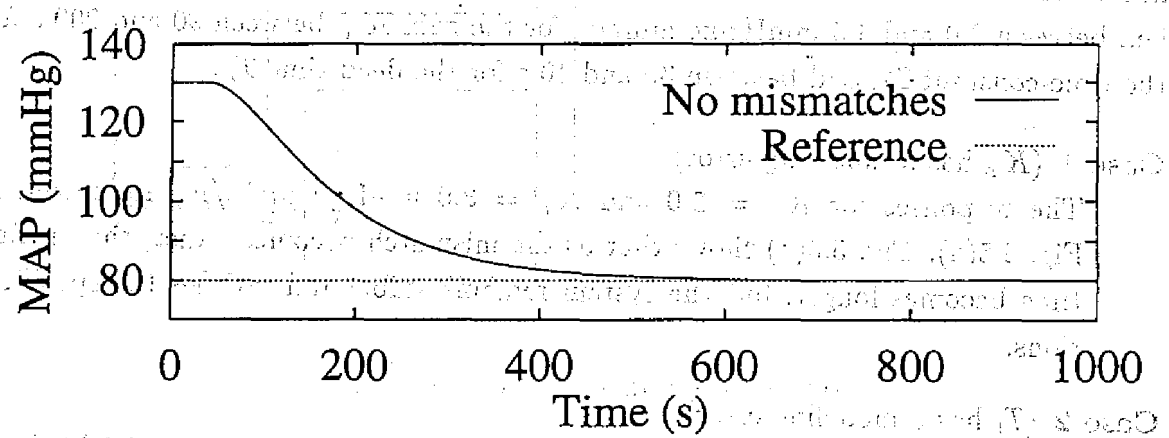

Fig. 5.4: Simulation result of the system with no mismatches

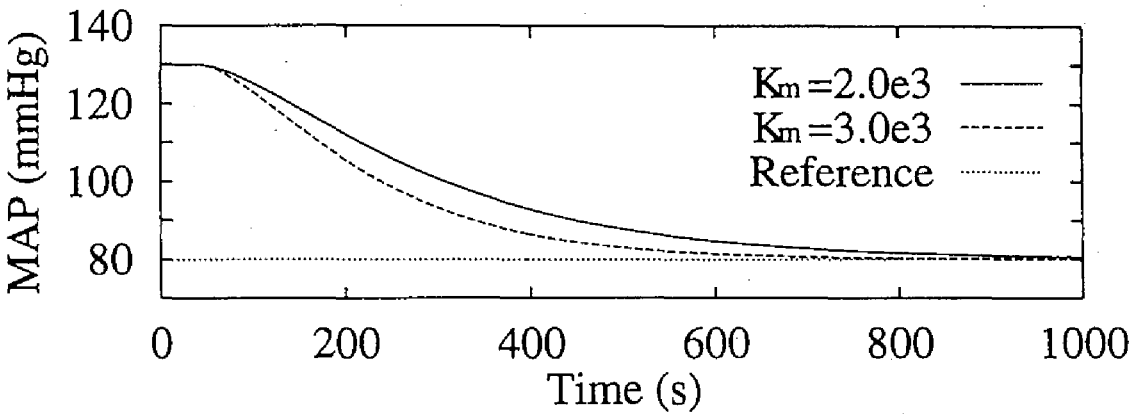

(a) Gain K_m has a modeling error

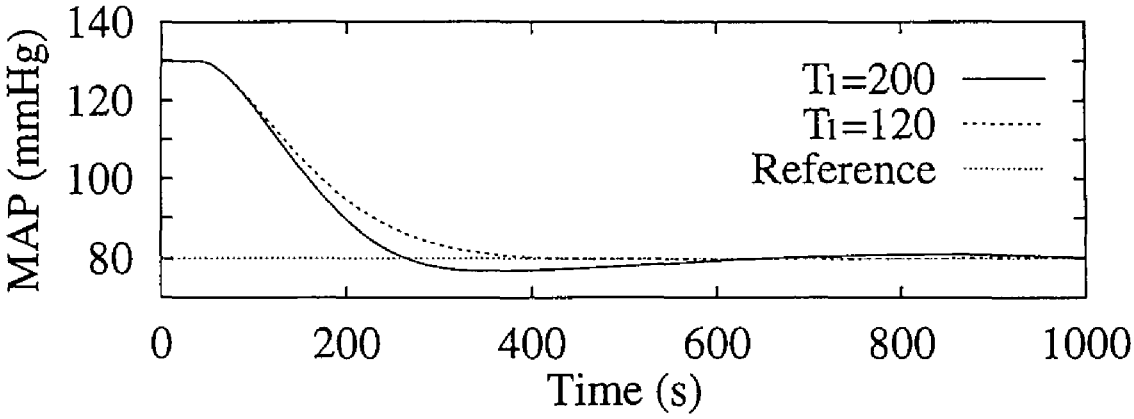

(b) Time constant T_1 has a modeling error

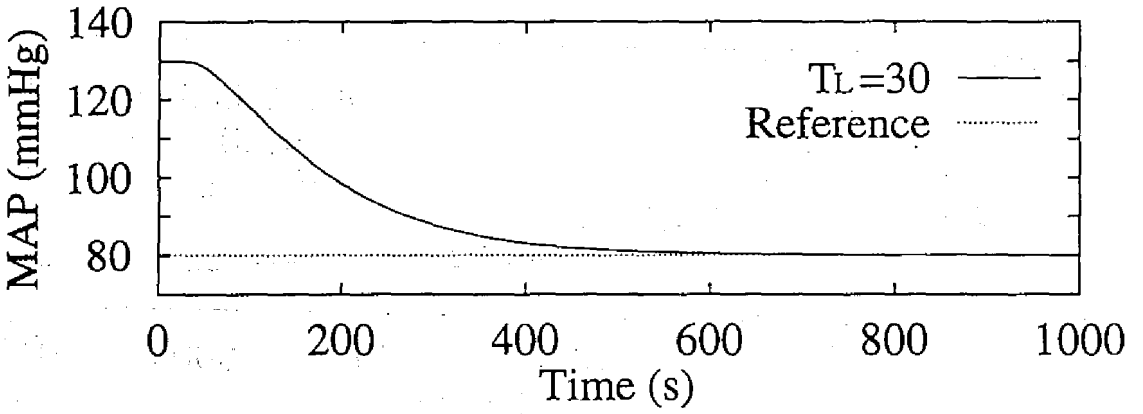

(c) Dead time T_L has a modeling error

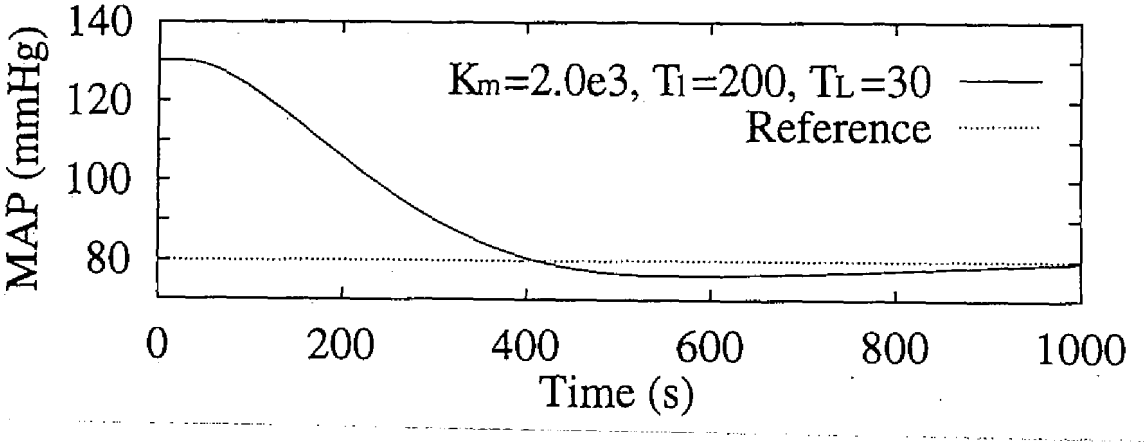

(d) K_m, T_1 and T_L have modeling errors

Fig. 5.5: Simulation results of the system with mismatches

Furthermore, the stability region of this control system in the gain–delay plane obtained using the robust stability criterion derived in Chapter 4 is shown in Fig. 5.6. This figure shows that the control system has enough stability margin.

From the above consideration, we concluded that the blood pressure control system satisfies the specifications even if the model has the mismatches in the range of Table 5.2, and has enough stability.

5.3 Experiments

In this section, we report the implementation of the blood pressure control system designed in Section 5.2 and the results of the experiments of blood pressure control on dogs.

5.3.1 Structure of blood pressure control system

The structure of the blood pressure control system is shown in Fig. 5.7. The system measures the three values: MAP, heart rate and blood loss. MAP is measured by a blood pressure amplifier (Nihon Koden AP-641G) with a pressure/voltage transducer connected with a cannula inserted into the artery of dogs. The heart rate is measured by an instantaneous heart rate measuring instrument (Nihon Koden AT-601G) and a strain pressure wave amplifier (Nihon Koden AP-601G) from the blood pressure values measured by AP-641G. The blood loss is measured by a balance (Chyo Balance MF6000). The values of MAP, heart rate and blood loss are transferred as analogue signals to an A/D converter (Micro Science DAS-1098), and converted to digital signals. Then, they are transferred to a personal computer (NEC PC-H98 model 70). Harvard Pump 22 is used as an infusion pump for the hypotensive drug, and IVAC 560 is used as an intravenous fluid pump. The infusion pump and the intravenous fluid pump are connected with personal computer by RS-232C cables, and controlled by communication.

In experiments, the condition of dogs are analyzed from the values of MAP, heart rate and blood loss, and the infusion rate of hypotensive drug is determined and sent out to the pump every 1 second. The infusion rate of intravenous fluid is determined every 10 seconds.

MAP, heart rate, total blood loss, blood loss per hour, the infusion rate of hypotensive drug and the infusion rate of intravenous fluid are displayed on the computer display, and the changes of MAP, heart rate and total blood loss are shown on the display graphically.

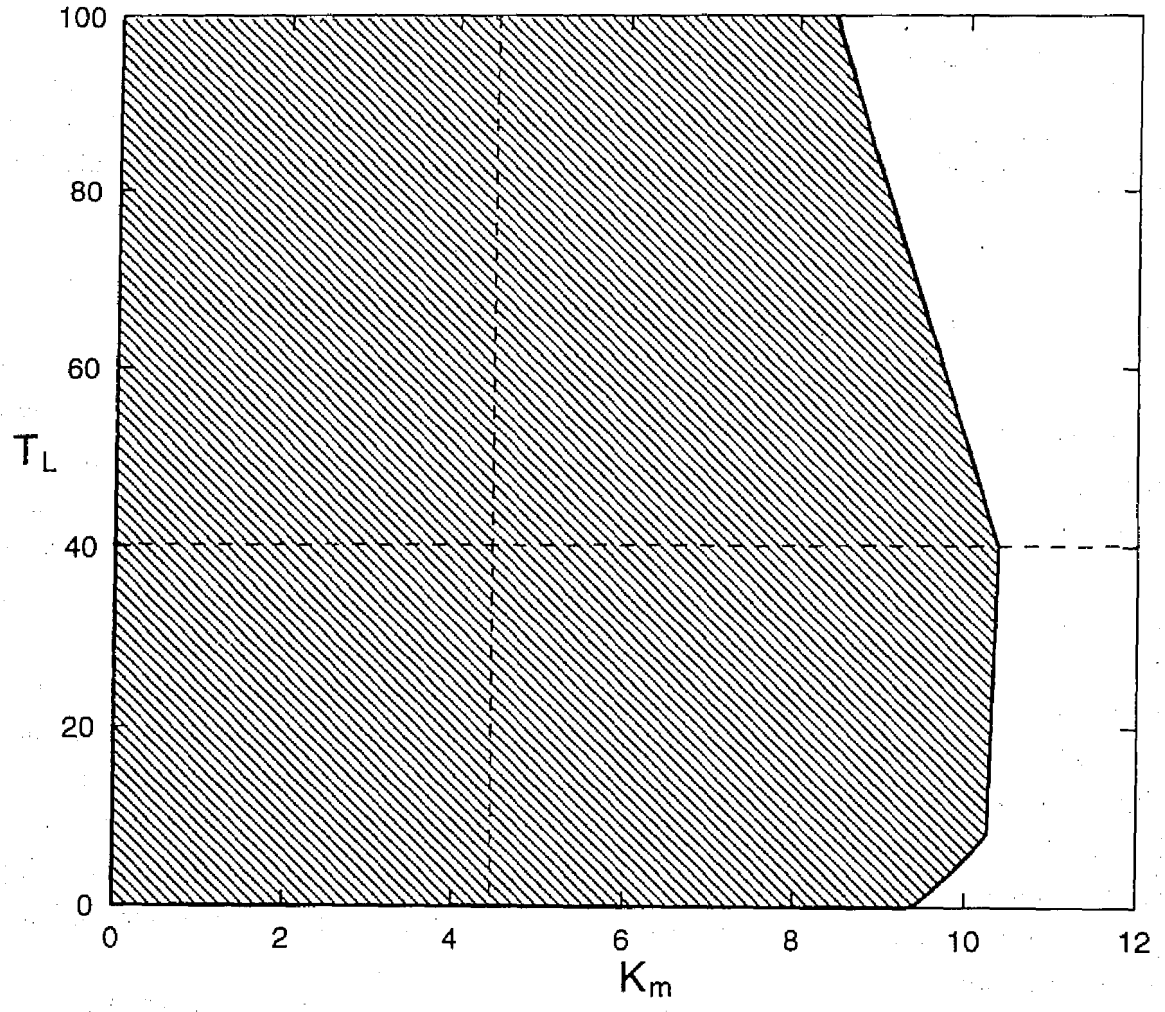

Fig. 5.6: Stability region of the blood pressure control system

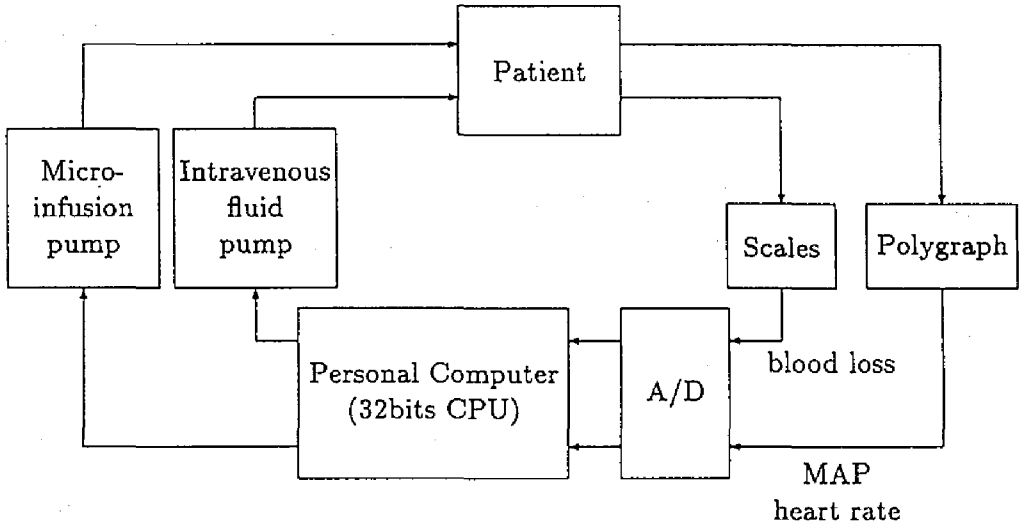

Fig. 5.7: Structure of the blood pressure control system

5.3.2 Risk preventing system

During surgical operations, it is possible that the dog is placed in danger because of various causes (e.g., too much blood loss), and that the blood pressure of the dog does not decrease enough because of the tolerance against the hypotensive drug and individual difference of dogs. In order to cope with these situations, we use the following method.

The system always analyzes the condition of the dogs, and if the dog is found to be in danger (this condition is referred to as an *emergent condition*), it starts a procedure to save the dogs out of danger (back to a *normal condition*). This is accomplished as follows. The ranges of MAP, heart rate and blood loss in which we are sure that the dog is not in danger are

- MAP: 40~200 mmHg
- heart rate: 50~300 times/min
- blood loss: 0~200 ml

If any values are out of these ranges, we regard the condition of the dogs as the emergent condition, and otherwise as the normal condition. In the normal condition, hypotensive drug is infused by the rate determined by the state-predictive servo controller. In the emergent condition, the system sounds the alarm to inform that the dog is in danger, and shows what is happening on the display. In addition, if the dog is in a very dangerous condition, i.e., the MAP is very low or blood loss is too much, then the

infusion of hypotensive drug is stopped and the infusion rate of intravenous fluid is increased, and the system waits until the MAP is in the safe range. The infusion rate of intravenous fluid is changed as follows.

- If the MAP is lower than $r - 10$ mmHg (r is the reference MAP), the infusion rate of intravenous fluid is increased to 1.5 times the current rate every 100 s.
- If the MAP is lower than 40 mmHg, the infusion rate of intravenous fluid is set to the maximal rate (999 ml/h).
- If the MAP becomes higher than r, the infusion rate is set to the initial rate.

Furthermore, in the case that the MAP becomes too low, the infusion rate of hypotensive drug is decreased as follows.

- If the MAP is lower than $r - 10$ mmHg, then the gain of the controller is divided by 1.2 in every 60 s. If the MAP is between $r - 10$ and $r - 5$ mmHg, then the gain of the controller is divided by 1.1 in every 60 s.
- If the MAP is lower than 50 mmHg, then the infusion rate of hypotensive drug is set to the half of the value determined by the state-predictive servo controller.

For the case that MAP does not decrease enough because of the tolerance against the hypotensive drug or individual differences of dogs, the infusion rate of hypotensive drug is increased as follows.

- If the MAP does not become lower than $r + 15$ mmHg within five minutes, then the gain of the controller is multiplied by 1.2.
- After five minutes, if the MAP is not lower than $r + 10$ mmHg, then the gain of the controller is multiplied by 1.2 in every 100 s. If the MAP is between $r + 10$ and $r + 7$ mmHg, then the gain of the controller is multiplied by 1.1 in every 100 s.

We dealt with the difference of the preinfusion MAP between the model and the dogs for experiments as follows, with consideration of safety of the dogs. If the preinfusion MAP is lower than 130 mmHg, the controller for the model whose equilibrium point is shifted by the difference of the preinfusion MAP is used, and otherwise the controller for the model whose equilibrium point is shifted and whose parameters with relation to blood pressure are scaled up is used.

5.3.3 Experiments on dogs

We made blood pressure control experiments on dogs using the system described above. In these experiments, we did not do any surgical operations except the one necessary for measurements, and so, the blood loss is so little as not to need to be measured. We used the anesthesia with GOF under controlled respiration to maintain a constant depth of anesthesia and lactated Ringer as an intravenous fluid.

Experiment 1 Four adult mongrel dogs were used, and their MAP was controlled seven times by the above blood pressure control system. The reference MAP was set to 60 mmHg and the MAP was controlled for three hours after settling at the reference level. The initial infusion rate of intravenous fluid is set to be 100 ml/h in all experiments.

The behaviors of MAPs and the infusion rates of hypotensive drug in representative cases are shown in Fig. 5.8. Numerical results of experiments are shown in Table 5.3. Settling time is the time that the MAP reaches in the range of reference MAP$\pm$10%, A-MAP is the averaged MAP from the settling time to the end of control, S. D. is the standard deviation of MAP from A-MAP, C-time is the time of controlling MAP and Duration is the duration of error from the reference MAP$\pm$10%. The MAP reached at the reference level in 5.8 to 26.5 minutes (16.0 $\pm$ 6.8 minutes), and the duration of error from the reference MAP$\pm$10% was 2.3 $\pm$ 3.9 minutes per hour.

5.4 Discussion

Until now, various controllers have been applied to blood pressure control [40], [47], [3], [24], [44], [33], [14], [21]. Most of these controllers (e.g. PID controllers, adaptive controllers, optimal controllers, rule-based controllers, and so on) did not take the dead time of the blood pressure response for drugs into account, and determined the infusion rate of drugs from the current blood pressure. However, in the case where the drugs to which the blood pressure response has a small time-constant (e.g. sodium nitroprusside, trimethaphan camsilate, and so on) were used, the dead time has a great effect on the stability and the transient response. For this reason, we should take the dead time into account.

As controllers for systems with a dead time, the Smith controller [42] and state-predictive controllers [32], [16] are well-known. Woodruff and Northrop [48] used a Smith controller for blood pressure control. We choose a state-predictive servo con-

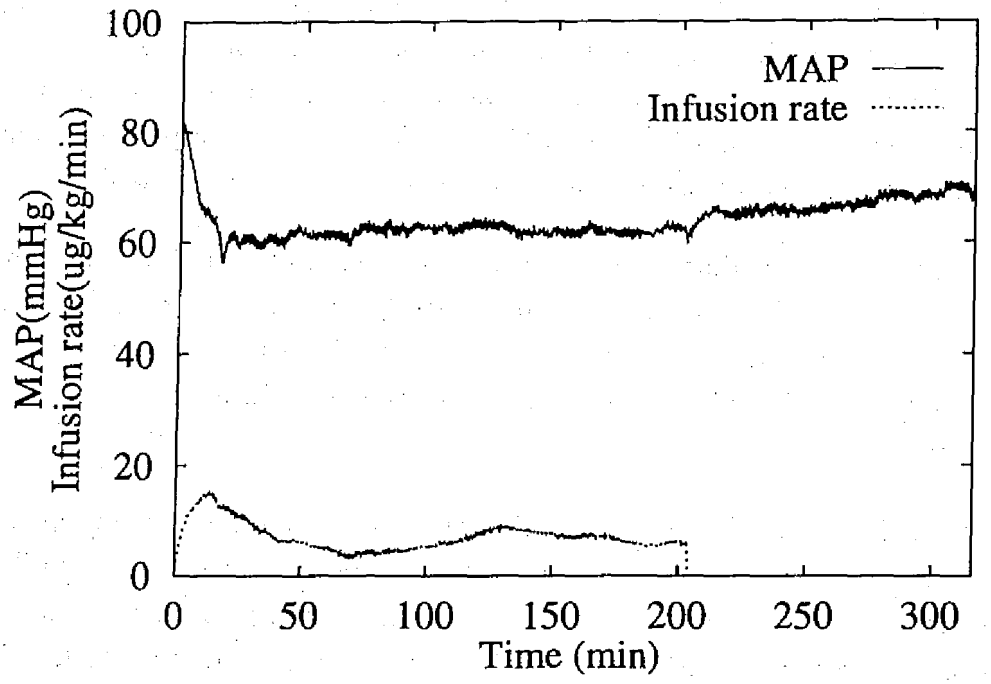

(a)

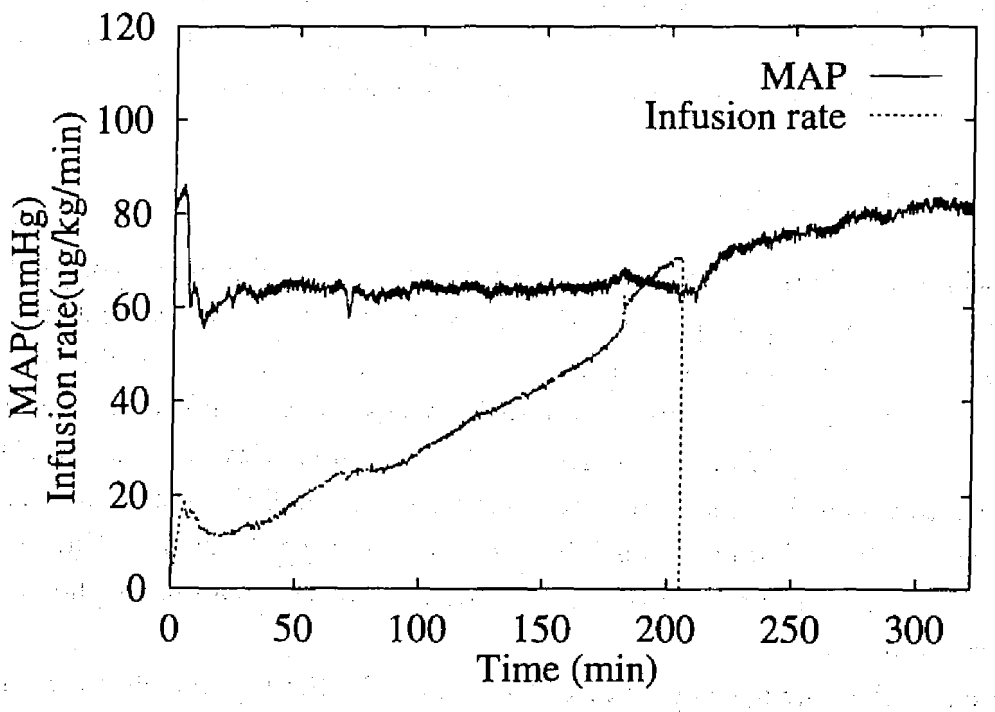

(b)

Fig. 5.8: MAP and infusion rate of Experiment 1

Table 5.3: Results of Experiment 1

	Initial MAP (mmHg)	T_s (min)	A_o (mmHg)	A-MAP (mmHg)	S. D. (mmHg)	C-time (min)	Duration (min/h)
1	111.0	16.2	26.5	63.8	0.51	194.6	3.1
2	82.5	9.7	3.2	61.7	0.20	194.1	0.0
3	83.0	5.8	0.5	63.6	1.24	199.3	0.1
4	85.0	24.1	10.2	59.9	0.51	185.9	0.2
5	108.5	13.8	17.5	64.9	0.62	200.8	11.5
6	95.0	26.5	11.5	61.9	0.41	193.3	0.2
7	87.0	16.1	12.8	62.1	0.62	202.9	0.8

T_s: Settling time
A_o: Overshoot
A-MAP: Averaged MAP from the settling time to the end of control
S. D.: Standard deviation of MAP from A-MAP
C-time: Time of controlling MAP
Duration: Duration of error from the reference MAP±10%

troller because the response speed of the system can be determined using a pole-assignment method or optimal method with respect to a quadratic performance index.

Comparing our results with other results [24], [33], times of controlling MAP of our results are much longer than the results of Koivo [24] and Masuzawa et al. [33], and S. D. of the MAP of ours are much less than theirs. Therefore, we can conclude that our system has much better stability than theirs, although the reference MAP was set to a lower level.

We tried to use nicardipine and PGE1 as hypotensive drugs. In these cases, the MAP could be maintained at 60 mmHg for more than three hours only by changing the parameters of state-predictive servo controllers. The result of an experiment using nicardipine is shown in Fig. 5.9.

However, the settling times and the overshoots of a few responses did not satisfy the specifications. From the results of these experiments, we found the following problems, which should be solved before applying our system to the clinical use.

- Overshoot caused by the initial mechanical error of the infusion pump:
  In some experiments, about 10mmHg overshoots happened. These are caused by the mechanical error of the infusion pump and the elasticity of the rubber part of syringe, namely, the real infusion rate does not coincide with the infusion rate

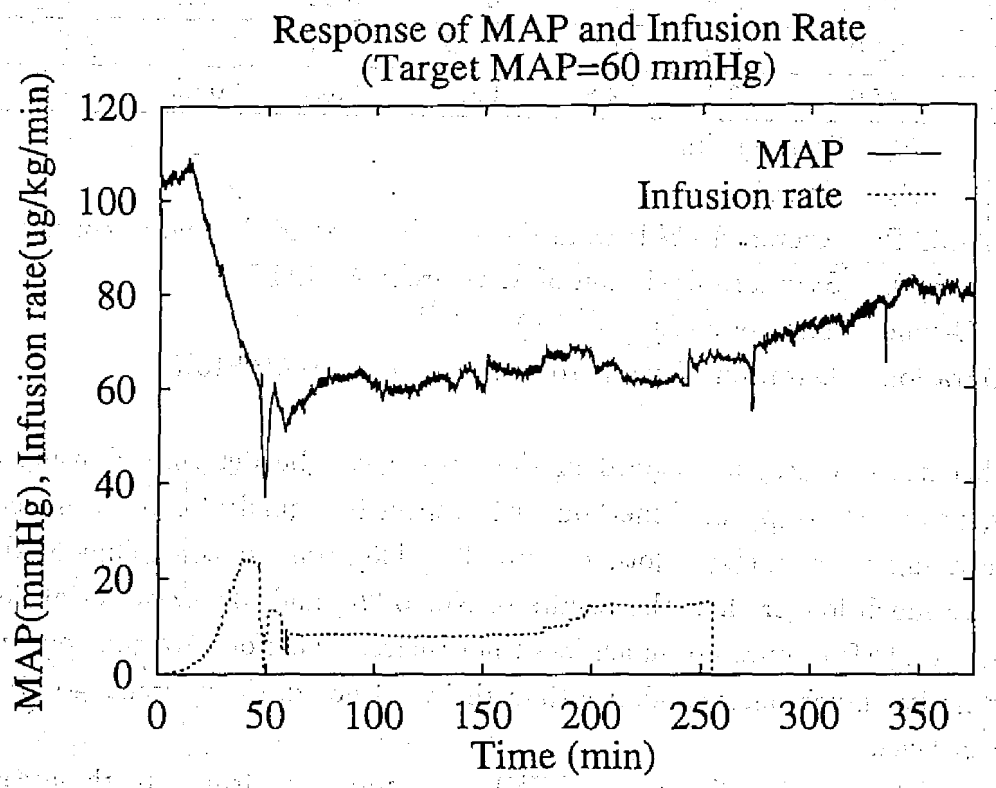

Fig. 5.9: MAP and infusion rate of an experiments using nicardipine as a hypotensive drug

determined by the state-predictive servo controller. This problem could be solved by reducing the density of hypotensive drug, but, for this, we need to change the structure of the control system and the rule for infusion rate of intravenous fluid.

- Insufficiency of the condition analysis:
  Dogs are not always safe even when MAP, heart rate and blood loss are in the safe ranges given in Subsection 5.3.2, respectively. It is necessary to make more analysis based on data covering enough kinds of situations. Further, we should add the infusion of a hypertensive drug and blood transfusion to the risk preventing system.

- Increase of the drug infusion rate:
  Since trimethaphan camsilate is a drug which dogs (and men) easily become tachyphylaxis, a very large infusion rate may sometimes be necessary to keep the MAP at a constant level for three hours. In fact, the changes of infusion rates can be classified into two types, namely, the type that the rates are almost constant regardless of time (Fig. 5.8(a)) and the type that the rates increase with time (Fig. 5.8(b)). In the case where the infusion rate increases with time, the total infusion volume becomes very large. This is not good from the safety point of view. We must find a method to keep low blood pressure by the drug infusion of a constant rate.

5.5 Concluding remarks

In order to maintain substantially low blood pressure, we developed a blood pressure control system using a state-predictive servo controller. First, we modeled the blood pressure response to hypotensive drug as a "pure delay plus a first order delay" system with a nonlinear feedback which is activated when the blood pressure is lower than a certain value. In order to cope with the dead time existing in the responses, we designed a state-predictive servo control system for this model. After simulation studies, we applied the system to dogs and assured that the control system can safely keep the blood pressure at a low level.

To increase the reliability of the system, we have to consider the following future topics.

1. eliminating the effect of mechanical error

2. coping with the tachyphylaxis

3. developing a fail-safe mechanism

4. identification of the individual dose response for increasing the accuracy and reliability of the system

Chapter 6

Conclusion

The results presented in this thesis are summarized in this chapter. In Chapter 2, we made a survey of the basic idea of the state-predictive control; i.e. we looked at the structures of the usual state-predictive servo system for the plant with a pure delay and the two-degree-of-freedom state-predictive servo system proposed by Araki and Watanabe [2]. We pointed out that the feedforward gain of the two-degree-of-freedom state-predictive servo system has been determined only by a trial-and-error method, and that the systematic design method has not been proposed.

In Chapter 3, we extended the two-degree-of-freedom design method of LQI servo systems [20] to the case in which the plant has a pure delay, based on the basic idea of state-predictive control. Moreover, we studied the property of the designed two-degree-of-freedom state-predictive LQI servo system incorporating an observer. The results can be summarized as follows.

- The feedback gain F_0 and feedforward gain H_0, which correspond to the tracking characteristics, and the feedback gain G, which corresponds to the feedback characteristics, can be determined independently. Furthermore, these gains can be determined optimally using independent quadratic-integral performance indices.

- As the state-weighting matrix of the performance index posed on the responses for step disturbances is made larger, the responses for step disturbances become quicker.

Furthermore, we studied the effect of the observer on disturbance responses and derived the optimal observer for state-predictive two-degree-of-freedom LQI servo system. The results can be summarized as follows.

- Comparing the asymptotic responses with those of the state feedback case, the

deterioration of disturbance rejection ability caused by the introduction of an observer is quantitatively clarified.

- The design method of the optimal observer that minimizes the deterioration of disturbance rejection ability caused by the introduction of an observer is established.

From the above results, we can obtain the optimal feedback and feedforward gains for responses for step references, the optimal feedback gain from the integrator for responses for step disturbances, and the optimal observer parameters for disturbance responses. This means that we obtained the complete solution for the optimal design problem of the state-predictive two-degree-of-freedom servo system.

In Chapter 4, we studied the robust stability of the state-predictive control system and the Smith control system. To put it concretely, we derived a theorem which gives a graphical method to obtain the stability margins in the case where the plant has modeling errors in the gain and in the delay. While the theorem derived by Bao and Araki [6] becomes conservative when γ, the relative error of the gain, is negative or when P-locus and $R[\gamma]$-locus cross at more than one points, this theorem gives a "practically necessary and sufficient" stability region around the nominal values on the gain–delay plane. By this theorem, we can take the robust stability into account in designing the state-predictive control system.

The design procedure of the state-predictive two-degree-of-freedom LQI servo system incorporating an observer developed in the above chapters can be summarized as follows.

1. Determine the feedback gain F_0 and the feedforward gain H_0, which determine tracking characteristics for step references, to minimize a quadratic-integral performance index.

2. Determine the parameters of an observer considering the feature of disturbances.

3. Construct a prediction mechanism.

4. Introduce an integrator and determine the feedback gain G from the integrator considering the tradeoff between the robust stability and the disturbance rejection ability.

In Chapter 5, we studied the blood pressure control system using a state-predictive controller. The response of the blood pressure to the infusion of a hypotensive drug can be considered as a typical plant with a pure delay. We developed a blood pressure

control system for keeping blood pressure at a low level using a state-predictive servo controller in order to spare blood transfusion and prevent the side-effects of blood transfusion. The response of the blood pressure to the infusion of a hypotensive drug can be modeled as a first order delay with a nonlinear feedback plus a pure delay. For this model, we designed a state-predictive servo system, and made blood pressure control experiments on dogs. Comparing our results with other former results, we can conclude that our system has much better stability and accuracy.

We have the following future topics. In Chapter 4, a method of robust stability analysis of state-predictive control systems and the Smith systems was given. However, this method is for the case where the plant model has the modeling error only in the gain and delay. The results in Chapter 4 can be extended to the case of general modeling errors.

The state-predictive servo controller to keep the blood pressure at a low level developed in Chapter 5 was actually used for surgical operations and performed a satisfactory function [38]. It is expected to develop similar systems which can be applied to the control of other physiological regulatory systems as medical treatments, e.g., artificial pancreas to keep the blood glucose of the subjects of diabetes at a normal level, an anesthesia control system during surgical operations, and so on.

Bibliography

[1] K. Aida and T. Kitamori: Feedback properties of the reduced sensitivity optimal robust servo system (in Japanese); Proc. the 29th SICE Annual Conference, Tokyo, pp. 61–62 (1990)

[2] M. Araki and K. Watanabe: Two-degree-of-freedom predictive control of plants with a pure delay (in Japanese); Preprint of the 14th SICE Symp. on Control Theory, pp. 203–206 (1985)

[3] J. M. Arnsparger, B. C. McInnis, J. R. Glover and N. A. Normann: Adaptive control of blood pressure; *IEEE Trans. Biomed. Eng.*, Vol. BME-30, No. 3, pp. 168–176 (1983)

[4] K. J. Astrom, C. C. Hang and B. C. Lim: A new Smith predictor for controlling a process with an integrator and long dead-time; *IEEE Trans. Automatic Control*, Vol. 39, No. 2, pp. 343–345 (1994)

[5] M. Athans: The matrix minimum principle; *Information and Control*, Vol. 11, pp. 592–606 (1968)

[6] S. Bao and M. Araki: On robust stability of state predictive control systems for plant with pure delay (in Japanese); *Systems and Control*, Vol. 32, No. 1, pp. 58–65 (1988)

[7] E. J. Davison and S. H. Wang: Properties and calculation of transmission zeros of linear multivariable systems; *Automatica*, Vol. 10, pp. 643–658 (1974)

[8] E. J. Davison: The robust control of a servomechanism problem for linear time-invariant multivariable systems; *IEEE Trans. Automatic Control*, Vol. AC-21, No. 1, pp. 25–34 (1976)

[9] J. C. Doyle and G. Stein: Robustness with observers; *IEEE Trans. Automatic Control*, Vol. AC-24, No. 4, pp. 607–611 (1979)

[10] B. A. Francis and W. M. Wonham: The internal model principle for linear multivariable regulators; *Applied Mathematics & Optimization*, Vol. 2, No. 2, pp. 170–194 (1975)

[11] Y. Fujisaki and M. Ikeda: Synthesis of two-degree-of-freedom optimal servosystems (in Japanese); *Trans. Society of Instrument and Control Engineers*, Vol. 27, No. 8, pp. 907–914 (1991); see also: Y. Fujisaki and M. Ikeda: A two-degree-of-freedom design of optimal servosystems; Proc. the 31st IEEE Conference on Decision and Control, pp. 3588-3589, Tucson, Arizona (1992)

[12] Y. Fujisaki and M. Ikeda: A two-degree-of-freedom design of servosystems incorporating an observer (in Japanese); *Trans. Institute of Systems, Control and Information Engineers*, Vol. 6, No. 7, pp. 347–349 (1993)

[13] Y. Fujisaki, M. Ikeda and Y. Kuboyama: Two-degree-of-freedom optimal servosystems for plants with delay (in Japanese); *Trans. the Institute of Systems, Control and Information Engineers*, Vol. 7, No. 1, pp. 32–34 (1994)

[14] Y. Fukui and T. Masuzawa, Development of fuzzy blood pressure control system (in Japanese); *Jpn. J. Med. Electron. Biol. Eng.*, Vol. 27, No. 2, pp. 19–25 (1989)

[15] T. Furukawa and E. Shimemura: Predictive control for systems with time delay; *Int. J. Control*, Vol. 37, No. 2, pp. 399–412 (1983)

[16] E. Furutani, S. Bao and M. Araki: A-TDS: A CADCS package for plants with a pure delay; *Recent Advances in Computer-Aided Control Systems Engineering* (edited by M. Jamshidi and C. J. Herget), pp. 247–272 (1992)

[17] T. Hagiwara, Y. Ohtani and M. Araki: A design method of LQI servo systems with two degrees of freedom (in Japanese); *Trans. Institute of Systems, Control and Information Engineers*, Vol. 4, No. 12, pp. 501–510 (1991)

[18] T. Hagiwara and M. Araki: A successive optimal construction procedure for state feedback gains; *Linear Algebra and Its Applications*, Vol. 203-204, pp. 659–673 (1994)

[19] T. Hagiwara, T. Yamasaki and M. Araki: Two-degree-of-freedom design method of LQI servo systems: disturbance rejection by constant state feedback; *Int. J. Control*, Vol. 63, No. 4, pp. 703–719 (1996)

[20] T. Hagiwara, E. Furutani and M. Araki: Two-degree-of-freedom design method of linear-quadratic servo systems with an integral compensator: Analysis of the performance deterioration by the introduction of an observer; *Int. J. Control*, Vol. 64, No. 5, pp. 941–958 (1996)

[21] S. Isaka and A. V. Sebald: Control strategies for arterial blood pressure regulation; *IEEE Trans. Biomed. Eng.*, Vol. BME-40, No. 4, pp. 353–363 (1993)

[22] M. Ito and K. Watanabe: ; *Systems and Control*, Vol. 26, No. 8, pp. 479–488 (1982)

[23] H. Kimura and T. Fujii: Theory of multivariable control systems and applications–II (in Japanese), *Systems and Control*, Vol. 22, No. 6, pp. 340–349 (1978)

[24] A. J. Koivo: Automatic continuous-time blood pressure control in dogs by means of hypotensive drug injection; *IEEE Trans. Biomed. Eng.*, Vol. BME-27, No. 10, pp. 574–581 (1980)

[25] R. L. Kosut: Suboptimal control of linear time-invariant systems subject to control structure constraints; *IEEE Trans. Automatic Control*, Vol. AC-15, No. 5, pp. 557–563 (1970)

[26] P. Kudva, N. Viswanadham and A. Ramakrishna: Observers for linear systems with unknown inputs; *IEEE Trans. Automatic Control*, Vol. AC-25, No. 1, pp. 113–115 (1980)

[27] H. Kwakernaak and R. Sivan: The maximally achievable accuracy of linear optimal regulators and linear optimal filters; *IEEE Trans. Automatic Control*, Vol. AC-17, No. 1, pp. 79–86 (1972)

[28] W. S. Levine and M. Athans: On the determination of the optimal constant output feedback gains for linear multivariable systems; *IEEE Trans. Automatic Control*, Vol. AC-15, No. 1, pp. 44–48 (1970)

[29] D. G. Luenberger: Observers for multivariable systems; *IEEE Trans. Automatic Control*, Vol. AC-11, 190–196 (1966)

[30] H. Maeda and H. Hino: Design of optimal observers for linear time-invariant systems; *Int. J. Control*, Vol. 19, No. 5, pp. 993–1004 (1974)

[31] F. T. Man: Some inequalities for positive definite symmetric matrices; SIAM J. Applied Mathematics, Vol. 19, No. 4, pp. 679–681 (1970)

[32] A. Manitius and A. W. Olbrot: Finite spectrum assignment problem for systems with delays; *IEEE Trans. Automatic Control*, Vol. AC-24, No. 4, pp. 541–553 (1979)

[33] T. Masuzawa and Y. Fukui: The control system for physiological system –Optimal control of blood-pressure by using vaso-active drug (in Japanese); *J. Jpn. Soc. Precis. Eng.*, Vol. 55, No. 2, pp. 406–411 (1989)

[34] P. S. Maybeck: *Stochastic Models, Estimation, and Control*; Academic Press, New York (1982)

[35] R. A. Miller: Specific optimal control of the linear regulator using a minimal order observer; *Int. J. Control*, Vol. 18, No. 1, pp. 139–159 (1973)

[36] P. S. Pak, Y. Suzuki and K. Fujii: Synthesis of multivariable optimal servo system (in Japanese); *Trans. Society of Instrument and Control Engineers*, Vol. 8, No. 5, pp. 568–575 (1972)

[37] Z. Palmor: Stability properties of Smith dead-time compensator controller; *Int. J. Control*, Vol. 32, No. 6, pp. 937–949 (1980)

[38] T. Sakamoto, E. Furutani, H. Onodera, S. Kan, G. Shirakami, M. Araki, S. Maetani, K. Mori and M. Imamura: Clinical application of an automatic blood pressure control system (in Japanese); The 34th Annual Meeting of Japanese Society for Artificial Organs (1996)

[39] S. Sawano: Control of processes with dead time (in Japanese); *Automatic Control*, Vol. 7, No. 5, pp. 248–254 (1960)

[40] L. C. Sheppard: Computer control of the infusion of vasoactive drugs; *Ann. Biomed. Eng.*, Vol. 8, pp. 431–444 (1980)

[41] J. B. Slate, L. C. Sheppard, V. C. Rideout and E. H. Blackstone: A model for design of a blood pressure controller for hypertensive patients; *Proceedings of 5th IFAC Symposium on Identification and System Parameter Estimation*, edited by R. Isermann, pp. 867–874, Pergamon (1979)

[42] O. J. M. Smith: A controller to overcome dead time; *ISA J.*, Vol. 6, No. 2, pp. 28–33 (1959)

[43] G. Stein and M. Athans: The LQG/LTR procedure for multivariable feedback control design; *IEEE Trans. Automatic Control*, Vol. AC-32, No. 2, pp. 105–114 (1987)

[44] G. I. Voss, P. G. Katona and H. J. Chizeck: Adaptive multivariable drug delivery: Control of arterial pressure and cardiac output in anesthetized dogs; *IEEE Trans. Biomed. Eng.*, Vol. BME-34, No. 8, pp. 617–623 (1987)

[45] K. Watanabe and M. Ito: Disturbance rejection of Smith predictor control system (in Japanese); *Trans. Society of Instrument and Control Engineers*, Vol. 19, No. 3, pp. 187–192 (1983)

[46] K. Watanabe: On robust stability of control systems for plant with delay (in Japanese); Preprint of the 8th Dynamical System Theory Symp., pp. 9–12 (1985)

[47] B. Widrow: Adaptive model control applied to realtime blood-pressure regulation; in *Pattern recognition and machine learning*, edited by K. S. Fu, pp. 310–324, Plenum Inc. (1971)

[48] E. A. Woodruff and R. B. Northrop: Closed-loop regulation of a physiological parameter by an IPFM/SDC (integral pulse frequency modulated/Smith delay compensator) controller; *IEEE Trans. Biomed. Eng.*, Vol. BME-34, No. 8, pp. 595–602 (1987)

List of Publications by the Author

Journal Papers

1. T. Sakamoto, H. Onodera, S. Maetani, E. Furutani and M. Araki: Development of blood pressure control system (in Japanese); *Jpn. J. Artif. Organs*, Vol. 22, No. 3, pp. 1009–1013 (1993)

2. T. Sakamoto, H. Onodera, M. Imamura, S. Maetani, E. Furutani and M. Araki: Blood pressure control systems based on state-predictive control method; *Artificial Organs Today*, Vol. 4, No. 2, pp. 141–149 (1994)

3. E. Furutani, M. Saeki and M. Araki: Shifted Popov criterion (in Japanese); *Trans. Inst. Syst. Contr. Inform. Eng.*, Vol. 7, No. 7, pp. 247–254 (1994)

4. E. Furutani, M. Araki, T. Sakamoto and S. Maetani: Blood pressure control during surgical operations; *IEEE Trans. Biomed. Eng.*, Vol. 42, No. 10, pp. 999–1006 (1995)

5. T. Sakamoto, E. Furutani, H. Onodera, M. Imamura, S. Maetani and M. Araki: Further inprovement of blood pressure control system toward clinical use (in Japanese); *Jpn. J. Artif. Organs*, Vol. 24, No. 5, pp. 982–988 (1995)

6. T. Sakamoto, E. Furutani, H. Onodera, M. Imamura, S. Maetani and M. Araki: Automatic blood pressure control system —For clinical use— (in Japanese); *Clinical Pharmacology and Therapy*, Vol. 5, No. 7, pp. 1257–1261 (1995)

7. T. Hagiwara, E. Furutani and M. Araki: Two-degree-of-freedom design method of linear-quadratic servo systems with an integral compensator: Analysis of the performance deterioration by the introduction of an observer; *Int. J. Contr.*, Vol. 64, No. 5, pp. 941–958 (1996)

8. T. Hagiwara, E. Furutani and M. Araki: Optimal observers for disturbance rejection in two-degree-of-freedom LQI servo systems; submitted to *IEE Proceedings*

9. T. Sakamoto, E. Furutani, H. Onodera, S. Kan, G. Shirakami, M. Araki, S. Maetani, K. Mori and M. Imamura: Clinical application of an automatic blood pressure control system (in Japanese); submitted to *Jpn. J. Artif. Organs*

Conference Papers

1. S. Bao, E. Furutani, M. Araki and A. Sugikawa: A CAD package "A-TDS" for plants with a pure delay (in Japanese); Report of Researching Group on Systems and Control, Institute of Electrical Engineers of Japan, pp. 11–20 (1987)

2. S. Bao, E. Furutani and M. Araki: CADCS package "A-TDS" for systems with pure delay; 4th IFAC Symposium on Computer Aided Design in Control Systems, Beijing, P. R. China, pp. 290–294 (Aug. 1988)

3. S. Suzuki, E. Furutani and M. Araki: Control systems with self-breeding controllers (in Japanese); Preprints of the 31st Japan Joint Automatic Control Conference, pp. 547–548 (1988)

4. E. Furutani and M. Araki: Modified algorithm of self-breeding controllers (in Japanese); Proc. of the 33rd Annual Conference of the Institute of Systems, Control and Information Engineers, pp. 71–72 (1989)

5. E. Furutani and M. Araki: Design method for control systems with two-degrees of freedom based on frequency response – I (in Japanese); Proc. of the 28th SICE Annual Conference, pp. 211–212 (1989)

6. E. Furutani and M. Araki: Design method for control systems with two-degrees of freedom based on frequency response – II (in Japanese); Proc. of the 28th SICE Annual Conference, pp. 213–214 (1989)

7. E. Furutani and M. Araki: Identification of the frequency-domain characteristics from the response of closed-loop systems (in Japanese); Proc. of the 28th SICE Annual Conference, pp. 715–716 (1989)

8. E. Furutani and M. Araki: A tuning method of D element and identification of the frequency response (in Japanese); Report of Researching Group on Systems and Control, Institute of Electrical Engineers of Japan, pp. 1–9 (1990)

9. M. Araki, E. Furutani and M. Saeki: Stability criterion for nonlinear systems and its application to fuzzy control systems (in Japanese); Proc. of the Annual Conference of the Japan Society for Industrial and Applied Mathematics, pp. 37–38 (1991)

10. E. Furutani and M. Araki: A stability condition for fuzzy control systems — Application of an extended Popov criterion— (in Japanese); Preprints of the 34th Japan Joint Automatic Control Conference, pp. 5–6 (1991)

11. M. Araki, E. Furutani and M. Saeki: Shifted Popov criterion —Filling the gap between time-varying and time-invariant systems (in Japanese); IEICJ, pp. 23–30 (1991)

12. E. Furutani and M. Araki: Application of the shifted Popov criterion to fuzzy control systems (in Japanese); Proc. of the 36th Annual Conference of the Institute of Systems, Control and Information Engineers, pp. 193–194 (1992)

13. W. Mizuta, E. Furutani, M. Araki, T. Sakamoto and S. Maetani: Application of state predictive control to blood pressure control system (in Japanese); Proc. of the 36th Annual Conference of the Institute of Systems, Control and Information Engineers, pp. 411–412 (1992)

14. E. Furutani, M. Saeki and M. Araki: Shifted Popov criterion and stability analysis of fuzzy control systems (in Japanese); Proc. of the 21st SICE Symposium on Control Theory, pp. 227–232 (1992)

15. E. Furutani, T. Hagiwara and M. Araki: Plant-variable-optimal LQI servo systems with two degrees of freedom incorporating an observer (in Japanese); Proc. of the 31st SICE Annual Conference, pp. 29–30 (1992)

16. E. Furutani, T. Hagiwara and M. Araki: Plant-variable-optimal state-predictive servo systems with two degrees of freedom (in Japanese); Preprints of the 35th Japan Joint Automatic Control Conference, pp. 133–134 (1992)

17. T. Sakamoto, H. Onodera, S. Maetani, E. Furutani and M. Araki: Blood pressure control system using micro-computer (in Japanese); The 30th Annual Meeting of Japanese Society for Artificial Organs (1992)

18. E. Furutani, M. Saeki and M. Araki: Shifted Popov criterion and stability analysis of fuzzy control systems; 31st IEEE Conference on Decision and Control, Tucson, Arizona, U.S.A., pp. 2790–2795 (Dec. 1992)

19. T. Sakamoto, H. Onodera, S. Maetani, E. Furutani and M. Araki: Development of an automatic blood pressure control system (in Japanese); The 93rd Annual Conference of Japanese Society for Surgery (1993)

20. E. Furutani, T. Hagiwara, K. Yoshihara and M. Araki: A design method of observers for plant-variable-optimal LQI servo systems (in Japanese); Proc. of the 37th Annual Conference of the Institute of Systems, Control and Information Engineers, pp. 199–200 (1993)

21. H. Watanabe, E. Furutani, M. Araki, T. Sakamoto, H. Onodera and S. Maetani: Danger protecting system in blood pressure control during surgical operations (in Japanese); Proc. of the 37th Annual Conference of the Institute of Systems, Control and Information Engineers, pp. 345–346 (1993)

22. E. Furutani, T. Hagiwara and M. Araki: State-predictive LQI servo systems with two degrees of freedom (in Japanese); Proc. of the 22nd SICE Symposium on Control Theory, pp. 239–244 (1993)

23. E. Furutani, T. Hagiwara and M. Araki: Two-degree-of-freedom LQI servo systems incorporating an observer (in Japanese); Report of Researching Group on Systems and Control, Institute of Electrical Engineers of Japan, pp. 39–48 (1993)

24. T. Hagiwara, E. Furutani and M. Araki: Optimal minimal-order observers for disturbance rejection in two-degree-of-freedom LQI servo systems (in Japanese); Preprints of the 36th Japan Joint Automatic Control Conference, pp. 89–90 (1993)

25. T. Sakamoto, E. Furutani, H. Onodera, M. Imamura, S. Maetani and M. Araki: Optimal control of blood pressure and other variables in acute blood loss: Experimental studies using automatic BP control system; The Society of University Surgeons 55th Annual Meeting & 9th Tripartite Meeting, Jackson, Mississippi, U.S.A. (Feb. 1994)

26. T. Sakamoto, E. Furutani, H. Onodera, M. Imamura, S. Maetani and M. Araki: Effects of automatic control of blood pressure and intravenous fluid for bleeding (in Japanese); The 93rd Annual Conference of Japanese Society for Surgery (1994)

27. T. Murotani, E. Furutani, M. Araki, T. Sakamoto, H. Onodera and S. Maetani: Identification systems for blood pressure control (in Japanese); Proc. of the 38th Annual Conference of the Institute of Systems, Control and Information Engineers, pp. 269–270 (1994)

28. T. Sakamoto, E. Furutani, H. Onodera, M. Imamura, S. Maetani and M. Araki: Improvement of automatic blood pressure control systems using a state-predictive controller for clinical use (in Japanese); The 32nd Annual Meeting of Japanese Society for Artificial Organs (1994)

29. E. Furutani, T. Hagiwara and M. Araki: Two-degree-of-freedom digital LQI servo systems incorporating an observer (in Japanese); Preprints of the 37th Japan Joint Automatic Control Conference, pp. 153–154 (1994)

30. T. Hagiwara, E. Furutani and M. Araki: Two-degree-of-freedom design method of LQI servo systems —Performance deterioration by the introduction of an observer and optimal observer design—; The 33rd IEEE Conference on Decision and Control, Lake Buena Vista, Florida, U.S.A., pp. 4204–4209 (Dec. 1994)

31. E. Furutani, T. Hagiwara and M. Araki: Two-degree-of-freedom design method of state-predictive LQI servo systems; The 33rd IEEE Conference on Decision and Control, Lake Buena Vista, Florida, U.S.A., pp. 3581–3586 (Dec. 1994)

32. T. Sakamoto, E. Furutani, H. Onodera, M. Imamura, S. Maetani and M. Araki: Automatic blood pressure control system —For clinical use— (in Japanese); The 7th Annual Conference of Japanese Society for Therapeutics & Engineering, p. 66 (1995)

33. E. Furutani, M. Araki, T. Sakamoto, H. Onodera and S. Maetani: A blood pressure control system using a state-predictive controller (in Japanese); Proc. of the 3rd SICE Symposium on Application of Control Theory, pp. 79–84 (1995)

34. E. Furutani and M. Araki: On robust stability of state-predictive control systems; Proc. of the 34th SICE Annual Conference, pp. 1059–1060 (1995)

35. H. Shigei, E. Furutani, M. Araki, T. Sakamoto, H. Onodera and S. Maetani: Improved fail-safe mechanism for blood pressure control; Proc. of the 40th Annual Conference of the Institute of Systems, Control and Information Engineers, pp. 477–478 (1996)

36. M. Sugano, E. Furutani, M. Araki, T. Sakamoto, H. Onodera and S. Maetani: A blood pressure control system using a model predictive controller; Proc. of the 40th Annual Conference of the Institute of Systems, Control and Information Engineers, pp. 479–480 (1996)

37. S. Tonegawa, E. Furutani and M. Araki: Pharmacological and physiological modeling of blood pressure regulating mechanism for blood pressure control; Proc. of the 40th Annual Conference of the Institute of Systems, Control and Information Engineers, pp. 123–124 (1996)

38. T. Sakamoto, E. Furutani, H. Onodera, S. Kan, G. Shirakami, M. Araki, S. Maetani, K. Mori and M. Imamura: Clinical application of an automatic blood pressure control system (in Japanese); The 34th Annual Meeting of Japanese Society for Artificial Organs (1996)

Books

1. E. Furutani, S. Bao and M. Araki; A-TDS: A CADCS package for plants with a pure delay, in *Recent Advances in Computer Aided Control Systems Engineering* (eds. M. Jamshidi and C. J. Herget), pp. 247–272, Elsevier (1992)